Dissertation

submitted to the

Combined Faculties for the Natural Sciences and for Mathematics

of the Ruperto-Carola University of Heidelberg, Germany

for the degree of

Doctor of Natural Sciences

presented by

Masters in Biology Anna Dondzillo

from Warsaw, Poland

Oral-examination:_____

Active zone proteins Bassoon and Piccolo at the calyx of Held: age – dependent localization and targeted *in vivo* perturbation

Referees: Prof. Dr. Bert Sakmann

Prof. Dr. Thomas Kuner

I hereby declare that this submission is my own work and that, to the best of my knowledge and belief, it contains no material previously published or written by another person nor material which to a substantial extent has been accepted for the award of any other degree or diploma of the university or other institute of higher learning, except where due acknowledgment has been made in the text.

Heidelberg, 27 November 2007 _____

Anna Dondzillo

Active zone proteins Bassoon and Piccolo at the calyx of Held: age - dependent localization and targeted *in vivo* perturbation

Summary

Neurons communicate with each other via synaptic transmission. Chemical synapses transfer information through the release of neurotransmitter. This process involves a cascade of tightly controlled molecular reactions, designed to allow reliable transmission of activity and to accommodate mechanisms of experience-dependent plasticity. In contrast to the very detailed knowledge of the functional capabilities of synapses and the fact that most presynaptic proteins have been identified, the molecular mechanisms underlying neurotransmitter release remain poorly understood.

The active zone (AZ), the site of Ca^{2+}-dependent neurotransmitter release in nerve terminals, is a morphological specialization of the presynaptic plasma membrane with a set of proteins necessary for the organization of exo- and endocytotic molecular machineries. Bassoon and Piccolo are structurally related, large multidomain proteins specifically and exclusively located in AZs of the mammalian nervous system. In conjunction with Rim, CAST, Munc13 and ELKS, Bassoon and Piccolo are thought to organize AZs through their multidomain capability of interaction with many other proteins.

Specific deletion of Bassoon in mice resulted in a significantly lower number of active synapses in hippocampal autaptic cultures. Bassoon deletion did not result in compensatory changes of AZ proteins but Piccolo, which was increased 1.4 times. Hence, the presence of Piccolo may prevent a loss of function in Bassoon knockout mice. To assess the role of Bassoon and Piccolo in neurotransmitter release, we examined their localization in the calyx of Held giant presynaptic terminal and attempted a simultaneous knockdown of both proteins using RNA interference.

First, we examined the three-dimensional (3D) localization of Bassoon and Piccolo in the rat calyx of Held between postnatal days (P) 9 and 24, a period characterized by pronounced structural and functional changes. To unequivocally assign immunohistochemical (IHC) signals to the calyx, we expressed membrane-anchored GFP (mGFP) or synaptophysin-GFP in the calyx using targeted stereotaxic delivery of adeno-associated virus (AAV) vectors. We then examined the distribution of Bassoon and Piccolo using IHC in slices containing calyces with labeled plasma membrane or synaptic vesicles (SV) using confocal microscopy and 3D reconstructions. We found that both Bassoon and Piccolo were arranged in clusters resembling the size of AZs. These clusters were located in the presynaptic membrane

facing the principal cell, close to and partially overlapping with SV clusters. Simultaneous application of both antibodies revealed a ~90% overlap, indicating that both proteins co-localize. We found about 200-400 clusters in both P9 and P24 calyces. The number and distribution of clusters did not differ, suggesting that these parameters do not contribute to postnatal functional maturation. Furthermore, we observed IHC-signals in the spaces between finger-like protrusions of the calyx, consistent with intermingled non-calyceal inputs located on the principal cell. As these signals mimic a calyx-like distribution, particularly in 2D images, pre-labeled calyces are essential for IHC studies of protein distribution in the calyx of Held.

To understand the function of Bassoon and Piccolo in AZ organization and their contribution to neurotransmitter release, we attempted to down-regulate each of these proteins *in vivo* in the calyx of Held using RNA interference. Small hairpin RNAs (shRNA) directed against Bassoon and Piccolo were expressed through AAV vectors. Viral particles were stereotaxically delivered to the ventral cochlear nucleus, where the somata of neurons giving rise to calyx terminals are located. Using 3D fluorescence immunohistochemistry, we could demonstrate a down-regulation of Piccolo at its most relevant site - the nerve terminal. With this approach we were able to show a decreased amount of Piccolo in the calyces treated with shRNA as compared to control calyces. Preliminary results suggest a knockdown of Bassoon using the same approach. However, low titers of the virus preparations did not yield numbers of perturbed calyces sufficient for functional analyses in brain slices. This also precluded knocking down Bassoon and Piccolo simultaneously. Attempts of improving viral titers remained unsuccessful, posing a potential general limitation to AAV-mediated applications of shRNAs for targeted *in vivo* RNA interference.

In summary, we developed a novel approach to quantify *in vivo* perturbation of proteins at the level of a single synapse. Furthermore, we show that any immunohistochemistry-based characterization of proteins in the calyx of Held requires the prelabelled calyces. We found that the number of AZs as identified with Bassoon and Piccolo fluorescent immunohistochemistry did not change in development of the calyx of Held, suggesting that this parameter is not involved in increasing release efficiency during postnatal maturation.

Active zone proteins Bassoon and Piccolo at the calyx of Held: age - dependent localization and targeted in vivo perturbation

Zusammenfassung

Nervenzellen kommunizieren untereinander über Synapsen, wobei chemische Synapsen die Information durch die Ausschüttung von Neurotransmittern übertragen. Dieser Prozess beinhaltet eine Kaskade stark regulierter Protein-Protein Wechselwirkungen die eine zuverlässige Übertragung der elektrischen Aktivität garantieren und gleichzeitig Mechanismen der synaptischen Plastizität zulassen. Während die funktionellen Aspekte der Präsynapse gut untersucht und die meisten der ihrer Proteine identifiziert sind, bleiben die exakten molekularen Mechanismen die zur Ausschüttung der Neurotransmitter führen unklar.

Die aktive Zone (AZ), der Ort in den Nervenendigungen, an dem die Ca^{2+}-abhängige Neurotransmitterausschüttung stattfindet, ist ein spezieller Abschnitt der präsynaptischen Plasmamembran, der sich morphologisch von Rest der Zelle unterscheidet, und in dem Proteine der Exo- und Endocytosemaschinerie vorliegen. Bassoon und Piccolo sind strukturell verwandte, große Multidomänenproteine die spezifisch und exklusiv in den AZs des Nervensystems von Säugern vorliegen. Es wird vermutet, dass Bassoon und Piccolo zusammen mit Rim, CAST, Munc13 und ELKS die Grundstruktur der AZ bilden, wobei ihr Multidomänenaufbau die Wechselwirkung mit diversen anderen Proteinen der AZ erlaubt.

Die spezifische Ausschaltung von Bassoon in Mäusen führte zu einer signifikanten Reduktion der Anzahl von Synapsen in autaptischen Kulturen des Hippocampus. Außer einer 1,4fachen Hochregulierung von Piccolo wurden jedoch keine durch die Ausschaltung von Bassoon verursachten kompensatorischen Veränderungen in den Mengen anderer AZ-Proteinen beobachtet. Die Anwesenheit von Piccolo könnte also einen Verlust der Funktion in Bassoon-knock-out-Mäusen verhindern. Zur genaueren Bestimmung der Rolle von Basson und Piccolo untersuchten wir ihre Lokalisation in der Heldschen Calyx, einer Riesennervenendigung, und versuchten beide Proteine mittels RNA interference auszuschalten.

Zunächst untersuchten wir die dreidimensionale (3D) Lokalisation von Bassoon und Piccolo in der Heldschen Calyx der Ratte zwischen dem neunten und vierundzwanzigsten Tag nach der Geburt, einer Phase in der bedeutende strukturelle und funktionelle Veränderungen der Synapse stattfinden. Um immunhistochemische Signale zweifelsfrei der Calyx zuordnen zu können, wurden membrangebundenes GFP (mGFP) oder Synaptophysin-GFP gezielt in der Calyx exprimiert. Dabei wurden stereotaktische Injektionen von adeno-assoziierten Viren (AAV) als Vektoren für die GFP-Konstrukte benutzt. Danach bestimmten wir die Verteilung von IHC-Signalen gegen Basson und Piccolo in Hirnschnitten markierter Calyces (Plasmamembran oder synaptische Vesikel (SV)). Dazu wurden konfokale Mikroskopie und 3D-Rekonstruktionen verwendet. Hierbei stellten wir fest, dass sowohl Bassoon als auch Piccolo in Clustern, die der Größe der AZ entsprachen, organisiert waren. Diese Cluster

befanden sich in der Plasmamembran der Calyx, die der Prinzipalzelle zugewandt war, wobei in der Nähe und teilweise mit dem IHC-Signal von Bassoon und Piccolo überlappend, SV-Cluster detektiert wurden. Die gleichzeitige Applikation von Antikörpern gegen beide Proteine führte dazu, dass eine ca. 90%ige Überlappung der IHC-Signale erhalten wurde, was darauf hindeutet, dass die beiden Proteine kolokalisiert vorlagen. Es wurden sowohl in P9 als auch in P24 Ratten 200-400 Bassoon- bzw. Piccolo-Cluster pro Calyx detektiert. Weder die Anzahl noch die Verteilung der Cluster unterschieden sich in den beiden Altersgruppen, was zu der Annahme führt, dass diese beiden Parameter keine Rolle bei der funktionellen Reifung des Calyx spielen. Außerdem fanden wir IHC-Signale zwischen den fingerähnlichen Fortsätzen des Calyx, welche zu anderen Synapsen der Prinzipalzelle als der Calyx gehören. Da diese Signale aber besonders in 2D-Bildern eine Calyx-ähnliche Verteilung besitzen, ist eine vorher markierte Calyx, beispielsweise mit mGFP, essentiell um IHC-Studien in der Heldschen Calyx durchführen zu können.

Um die Funktion von Bassoon und Piccolo bei der Organisation der AZ und ihren Beitrag zur Neurotransmitterfreisetzung besser zu verstehen, versuchten wir jedes der Proteine mittels RNA interference *in vivo* herunter zu regulieren. Small hairpin RNAs (shRNAs), gegen Bassoon oder Piccolo gerichtet, wurden mittels AAV-Vektoren exprimiert. Dazu wurden Viruspartikel stereotaktisch in den ventralen cochlearen Nukleus, der die Somata der Neuronen welche die Heldsche Calyx bilden enthält, injiziert. Mit Hilfe von 3D Fluoreszenzimmunhistochemie konnten wir eine Herunterregulierung von Piccolo in shRNA exprimierenden Calyces detektieren. Ähnliche, vorläufige Ergebnisse wurden mit dieser Methode bei entsprechenden Versuchen zur Herunterregulierung von Bassoon erhalten. Die niedrigen Titer der Viruspräparationen führten allerdings nicht zu einer für die funktionelle Analyse ausreichenden Anzahl von Calyces die shRNA exprimierten. Das gleiche Problem trat auch bei dem Versuch auf Bassoon und Piccolo gleichzeitig herunterzuregulieren. Eine Erhöhung der Virustiter war nicht möglich, so dass hier eventuell eine generelle Grenze der Anwendbarkeit von AAV-vermittelter shRNA-Expression zur gezielten RNA interference *in vivo* erreicht wurde.

Zusammenfassend kann gesagt werden, dass hier ein neuer Ansatz zur Quantifizierung der Proteinpertubation in einzelnen Synapsen, *in vivo*, entwickelt wurde. Außerdem konnten wir zeigen, dass eine vorherige Markierung der Calyx, beispielsweise durch mGFP, für immunhistochemische Charakterisierungen von Proteinen in der Heldschen Calyx unerlässlich ist. Wir fanden mit Hilfe von Fluoreszenzimmunhistochemie heraus, dass die Anzahl der mittels Bassoon und Piccolo identifizierten AZs sich während der Entwicklung nicht veränderte. Daraus schließen wir, dass die Anzahl der AZs nicht an der Steigerung der Freisetzungseffizienz während der postnatalen Reifung der Heldschen Calyx beteiligt ist.

List of contents

1 Introduction

Nerve cells basic structure remains similar to that of other cells. Each neuron has a nucleus, Golgi apparatus, endoplasmic reticulum, ribosomes, mitochondria and other organelles essential for any cell to function. Neurons differ from other cells and each other by specific morphological and functional features. They have one property in common: integration of incoming information. In the human nervous system, a single neuron can receive from 1 to 100 000 inputs (Purves et al., 2004), and this variability depends on the type and function of any given neuron. In general, the information received from the inputs is conducted via a regenerating electrical impulse – the action potential (AP), along neuronal axon. In the majority of the central nervous system (CNS) nerve cells, the signal is received at the dendrites or the soma and conducted to the axon terminal.

1. 1 Different types of synapses in the brain

Information is passed between neurons via specialized site called synapse. In general, a synapse consists of a pre-synaptic compartment, which is located on an axon terminal, and a post-synaptic compartment, often a dendrite or a cell soma of the next neuron. Usually both pre- and post-synaptic sites are physically separated by an extracellular gap – the synaptic cleft. The synaptic cleft can be extremely small in electrical synapses or bigger in chemical ones. In chemical type of synapses, information has to be first converted from the incoming AP to a chemical signal and then back to an AP after crossing the synaptic cleft. Another type of synapse, less common in the CNS, has a very small gap, so small that there is a physical connection established between pre- and post-synaptic compartments. Communication between such synapses is based on direct electrical transduction hence these synapses are called electrical synapses.

1. 1. 1 Synaptic communication

The information about stimulus intensity is encoded in spike frequency and send along neuronal axon. Such coding features temporal and electrical potential characteristics: frequency, length of occurrence (represented by width at half-maximal action potential amplitude), and amplitude of the AP. Transfer of the AP down the axon without losing any of the characteristics requires active electrical conductances, which are based on the electrical gradient present across the axon membrane and controlled permeability of the membrane for negatively and positively charged ions. This selective permeability of a membrane for ions is achieved via ion channels spanning the membrane. When the AP arrives at the terminus of the axon it has to be passed to the next neuron. There are two fundamentally different transmission mechanisms used for such inter – neuronal transmission. The one at chemical synapses involves transforming an electrical impulse to a chemical signal at a specialized terminal, the second mechanism seen at electrical synapses permit current to flow passively through intracellular channels between two contacting neurons.

1. 1. 2 Chemical and electrical synapses

In vertebrates the electrical synapses, identified by their molecular substrates, have been found in glia astrocytes and oligodendrocytes, as well as in some neuronal subpopulation e.g. in the brain stem, in the basal ganglia etc (Dermietzel and Spray, 1993). The electrical synapse consists of a pre- and postsynaptic compartment, but that is where the similarity to chemical synapse ends. The two communicating neurons are very close to each other at the synapse so that there is very little space (~3nm) in between pre- and postsynaptic compartments. Pairs of channels formed by connexins, members of larger family of proteins, are located in pre- and postsynaptic membrane and aligned with each other creating an aqueous pore of ~ 1.5 nm diameter through the two membranes. This complex is called gap junction. The communication is based on passive ionic current flow through the gap junction pores from one neuron to the downstream one. Such connection can be bidirectional since it depends on the potential difference between two connected neurons, which is generated locally by the AP. Thus depending on which neuron receives an AP the connection will act in the direction from higher to lower potential. However, unidirectional electrical synapses

have also been described. Another feature of electrical synapses is their speed of transmission, which is almost instantaneous at ≤0.1ms (versus ~0.5ms delay between neurons connected with chemical synapse). For that reason electrical synapses exist in systems where extremely fast reaction from sensory input to motor response is required e.g. neurons involved in crayfish escape behavior. Neurons connected with electrical synapses are also present in systems where electrical activity of neurons needs synchronization, e.g. hormone-secreting neurons within mammalian hypothalamus or neural coupling in control of electric organs of fishes (for review see Bennett, 1997).

At the chemical synapse, signal has to be converted from digitally encoded all or nothing AP wave to analog chemical information. Such incoming AP is converted into chemical signal at the presynaptic compartment. An analog phase of neuronal transmission allows for integration of the information. At the conversion phase the characteristics of AP are read out. Chemical transfer requires different morphological specializations than that of electrical transfer, and allows for connecting interface to convert, integrate, and filter of the passing information. Chemical neurotransmitter is stored in small ~40nm diameter synaptic vesicles (SV) located in the presynaptic compartment. Because of such packaging of neurotransmitter in SVs the release of it is quantal and offers potential for spatial and temporal summation. Anatomically chemical synapse consist of three compartments: presynaptic compartment – mostly axon terminal that releases chemical neurotransmitter in response to calcium influx triggered by incoming AP, postsynaptic compartment – a dendrite or cell soma with neurotransmitter receptors, and a synaptic cleft – a space of ~20 – 30 nm width between pre- and postsynaptic compartments filled with fuzzy electron dense material into which chemical neurotransmitter diffuses. Complex ultrastructural machinery of protein interactions coordinates the series of presynaptic events leading to a fusion of the synaptic vesicles with the presynaptic membrane and a release of neurotransmitter to the synaptic cleft. Neurotransmitter diffuses in the cleft and binds to the receptors located on the postsynaptic neuron. This invokes either excitatory or inhibitory action on the recipient neuron. Whether neuron is excitatory or inhibitory depends on the type of the neurotransmitter it produces, the type of the postsynaptic receptors ion channels and the postsynaptic transmembrane ion gradients that set the polarity and driving force of the channel-mediated current. Majority of neurons however can be

qualified based on their neurotransmitter as being excitatory – with glutamate or inhibitory – with gamma-amino butyric acid (GABA) or glycine as their neurotransmitters.

1. 1. 3 Excitatory and inhibitory chemical synapses

Synapses of the inhibitory neurons differ morphologically from those of the excitatory neurons. Gray (1959) described two types of chemical synapses based on the EM images: symmetrical or type II synapses and asymmetrical or type I synapses. The symmetrical synapses were later confirmed to be inhibitory synapses while asymmetrical or type I – excitatory. Morphologically symmetrical synapses both pre- and postsynaptic membranes look alike, with very few electron dense structures at the juxtaposed membranes. These synapses are having no clear postsynaptic density (PSD), neither clearly visible distinct release site called active zone (AZ). Also, synaptic vesicles located at the presynaptic membrane, are not circular but rather elongated (Somogyi and Cowey, 1981). Molecular components of inhibitory synapses differ also from those of excitatory mainly with neurotransmitter type at the presynaptic site and different receptor types and scaffolding proteins at the postsynaptic compartments. A major postsynaptic protein in the inhibitory synapses indicated in anchoring of the receptors at the postsynaptic membrane is gephyrin. In excitatory synapses this function is played mostly by Post Synaptic Density of 95 kDa protein (PSD 95). GABA and glycine, major inhibitory neurotransmitters of central nervous system (CNS) bind to their receptors after diffusion into the cleft. GABA receptors can further be divided into ligand-gated ionotropic $GABA_A$ receptors ($GABA_A$Rs) and metabotropic ((G)-protein-coupled) $GABA_B$ receptors ($GABA_B$Rs).

Morphologically the excitatory, glutamatergic synapse is characterized with electron dense structures at both pre- and postsynaptic membrane, although the latter one appears thicker (hence the apparent asymmetry). The presynaptic compartment has distinct AZs visible as electron dense area. It appears to contain structures reaching up to ~ 100 nm from the membrane to the cytoplasm in EM images (Landis, et al., 1988), these structures are thought to represent scaffolding proteins. The AZ is a specialized release site with proteins involved in recruiting SVs to the membrane (Bassoon, RIM1), docking and priming (Munc13, Munc18) and fusing (soluble N-ethylmaleimide sensitive factor attachment receptor - SNARE complex) of the SVs

membrane with the presynaptic membrane. At the AZ, few SVs (depending on the type of synapse from 2-3 in the giant terminal of the calyx of Held, to 8 -10 in nerve terminals in cerebellum, hippocampus and cortex) are docked and primed for Ca^{2+}-dependent fusion with the presynaptic membrane. These vesicles are thought to belong to the readily releasable pool (RRP) (Elmqvist and Quastel, 1965) which consists of ~1% of all the SVs present in the compartment. The classical three-pool model (see rev. Rizzoli and Betz, 2005) includes also the reserve pool (80-90% of the total pool of SVs) (Heuser and Reese, 1973), and smaller recycling pool ~10-15% (Pyle et al., 2000). The recycling pool is thought to be maintaining physiological rate of release, while the reserve pool is only involved during the intense stimulation.

In response to Ca^{2+} entering the presynaptic compartment through voltage gated calcium channels, the calcium sensing protein synaptotagmin triggers SVs fusion with the presynaptic membrane and release of neurotransmitter into the cleft. Neurotransmitter passively diffuses within the cleft and binds to specific neurotransmitter receptors located on the membrane of the postsynaptic neuron. The PSD region of the membrane is precisely aligned with the AZ of presynaptic neuron and contains the neurotransmitter receptors. In vertebrates CNS glutamate is a major excitatory neurotransmitter and in general it involves both ionotropic and metabotropic glutamate receptors. The ionotropic receptors can further be divided based on their pharmacological properties (Jonas and Moneyer, 1999) in L-alpha-amino-3-hydroxy-5-methyl-4-isoxazolepropionate receptors (AMPARs), kainate receptors (KARs) and N-methyl-D-aspartate receptors (NMDARs). Different neurons express different receptors depending on the network in which they are located and the tasks they perform. Some neurons, like neurons of the inferior colliculus, are involved in integration of inputs from multiple sensory areas, or thalamocortical neurons involved in filtering of the information send from one layer of the neo-cortex to another. In the auditory system, which relies on the interaural time difference for detection of the location of sound sources, neurons have to carry the information fast and reliably. In the lower auditory pathway of the mammalian brainstem neurons relaying information with high temporal fidelity have large calyx-like synaptic terminals for reliable transmission. Primary auditory neurons, which receive the excitatory input from cochlear hair cells form giant synapses called end bulbs of Held with neurons located in the cochlear nucleus (CN).

1. 1. 4 Calyx of Held as a model system of excitatory synapses

The auditory system utilizes precise timing detection for spatial localization of the sound source. This requires neurons transmitting the information to have a phase locking capability. Such transmission has to be reliable and thus neurons have to be able to fire with high fidelity (review McAlpine, 2005). In mammalian auditory brainstem excitatory globular bushy cells (GBC) specialized both morphologically and functionally to reliably carry the signal from the ventral cochlear nucleus (VCN) to the contralateral side of the brainstem. Their axons, the largest diameter fibers of the trapezoid body (5-10 μm in cats: Rowland et al., 2000) and <2 μm in rats (Rodriguez-Contreras et al., 2006) terminate in a giant synaptic ending (~ 20μm diameter) known as calyx of Held located in the medial nucleus of the trapezoid body (MNTB; Spirou et al., 1990; Kuwabara et al., 1991; Smith et al., 1991). The calyx of Held is a glutamatergic terminal (Grandes and Streit, 1989; Banks and Smith, 1992), which serves as sign-inverting relay in the sound-source localization pathway. The principal neurons of MNTB innervated by the calyx of Held synapse send their inhibitory efferents to ipsi-lateral lateral superior olive (LSO).

Initially the calyx of Held has become the synapse of choice for electrophysiological analysis of mammalian synaptic transmission because its large size allows simultaneous pre- and postsynaptic recordings. Besides the size of the calyx, other features like compartmentalization, a few millimeters distance between the cell soma and terminal make it ideal for acute genetic perturbations. Since injection side does not interfere with the terminal itself. The calyx profound morphological and functional developmental changes suit well the analysis of molecular mechanisms underlying increasing efficiency of transmission.

1. 2 Morphology of the calyx of Held

The calyx of Held does not reach its full synaptic capabilities instantaneously but rather it develops morphologically and functionally throughout the first three weeks of postnatal life in the rat. The ontogeny of the efferent projections from cochlear nucleus (CN) can be divided in three major periods (Kandler and Friauf, 1993). The first period still at the embryonic days (E15-E17) is characterized by axonal outgrowth. During the second period E18 to postnatal day 5 (P5) collaterals of the CN

fibers develop in the auditory brainstem nuclei. Third period P5 – P14 comprise further maturation of terminal structures. As for the establishing of functional synapses, it is not clear whether and how long of a waiting time occurs between CN axons invading MNTB and establishing synapses. However the first events of synaptic transmission at the calyx of Held synapse has been recorded in P2 rats. In young animals axons of developing calyces are free of myelin sheath which makes the calyces easily accessible for the recording electrodes. The size of the calyx, already at the early stages (P8-P11) is also sufficient for presynaptic patching. These features made the calyx of Held an attractive target for uncovering physiological properties of the synapses in the vertebrate CNS. Additionally the postnatal development of both morphological and functional properties of the neuron with large, easily accessible terminal offers a unique insight into the structure-function interplay in the CNS neurons.

1. 2. 1 Postsynaptic compartment

Principal cells of the MNTB form inhibitory connections with neurons located in the medial and lateral superior olivary complex (SOC). SOC is thought to act as coincidence detector because it receives input from both contra-, and ipsilateral CN. Additional role for this pathway has been suggested by thin collaterals branching from calyceal axons as well as MNTB principal cells axons (Kuwabara, et al., 1991). Principal cells major excitatory input comes mostly from globular bushy cells of the contralateral CN via calyx of Held terminal (Warr, 1972; Tolbert et al., 1982; Glendenning et al., 1985; Friauf and Ostwald, 1988; Spirou et al., 1990; Smith et al., 1991). However, other mainly inhibitory (Guinan and Li, 1990; Awatramani et al., 2004) terminals are known to innervate principal cells as well. Intracellular labeling showed local afferents from ventral nucleus of the trapezoid body (VNTB), and from three other nuclei from the periolivary nuclei group but also descending projection presumably from higher brain regions like the lateral lemniscus (Kuwabara et al., 1991). Principal cells of MNTB have been shown to undergo a switch from $GABA_A$ receptor to glycine receptor mediated inhibition. In older animals (P25-P27) this inhibition can be strong enough to shunt calyx-driven excitation (Awatramani, et al., 2004). The source of this inhibition is not known but recurrent collaterals of the MNTB are the possible source. Immunocytochemical study of rat MNTB using

antibody against alpha-1 glycine receptor (GlyR) subunit revealed that developmental increase of this subunit in the MNTB starts at around P8. By P21 alpha 1 GlyR reaches an adult pattern (Friauf et al., 1997).

1. 2. 2 Presynaptic compartment

Protocalyces start forming at around P2 they still have growth cone filaments, which disappear a few days later. From P5 – P7, the calyx differentiates into a cup-like structure covering much of the postsynaptic cell. At this stage a calyx has an AP of slow kinetics (more than 2 fold slower than at P14), and pronounced short-term depression. The change of calyx shape from solid protocalyx at young age to digitiform with stalks and swellings (Morest, 1968; Kandler and Friauf, 1993) in the adult is due to the decrease in terminal substance, fenestration mechanism (Kandler and Friauf, 1993). At the age of P8-P10, calyx matures further and forms single, large compartment that covers about half of the principal cell. It potentially increases contact areas with the principal cell. From the time of ear canal opening (P11/12) to P16 the calyx is more fenestrated and its action potentials become faster and synaptic depression is less pronounced. The physiological maturation of the synapse is very advanced but not complete. In vitro recordings from P14 calyx at physiological temperature (35ºC) shown that the synapse is capable to reliably follow stimuli up to 800 Hz. This indicates parallel changes of the pre- and postsynaptic properties (Taschenberger and von Gersdorff, 2000). Several factors contribute to such increase in firing efficiency. Acceleration of an AP leads to decrease in Ca^{2+} influx but yet the EPSC amplitude increases in maturing calyces. Also inactivation and recovery from inactivation speeds up during development, these factors together suggest enhancement in coupling efficacy (Yang and Wang, 2006). Change in Ca^{2+} channel contribution from N-, R-, P-type to mostly P-type from around P10 in rats (Forsythe et al., 1998) is responsible for short lasting up to 100ms Ca^{2+} - dependent facilitation observed in maturing calyces (Borst and Sakmann, 1998; Cuttle et al., 1998). The increase in calyx physiological capabilities coincides with the finding, using fluorescent confocal microscopy and EM, that SVs clusters and AZs are organized in "donut"-like assemblies of ~1 μm in diameter (Wimmer et al., 2006). These "donuts" only appear during maturation at the time of the ear canal opening P11/12 (Blatchley et al., 1987; Geal-Dor et al., 1993). Such arrangement might reflect microstructural

optimization of the release apparatus leading to increased efficacy of the synapse. Described developmental phases ranging from P2 to P14 are characterized with high variability of calyceal structures including immature to very mature morphologies. The structural development of the calyx at P21 is probably complete although there is not much of the ultrastructural comparative study covering this age. The functional state of P21 calyx remains unknown, since due to an increase in myelination, the pre- and postsynaptic patch-clamp study becomes very hard if not impossible as of today.

1. 2. 3 Neurotransmitter release

At the ultrastructural level, electron microscopic (EM) study have shown that individual active zones of the calyx of Held are similar to those of conventional small nerve terminals. An EM reconstruction of an entire P9 calyx has shown that there is ~ 600 AZs per calyx located at an average nearest-neighbour distance of 0.6μm. An average active zone surface area has been shown to be 0.1μm^2 (Saetzler et al., 2002). Another study has shown that the extrapolated number of AZs increases from ~300 at P5 to ~680 at P14 (Taschenberger et al., 2002). All the AZs create something like parallel release sites each with its own Ca^{2+} channels clusters (model prediction Meinrenken et al., 2002; experimental work Wadel et al., 2007). Each release site experiences a local increase in Ca^{2+} concentration resulting in a microdomain with a Ca^{2+} gradient depending on the distance from the AZs. Incoming AP causes elevation of the Ca^{2+} concentration in the presynaptic compartment and triggers SVs fusion with the presynaptic membrane and neurotransmitter release. At the rat P8-P10 calyx influx of Ca^{2+} creates a microdomain in which Ca^{2+} concentration reaches 10μM (Bollmann et al., 2000) or 25μM when measured using a different method (Schneggenburger and Neher, 2000). The distance between calcium channels and SVs has not been directly measured. There are models that predict that about ten Ca^{2+} channels influence release within a microdomain of ~200nm (Meinrenken et al., 2003). Research on the developmental changes of Ca^{2+} influx triggering SVs fusion indicated tighter spatial coupling between the Ca^{2+} channels and sites of synaptic release (Fedchyshyn and Wang, 2005) in the older animals (P16-P18) as compared to younger (P8-P12). Calcium sensors, are located within the Ca^{2+} microdomains, which within ~300μs (Bollmann and Sakmann, 2005) gradually spreads over the surface of the AZ. Synaptic vesicles that are docked to the membrane at the release site are

primed for calcium dependent fusion, so that when Ca^{2+} concentration is elevated SVs immediately fuse with the presynaptic membrane and the neurotransmitter glutamate is released to the synaptic cleft. The gradient of Ca^{2+} in microdomains is responsible for different release probability of those docked readily releasable SVs.

1. 2. 4 Active zone as specialized area of neurotransmitter release

Docked synaptic vesicles are only present at the AZs and therefore transmitter release is restricted to this specific site. This is the first - organizational role of the AZ – a precise alignment of the release site with its postsynaptic counterpart PSD containing neurotransmitter receptors. Formation of AZs in primary hippocampal cultures has been shown to occur as early as at 11 day *in vitro* (div) from "transport packets" a subset of dense core vesicles (Ahmari et al., 2000). Another study (Zhai et al., 2001) described 80 nm Golgi-derived AZs precursor vesicles containing active zone proteins Piccolo and Bassoon. The authors concluded that such Piccolo-Bassoon transport vesicles (PTV) may very well carry all necessary structural components of an AZ. Considering the surface of a single granulated vesicle they approximated that single PTV would, after fusion with the presynaptic membrane, establish ~3-4 release sites. The docking site of the SV is its most likely fusion site, and the concentration of docking sites within AZ and the size of AZ most likely define the number of SVs docked at the AZ. EM studies in which the AZ surface was measured noted very large coefficient of variation. This could suggest either that the mechanism defining the size of AZs is quite inaccurate or that the size of AZs provides ready space for probably mobile release sites that have to be well aligned with postsynaptic spots of densely packed receptors.

1. 3 Molecular organization of the active zone

The active zone morphologically is a partition of presynaptic plasma membrane with a set of proteins probably necessary for the organization of exo- and endocytotic molecular machineries relative to each other and the presynaptic plasma membrane. Also, AZ proteins are thought to be involved in anchoring plasma membrane proteins, e.g. voltage gated Ca^{2+} channels, or cell adhesion molecules.

1. 3. 1 Active zone proteins

Most of the proteins present in the active zone can also be found in other cellular compartments. These proteins can be divided based on their function at the active zone into: 1) fusing SVs with the plasma membrane e.g. syntaxin, SNAP-25; 2) scaffolding proteins like CASK, Mint, SAP97 and Velis/MALS; 3) cytoskeletal proteins, e.g. actin, tubulin, myosin, spectrin and beta-catenin; 4) voltage gated Ca^{2+} channels; 5) cell adhesion molecules e.g. neurexins, cadherins. Proteins specific for the AZs belong to seven families: Munc13, RIMs, ELKS/CAST/ERC, Bassoon, Piccolo/Aczonin, Liprin-α, and RIM-BPs (RIM-binding proteins) (Schoch and Gundelfinger, 2006). These multidomain proteins are thought to be directly involved in scaffolding of the AZ, and indirectly via their interacting partners, in mechanisms underlying neurotransmitter release. Interaction partners of Bassoon and Piccolo as well as other AZ proteins are depicted in Fig.1.1.

In vertebrates there are four isoforms of Munc13 (1 to 4, with Munc13-2 having further two isoforms, one ubiquitously and one brain expressed (Betz et al., 2001). Munc13 proteins are necessary for priming – preparing SVs for Ca^{2+} - dependent fusion. In vitro Munc13-1 binds syntaxin (Betz et al., 1997) therefore its thought to promote formation of the SNARE complex.

RIMs (Rab3-interacting molecule) have six isoforms (RIM1α, RIM2α, RIM2β, RIM2γ, RIM3γ, RIM4γ) (Wang et al., 1997, 2000; Wang and Sudhof 2003). RIMs have been found to interact with ~10 different proteins (for the review see Schoch and Gundelfinger, 2006). Through these interactions diverse functions of RIMs are proposed, e.g. scaffolding, stabilization, calcium-dependent plasticity, cytoskeleton anchoring and regulation, SVs priming, SNARE complex regulation, presynaptic long-term plasticity and many others.

Total of two proteins belong to ELKS/CAST/ERC family. ELKS1 protein has two isoforms: ELKS1A and ELKS1B and ELKS2 protein is present in one isoform. The expression of ELKS1B and ELKS2 proteins starts within embryonic development (~E14) and is restricted to the brain, while the ELKS1A is exclusively synthesized outside the brain early during development (Wang et al., 2002). The ELKS1B and ELKS2 interact with RIMs (Ohtsuka et al., 2002; Wang et al., 2002) and Piccolo/Aczonin and Bassoon (Takao-Rikitsu et al., 2004) among other interacting partners. Study of the ELKS2 deletion mutants in cultured neurons

suggested that ELKS is necessary to localize RIM at the AZ (Ohtsuka et al., 2002). However, a study using *C.elegans*, that was missing ELKS homolog, showed that ELKS was not necessary for RIM to localize to the AZ (Deken et al., 2005). Whether ELKS play a different role in synaptic transmission in *C.elegans* than in mammals is not yet known.

Bassoon (tom Dieck et al., 1998) and Piccolo/Aczonin (Cases-Langhoff et al., 1996; Fenster et al., 2000; Wang et al., 1999) are structurally related and are the largest known AZ-specific proteins (420kDa and 530kDa respectively). They are not evolutionary conserved in worms and flies, but are only present in vertebrates. Bassoon and Piccolo are indicated in scaffolding functions within the AZ. Spatially restricted to the AZ they together with RIMs, Munc13 and ELKS appear to have an organizational function mostly due to their multidomain capability of interaction with many other proteins (tom Dieck et al. 2005; Takao-Rikitsu et al. 2004; Fenster et al. 2003). Bassoon and Piccolo occur at excitatory and inhibitory CNS synapses but not in cholinergic synapses (Cases-Langhoff et al., 1996; Fenster et al., 2000; tom Dieck et al., 1998; Richter et al., 1999; Brandstatter et al., 1999). In primary cultures of hippocampal neurons both of the proteins colocalize at a majority of the synapses (Fenster et al., 2000; tom Dieck et al., 1998). However in the inner plexiform layer (IPL) of the retina, Bassoon and Piccolo have been found not to colocalize at all conventional synapses. Rather, Bassoon expression at GABA-ergic synapses is higher than that of Piccolo (Dick et al., 2001).

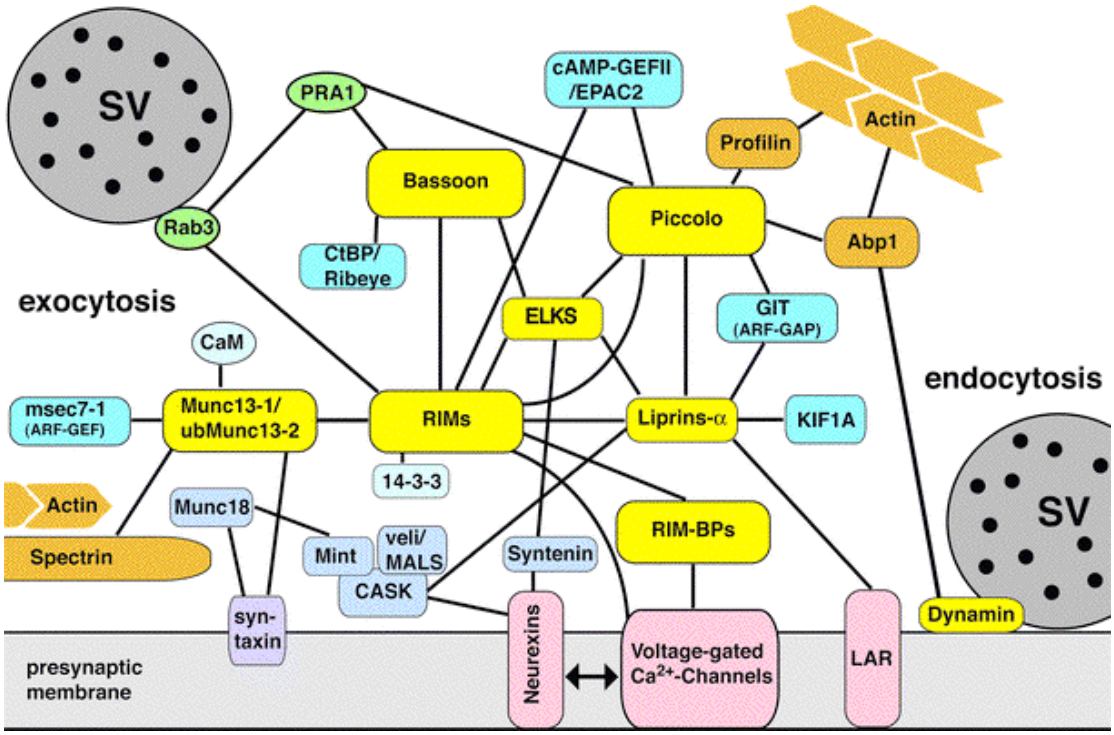

Fig.1.1: Schematic diagram of interactions of CAZ proteins and the resulting network at the active zone. The binding partners of all members of individual families are presented. *SV* synaptic vesicle, Abp actin binding protein, *ARF-GEF* ADP-ribosylation factor guanine nucleotide exchange factors, CaM calmodulin, *cAMP-GEFII* cAMP-dependent guanine nucleotide exchange factors, *CASK* a scaffolding protein *CtBPs* C-terminal-binding protein/connected to Bassoon and Piccolo, *GIT* G-protein-coupled receptor kinase interactor, KIF1A kinesin motor, *LAR* leukocyte common antigen-related receptor tyrosine phosphatase, *RIM-BPs* RIM-binding proteins) (from Schoch and Gundelfinger, 2006).

1. 3. 2 Bassoon

Structurally, Bassoon consists of two Zn^{2+} finger domains and three coiled coil (CC) domains. Post-translational modification adds myristoylate to the N-terminal of Bassoon (Dresbach et al., 2003). Interacting proteins for Bassoon are ELKS via the third CC domain of Bassoon (Takao-Rikitsu et al., 2004) and two members from family of CtBP (C-terminal binding protein) (tom Dieck et al., 2005).

Bassoon cDNA clone sap7f was found by screening λgt11 expression library with polyclonal antibodies generated against rat brain synaptic junction preparation. The cDNA clone sap7f (733bp) was later used for production of monoclonal antibody against Bassoon (tom Dieck et al., 1998). On western blot sap7f detects two major protein bands of > 400 and 350kDa. However, Northern blot analysis of RNA transcripts from different brain regions did not detect additional Bassoon transcripts. The authors concluded that smaller polypeptides visible on the Western blot are

products of proteolytic degradation and not alternatively spliced variants (tom Dieck et al., 1998). An EM immunogold analysis using sap7f antibody against Bassoon found gold particles between SVs and in close proximity - at about one synaptic vesicle diameter - distance from active zone in synaptosomal preparations, mossy fiber terminals in hippocampal CA3 region and in ribbon synapses (tom Dieck et al., 1998; Zhang et al, 2000, Brandstatter et al, 1999). In situ hybridization showed high levels of Bassoon transcripts in hippocampus and the cerebellum (tom Dieck et al., 1998) of the P30 rat brain. Developmental analysis (Zhai et al., 2000) of Bassoon mRNA using Northern blot method shown that it is synthesized as early as by E19 (total brain extract), and that its expression increases significantly until P10-P20 and reaches final adult level by ~ P40. Using in situ hybridization authors have shown that the peak expression of Bassoon in hippocampus occurs at P21, which is the time of neuronal differentiation and synaptogenesis. Bassoon protein is seen in the hippocampal primary culture as early as synaptotagmin1 at div2 (day *in vitro* 2) (Zhai et al., 2000). Elimination of the central region of Bassoon was used to create knock out (KO) mice (BsnΔEx4/5). The central region (between 1692 – 3263aa) is known to be essential for CAZ association of Bassoon (Dresbach et al., 2003). Physiologically, Bassoon deficient mice display significantly weaker synaptic depression during stimulus application in CA1 (*cornu Ammonis*) pyramidal cells and the number of active synapses is significantly reduced in KO neurons as compared to WT. Structurally, mutant hippocampal synapses look normal as evaluated with EM (Altrock et al., 2003). However, unlike in hippocampus, in the retina, lack of Bassoon disturbs formation of functional photoreceptor ribbon synapses because ribbons do not attach to the presynaptic membrane, but instead float in the cytoplasm (tom Dieck et al., 2005). Interestingly, in the Bassoon KO mice amounts of other CAZ proteins, like Munc13 and RIM remain unchanged but Piccolo protein level was up regulated 1.4 fold compared to WT.

Phenotypically Bassoon -/- mutant mice develop spontaneous epileptic seizures (Altrock et al., 2003). Anatomical characterization of Bassoon KO mice using Manganese-enhanced magnetic resonance imaging (ME-MRI) showed a marked increase in total brain volume as compared to WT. Also, disturbed formation of normal basal cortical activation patterns was found (Angenstein, et al., 2006). These two recent characteristics might indicate disturbed balance of excitatory and

inhibitory inputs. Recent metabonomic study using H-nuclear magnetic resonance (H-NMR) spectroscopy, focused on metabolic changes in the mice lacking functional Bassoon. The authors demonstrated cortex-layer dependent alterations in the ratio between neurons and glia cells. Furthermore, the authors observed metabolic disturbances in the glutamine-glutamate and N-acetyl aspartate (a neuron-associated metabolite, for a review see Baslow 2003) metabolism in the cortex and hippocampus but not in the cerebellum (Angenstein et al., 2007).

1. 3. 2 Piccolo/Aczonin

Piccolo/Aczonin consists of ten regions of high sequence similarity to the regions found in Bassoon. These regions are called Piccolo Bassoon homology domains (PBH). They include two zinc finger domains, and three CC domains. Piccolo but not Bassoon also has a PDZ-domain and two C2-domains (C2A and C2B) in its C-terminal region. The N-terminal has proline-rich Q-domain. Piccolo has been found as a result of screening of the components of the rat synaptic junction preparations (Cases-Langhoff et al., 1996). Screening chicken brain expression library with rabbit polyclonal antibodies against chicken brain synaptic plasma membranes lead to discovery of Aczonin. Aczonin is a chicken ortholog (same protein found in different species) of rat Piccolo. Piccolo has multiple splice variants with two manifesting by presence or absence of C2B-domain and resulting in short or long variants of Piccolo (Wang et al., 1999). Piccolo with its C-terminal C2A and C2B domains is the only known low-affinity Ca^{2+} sensor at the synapse (Gerber et al., 2001). Piccolo C2A domain is similar to synaptotagmin and other proteins C2-domains. However properties of Piccolo C2A domain calcium binding differs from those of C2-domain found in synaptotagmin. Piccolo C2A-domain binds Ca^{2+} with low affinity but high specificity. Binding of calcium to Piccolo C2A-domain evokes major conformational change in the entire domain (Gerber et al., 2001). Furthermore Piccolo C2A-domain also exists in two splice variants, with or without a short nine-residues sequence (Garcia et al., 2004). Depending on the splice variant, biophysical and biochemical properties of Piccolo C2A-domain differ. Lack of the nine-residues sequence increases Ca^{2+} affinity of the C2A-domain. Such unusual splice controlled C2A-calcium binding domain indicates possible role for Piccolo in signaling events.

Like Bassoon, Piccolo also interacts with ELKS via its third CC domain as well as with CtBP1 and CtBP2. Unique for Piccolo is the region between the first and second CC domain, which interacts with G-protein-coupled receptor kinase interactor (GIT) proteins. GIT proteins have been indicated in multiple functions such as reorganization of the actin cytoskeleton, membrane trafficking, and endocytosis (Kim et al., 2003). Piccolo functions inferred from its interacting partners are summarized below.

ELKS (Takao-Rikitsu et al. 2004)	Scaffolding
Abp1 - (actin-binding protein) (Fenster et al. 2003)	actin binding, endocytosis
PRA1 (Fenster et al. 2000)	actin binding, endocytosis
GIT (ARF-GAP) (Kim et al. 2003)	membrane trafficking
Profilin (actin binding protein) (Wang et al. 1999)	actin regulation
cAMP-GEFII (Shibasaki et al. 2004)	insulin secretion
RIMs (Shibasaki et al. 2004)	scaffolding
Piccolo (Shibasaki et al. 2004)	scaffolding

Table 1.1: Piccolo/Aczonin - interacting partners. Various binding partners of Piccolo (left column) suggest multiple functions in which Piccolo might be involved (right column).

In summary Bassoon and Piccolo are involved in AZs formation and possibly in synaptic neurotransmitter release. Also in most of the synapses they co-exist and very likely are able to take over each other function. However the exact Bassoon and Piccolo localization within synapse compartments, developmental change in the protein content and their functional significance at individual synapse are not known.

1. 4 Strategies of localizing proteins in tissue

All approaches to localization of endogenous proteins are based on antibody binding to its specific antigen. Protein can be detected in the sample that has been homogenized, or identified in an intact tissue (*in situ*). For homogenate, a wide variety of techniques are available e.g. electrophoretic separation and detection on Western blot with all its high throughput versions, or enzyme-linked immunosorbent assay (ELISA) if a protein is in the liquid solution and antibody immobilized to a

solid support. Alternatively, if it is a fixed cell that constitutes a support and antibody is in the solution. Methods based on tissue homogenization offer quantitative information about the protein presence in particular, tested regions. On the other hand, methods that preserve cellular entity of the sample are better for localization of the protein in its natural place of occurrence. Such localization methods are still based on antibodies typically applied on primary cell cultures, organotypic cultures or tissue slices. Direct and indirect methods of immuno-detection are available. The first method is based on labeled primary antibody binding specifically to its antigen, while the second method utilizes sandwiching effect of secondary antibody binding to an antigen-bound primary antibody. For the fluorescent detection the indirect method increases the number of fluorescent molecules per antigen. Also allows for colocalization of multiple proteins using different fluorescent molecules. Fluorochromes emit visible light after excitation with light of the shorter wavelength than the one they emit. There are fluorochromes emitting lights at wide range of visible spectrum and beyond it. None-fluorescent detection mostly utilizes enzymes as labels of the antibodies, e.g. horseradish peroxidase or alkaline phosphatase. Chromogen substrate for the enzyme forms darker precipitates in the site of reaction, that is at the site of antibody bound to antigen, one of the commonly used substrates is 3'-diaminobenzidine tetrahydrochloride (DAB).

In this work, we used indirect fluorescent immunohistochemical detection of the antigens, because we were interested in the specific localization of the proteins within confined area of individual synapse. Moreover we wanted to describe position of detected antigens relative to other fluorescently labeled structures.

1. 5 Molecular perturbation technologies

Complexes of proteins interacting with each other in their natural environment underlie various cell functions. Understanding protein interactions in situ is based on elimination of a single protein from the complex and analysis of the functional outcome at the cellular, network or behavioral level. In an ideal scenario only the protein of interest is removed, only in the region (spatially-specific) and at the time frame desired (temporally restricted) by an experimenter. Many techniques leading ultimately to elimination of a protein of interest have been developed. Approaches based on binding and inactivating the functional domain of the protein of interest or its functional target (dominant negative peptides, pharmacological agents, toxins), over-expressing the protein of interest which in some cases results in dominant negative behavior. Additionally genetical approaches, specifically reverse genetic when a gene of the protein of interest is known, but its function is not, are now also available. The latter technologies utilize targeted homologous recombination in embryonic stem cells (Thomas and Capecchi, 1987), which allows for developing mice with a specific mutation. Additionally conditional mutagenesis with use of site-specific DNA recombinase (e.g. Cre-lox inducible system (Rajewsky et al., 1996)) allows for precise and timely manner of switching the gene off. Other techniques are nucleic-acid based approaches that silence gene expression in the sequence specific manner, e.g. antisense oligodeoxyribonucleic acids (ODNs) and ribozymes both techniques are based on chemically modified molecules (for the review see Scherer and Rossi, 2003). The newest addition to the arsenal of methods leading to deactivation of a protein of interest is RNA interfering (RNAi) technique (Hamilton and Baulcombe, 1999). Such RNAi can be delivered to the cell directly in form of short interfering RNA (siRNA) fragments, or expression constructs, or via viral mediator. When naked siRNA is delivered the effect is only transient, however when it is expressed from a vector the effect can be long lasting.

1. 5. 1 RNA interference

Post-transcriptional gene silencing (PTGS) or RNA silencing conceptually introduced during 1990s has been described as specific degradation of a population of homologous RNAs and was first discovered in plants (for review see Vaucheret et al.,

2001). Study of transgene- or virus-induced PTGS in *Arabidopsis* plant found high number of short (21-25 nucleotide (nt)) RNA molecules complementary to both strands of the silenced gene. These short RNAs resulted from processing of a long dsRNA precursor (Hamilton and Baulcombe, 1999). In animals (*Caenorhabditis elegans*) siRNA-mediated interference activity was first described by Fire et al., 1998, the authors have also shown that double stranded RNA (dsRNA) silencing was more potent in silencing an endogenous gene activity than a single stranded RNA. In 2006 Andrew Fire and Craig C. Mello (the first and the last authors respectively) received a Nobel Prize in Physiology or Medicine "for their discovery of RNA interference – gene silencing by double-stranded RNA". In mammalian cell cultures the RNAi pathway has also been described and shown to be inducible by short dsRNA that mimics cell native endonuclease products (Elbashir et al., 2001).

Steps leading to silencing of endogenous mRNA with dsRNA partly overlap with endogenous micro RNA (miRNA) processing machinery (Fig. 1.2). They comprise an enzymatic cleavage of dsRNA into short 21-23nt RNA fragments mediated by enzyme Dicer. These short RNA fragments induce then the RNAi-induced silencing complex (RISC) and RISC cleaves endogenous mRNA, which matches to complementary antisense strain from the short RNA. The usefulness of the technique increased once it was discovered that dsRNA can be effective when derived from stem-loop form of RNA- short hairpin (shRNA) (Paddison et al., 2002) which in turn could be transcribed from DNA vector or virus.

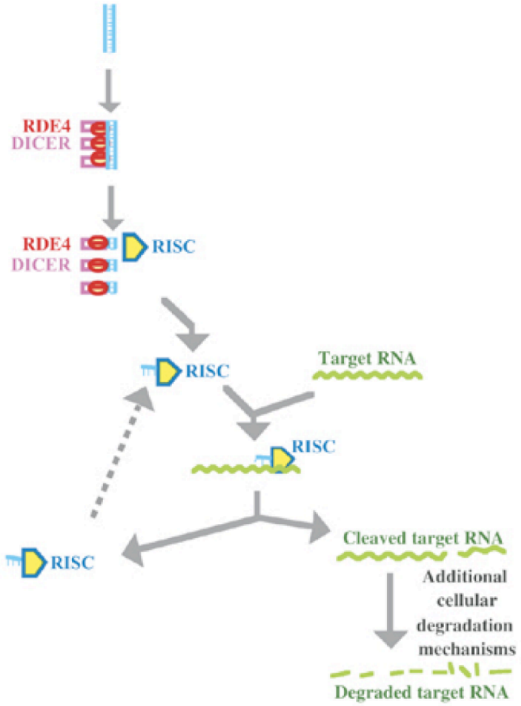

Fig. 1.2: A basic model for the conserved central core mechanism in RNAi. Once long dsRNA enters the cell it is recognized by dsRNA – binding protein and dsRNA-specific nuclease Dicer (RDE4 for *C.elegans*). This enzyme cleaves dsRNA into short dsRNA fragments, which are then inducing RNA-Induced-Silencing Complex (RISC). This complex looks for matching target mRNA sequences in the cell and then cleaves them which ultimately leads to their degradation (from Fire, 2007)

1. 5. 1. 1 Short hairpin RNA *in vivo* down regulation of genes

A transient effect of RNAi in mammalian cell culture can be achieved by transfecting these cells with exogenously generated shRNA. However, for the long lasting effect *in vitro* or for the siRNA effect *in vivo* transcription from DNA vector or virus is necessary. Polymerase III promoters (most commonly used U6, H1, or micro-RNA 7sK) mediate expression of shRNA from DNA vectors. Polymerase III characteristic features such as specific onset position and stretch of five thymidines for termination of transcription allow for generation of precise sequence of shRNA complementary to a fragment of mRNA of interest.

Many attempts of designing rules for selecting the most efficient shRNA has been made and some of the rules have proven valuable over time, while others shown no clear advantages (for an extensive review on designing effective siRNAs see Pei and Tuschl, 2006). Virus mediated delivery of shRNA is the most efficient way of targeting bulk of cells within mammalian organism. It also permits better control over

tissue specificity since many viruses have naturally occurring tropism toward particular cell types, or they can be engineered to reach expected target.

1. 5. 1. 2 Adeno-Associated virus mediated shRNA delivery system

In mammals delivery of shRNA and achieving stable long-term expression was of high interest mainly because of the potential medical application of shRNA in human. Because of this therapeutic potential viruses used should be: a) safe, b) specific, c) with high and long lasting expression and d) easy in production. Adeno-Associated virus fulfills most of these criteria in a manner superior to other viruses. AAV has been found in human as well as simian species with different serotypes being specific for either species. In fact one study have shown that in ~ 80% of human population AAV serotype 2 antibodies are present (Erles et al., 1999). This indicates wide spread of a virus in a population yet so far AAVs have not been associated with any human diseases. AAVs exist in a variety of serotypes that are naturally specific for certain tissues e.g. AAV1 is glia and neurons specific. AAVs are capable of multi particle infection, which potentially sets high number of shRNA copies from the beginning. The amount of shRNA expression however is rather difficult to predict, since it depends on its own promoter efficiency. Once AAV is expressed in a host cell it can remain active for years. Production of recombinant AAV has been significantly simplified and no adenovirus is necessary for AAV formation. Additionally different serotypes can be combined into a hybrid in order to increase infection efficiency and to obtain particular specificity. Such as for example AAV serotypes 1 and 2 can be assembled into a hybrid virus AAV1/2, which has high tropism for neurons and expresses more robustly than single AAV1 serotype.

1. 5. 2 Viral gene transfer

Virus particles expressing gene of interest can be delivered in precisely defined space and time to a living animal. Moreover, in combination with genetically modified mice with conditional mutagenesis, specifically injected viral particles can be used to spatially restrict conditional expression (suppression). Delivering of a various genetically encoded proteins in vivo has served in multiple applications. In anatomical studies expression of genetically encoded fluorescent proteins facilitated

tracing of neuronal projections and visualization of specific types of neurons and their synapses e.g. calyx of Held (Wimmer et al., 2004). Since the discovery of RNA interference and its applicability in a gene down-regulation viral transfer became essential for shRNA long term and tissue specific expression in mammals. In our study we used two very different virus types, namely AAV and sindbis virus.

1. 5. 2. 2 Sindbis virus

Sindbis virus is an alpha virus, a group of mosquitoes –borne viruses and belongs to Togaviridae family. Sindbis produces 40-50nm in diameter virions. Its genome of ~12 kb single, positive-strand RNA virus in encapsulated in icosahedral capsid with lipid envelope. Its genome consists of genes encoding for nonstructural proteins (nsP1-4) and structural proteins capsid and envelope glycoproteins (E1 and E2). Glycoproteins from the envelope mediate viral attachment, entry and fusion with the invaded cell. Sindbis virus shows strong tropism to neurons and high level of infectivity and fast onset of expression within ~ 5 hours after injection. These features together with cloning capacity of ~ 6 kb make Sindbis an excellent tool for delivery and expression of a gene of interest cloned into its genome. Sindbis does however induce cell death (apoptosis) when expression lasts over 24 hours. Also its safety level 2 makes it more difficult to handle. However, in our experiments where developmental analysis is of our interest Sindbis virus with fast onset and high expression is ideal, because it allows for expression analysis in as soon as ~16 hours after injection.

1.5.2.3 Adeno-Assocaciated Virus

Adeno-associate virus - single stranded DNA virus belonging to Parvoviridae family. Wild type AAV requires adeno-virus for productive infection, and thus it is considered naturally defective. Small ~ 20nm AAV virion consists of nonenveloped, icosahedral capsid, and contains linear DNA molecule. Viral genome is short (4681 nt – AAV2) and comprises two genes (*rep* and *cap*) that encode four nonstructural (Rep) and three structural (VP) proteins. The *rep* and *cap* genes are positioned between internal terminal repeats (ITRs) of an AAV genome. ITRs are responsible for packaging of the genome in the viral capsid. In infected cells ITRs are involved in converting single stranded to double stranded DNA, which occurs before the onset of

expression. The fact that ITRs are the only sequences in *cis* position required for successful packaging allowed for creating serotype hybrids by retaining ITRs from one serotype and providing capsid proteins from another. There are 108 AAV serotypes identified so far, 55 were isolated from human and 53 from nonhuman primates (Gao et al., 2004). These serotypes offer wide range of natural targets, such as for example AAV2 with natural tropism to neurons. In this study a chimera of serotype 1 and 2 namely AAV1/2 was used for it retains tropism for neurons, and has increased infectivity level as compared to AAV2 only.

1. 6 Goals of this work

Since we are interested in molecular mechanisms underlying neurotransmitter release, we wanted to investigate developmental changes in the number of AZs at the calyx of Held. Such structural change occurring during calyx maturation could potentially factor in increasing efficiency of the calyx transmission. Two closely related cytoskeletal active zone proteins Bassoon and Piccolo contribute to AZ formation and might in fact represent AZs. Therefore we first aimed to anatomically characterize their developmental changes in distribution and localization in the calyx of Held. Secondly, based on these proteins as active zone markers we expected to quantify potential changes in the active zone content within maturing calyces. Finally, we attempted to down-regulate both Bassoon and Piccolo using Acute Targeted Gene (ATG) transfer technique together with short hairpin RNA expression mediated by AAV1/2 virus and elucidate physiological effects of such perturbation on the calyx of Held. This was necessary because: 1) Bassoon KO have shown inconclusive results possibly due to up regulation of Piccolo expression, 2) double KO of Bassoon and Piccolo does not exist as of today, and 3) such approach allows for direct link between structural changes in the protein involved in AZ formation and the calyx of Held functional output.

2. Results

We are interested in potential contribution of presynaptic active zone proteins Bassoon and Piccolo to morphological changes in maturing calyx of Held. Thus we first describe our novel approach of localizing Bassoon and Piccolo specifically within 3D space of individual calyx. Next we describe localization of those proteins within sub-compartments of the calyx and in relation to SVs clusters, and finally we quantify fluorescent immunohistochemical labeling of Bassoon and Piccolo at two different ages, before (P8-10) and after onset of hearing (P21-25).

2.1 Localization of presynaptic proteins in the calyx of Held

Bassoon and Piccolo fluorescent immunohistochemical (FIHC) clusters created characteristic circular patterns within MNTB (Fig. 2.1 A and B). Outside borders of the MNTB both antibodies FIHC signal appeared in small densely distributed clusters (exemplified by Bassoon staining Fig. 2.1 A – white arrows), reminiscent of a pattern seen in primary hippocampal cultures stained with anti-Bassoon antibody. At the detailed examination we observed that the expected FIHC signal semi circular pattern often appeared as an entire circle (Fig. 2.1 C and D). Furthermore, we observed only a few FIHC clusters present in between the circular patterns, suggesting that only very few synapses did not terminate at the principal cells of the MNTB. We then checked whether such obtained staining allows for discrimination between calyceal and non-calyceal synapses. We used set of antibodies against pre- and postsynaptic proteins to label both parts of the synapse. We used antibody against CASK (belongs to MAGUKs scaffolding proteins family) – known to be present at both pre and postsynaptic compartment. It showed circular patterns, similar to that of Bassoon or Piccolo, but without giving any clue into which fluorescent cluster might be in the calyx (Fig. 2.2 A). Antibody against vesicular glutamate transporter protein (VGLUT1) – synaptic vesicle specific protein, revealed big fluorescent clusters highly reminiscent of a calyx shape, but without really delineating borders of the calyx (Fig. 2.2 B). Fluorescent signal detected after application of antibody against vesicular GABA transporter (VGAT) showed smaller and less abundant clusters that aligned along arched shapes (Fig. 2.2 C). Finally we also tried to visualize postsynaptic

density using an antibody against PSD95, a protein specific for postsynaptic density compartment. This antibody seemed to be not very specific and we only managed to stain tissue of one young (P9) rat (Fig. 2.2 D). Also antibody penetration of the tissue was very low, and we could not use it for adult animals since meylination there is much more profound than in young animals.

Do all the clusters present within circular pattern really belong to only one and the same calyx? Moreover, which FIHC clusters are from the collaterals that are known to be present within MNTB?

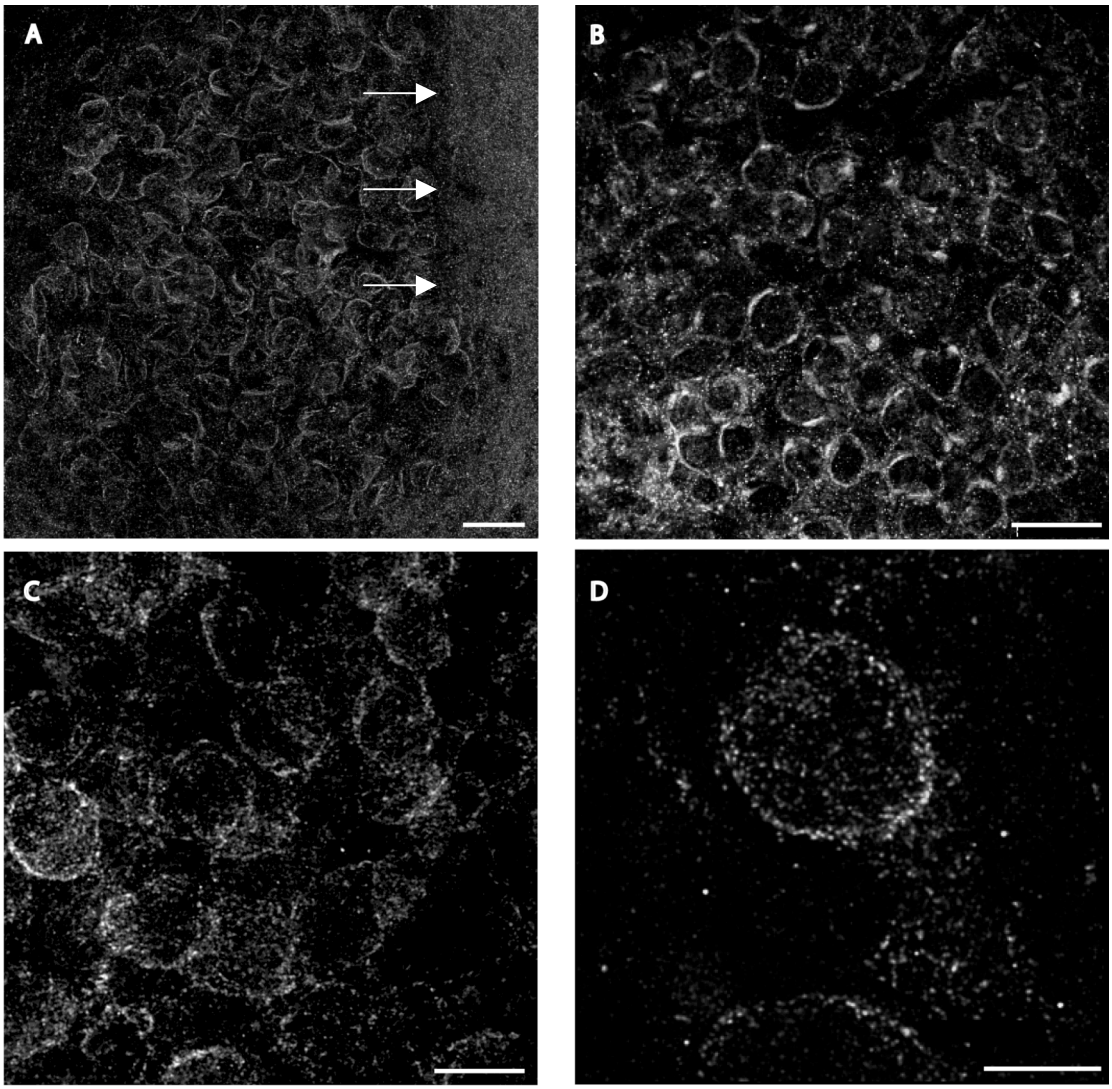

Figure 2.1: Overview of MNTB fragments treated with anti-Bassoon and anti-Piccolo fluorescent immunohistochemistry. A - circles of anti-Bassoon antibody indicate presence of the calyces. Note area outside the MNTB which lacks Bassoon circles – white arrows, rat P9. B - fluorescent immuno-clusters of anti-Piccolo, rat P13, also form circular patterns. C - circular pattern of anti-Bassoon fluorescent signal in higher zoom. Note absence of the fluorescent clusters in the areas between the circles, rat P21. D - highest zoomed circular pattern of anti-Piccolo antibody fluorescent clusters in the MNTB of P18 rat. Images A and C are projections along z-axis from a confocal stack of optical sections; images B and D are top

view of 3 D reconstruction of stack of confocal images. Scale bars: 40μm in A and B, 20μm in C, and 10μm in D.

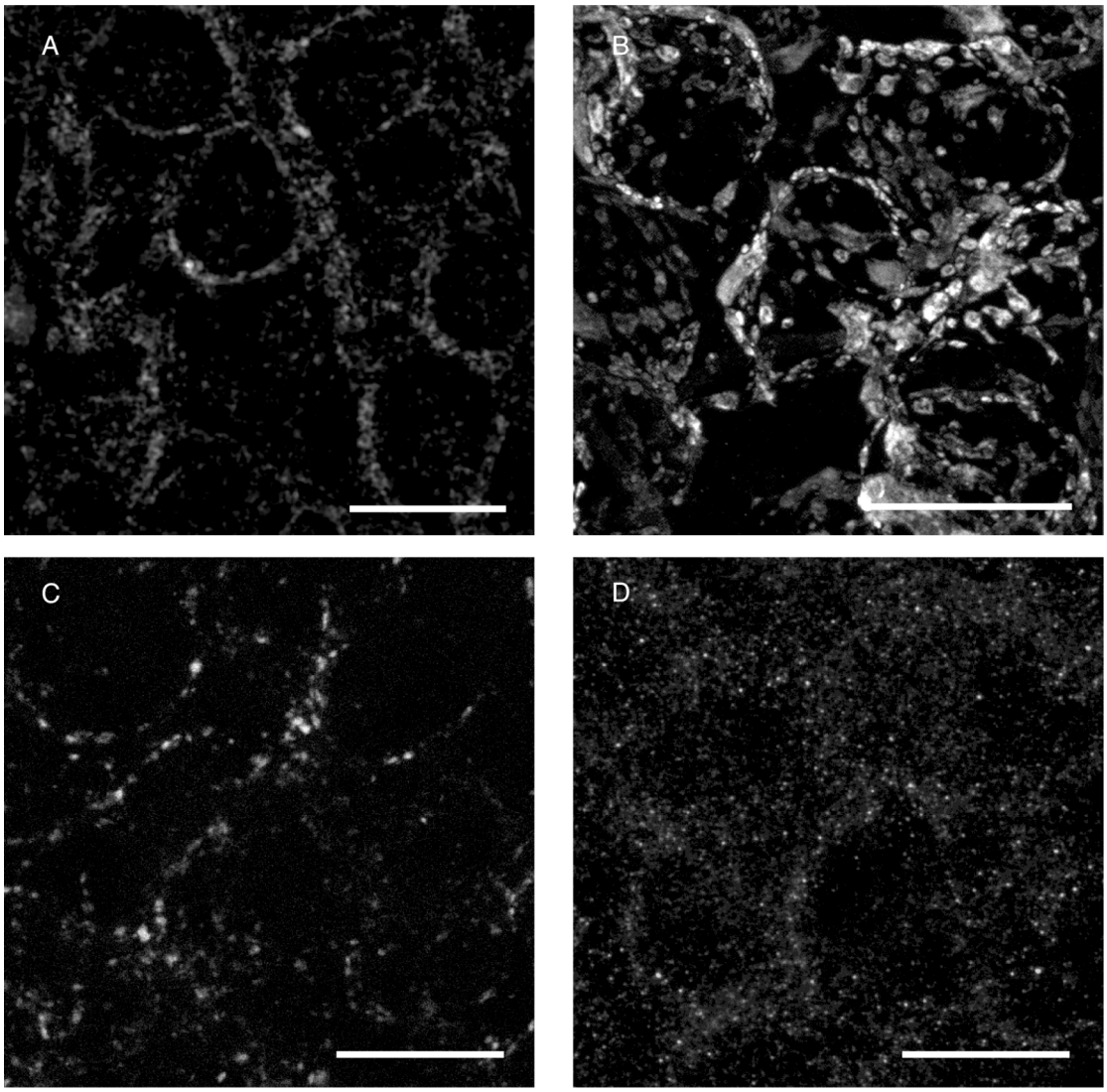

Figure 2.2: Overview of the MNTB fragments processed with various pre- and postsynaptic antibodies. A - FIHC of antibody against synaptic protein CASK, which is characterized as present in both pre- and postsynaptic compartments of contacting neurons. B - FIHC signal from VGLUT1 antibody against vesicular glutamate transporter indicates SVs clusters. C - FIHC signal after treatment with VGAT antibody against vesicular GABA transporter indicates inhibitory synapses. D - FIHC signal from antibody against postsynaptic density protein PSD95. The samples were prepared from: P9 A, D, C, and P11 - B rats. All the images are projections along z-axis from confocal stack. Scale bar 20μm.

2. 2 Labeling of calyx membrane with membrane-bound GFP

To assure calyceal localization of Bassoon and Piccolo fluorescent clusters we labeled calyces with genetically expressed mGFP tag (Fig. 2.3). This labeling revealed great morphological details of calyces at both age groups. We visualized calyces at great

details of individual distinct finger like protrusions in the adult calyces (Fig. 2.3 A). Also in young calyces we could trace many filopodia like extensions and some of them even for a few micrometers (Fig. 2.3 B).

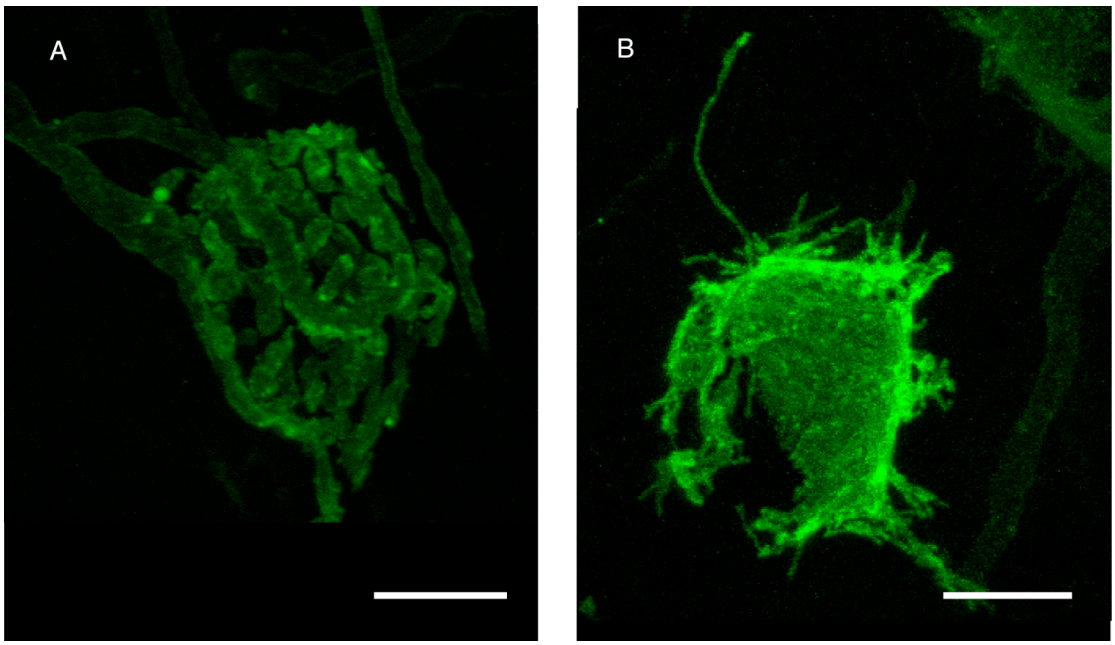

Figure 2. 3: Virus mediated membrane targeted GFP expression in the calyx of Held.
A - adult (P22) typically fenestrated calyx. B - young (P9) solid cup-like shape calyx with characteristic long protrusion. Both images are projections along z-axis from confocal stack of optical slices. Scale bar 10μm.

Furthermore this labeling allowed us to delineate borders of the calyx with precision of a single outer or inner part of the calyx membrane (Fig. 2.4). We have measured fluorescent signal intensity distribution in mGFP labeled calyceal axon (Fig. 2.4 A and B), and found that mGFP labeled membranes appear to be separated from each other by ~ 5μm (Fig. 2.4 C). Similarly using mGFP we could discern inner sub-compartments of the calyx: the membrane of the calyx that faces the principal cell, the cytoplasmic space between the membranes, and the outer membrane away from the principal cell (Fig. 2.4 D and E). Distance between plasma membrane facing principal cell and the outer plasma membrane of the calyx is smaller than that seen in the axon but can also be discerned by fluorescent intensity measurement (Fig. 2.4 F).

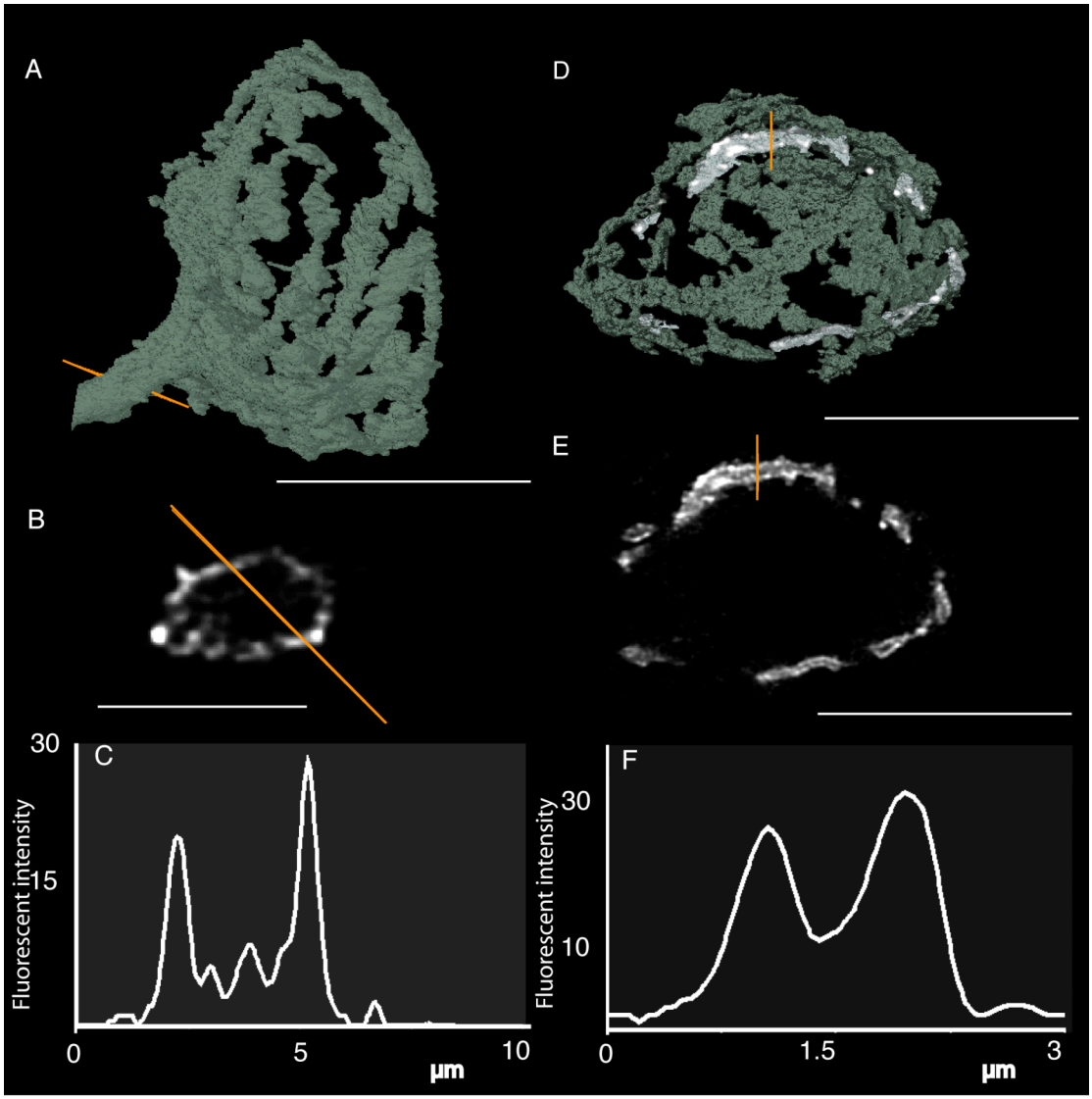

Figure 2.4: In the calyx of Held membrane targeted GFP allows for differentiation between plasma membrane side located toward principle cell of MNTB versus the outer side. A - surface rendered reconstruction of P24 calyx – green with probe line - orange across fragment of an axon. B - single cross section of the axon from A with the probe crossing its diameter. C - histogram of intensities along a probe line from A and B. Note two clearly separated peaks of intensity indicating membranes. D - surface rendered reconstruction of the calyx (same as in A) with top of the calyx removed and probe – orange located across one of the calyceal fingers. E - single cross section of the calyx from A and D with the probe D across calyceal finger. F - histogram of intensities along a probe line from D and E. Note two clearly separated peaks of intensity indicating membranes. Scale bars: 20μm in A, D, E and 5μm in B.

Pre-labeling of calyces with mGFP prompted us to develop an effective approach of isolating fluorescent antibody signal located within the calyx from the one beyond it. Excision of the immuno-labeled signal from the pre-labeled calyces was done via thresholding of the calyx channel and multiplying it by antibody channel (see

Methods, Fig. 2.5 A and B). The outcome of the procedure was a channel with immuno-labeled clusters remained within the calyx area only (Fig. 2. 5C and D).

Since calyces change their shape profoundly during development, it is also likely that their overall size changes. For further quantification of the proteins fluorescent clusters content within calyces it is important to know whether any potential difference in number of clusters could simply be related to different calyx sizes. To establish whether the volume of the calyces between age groups differs, we measured it in surface rendered 3D calyces. In total we measured 12 entire calyces from each age group and compared their average size. We have detected no difference on average size of the calyx between young (P9-P10) and adult (P21-P25) calyces (Fig. 2.6). However we observed large variability of calyx size within age groups.

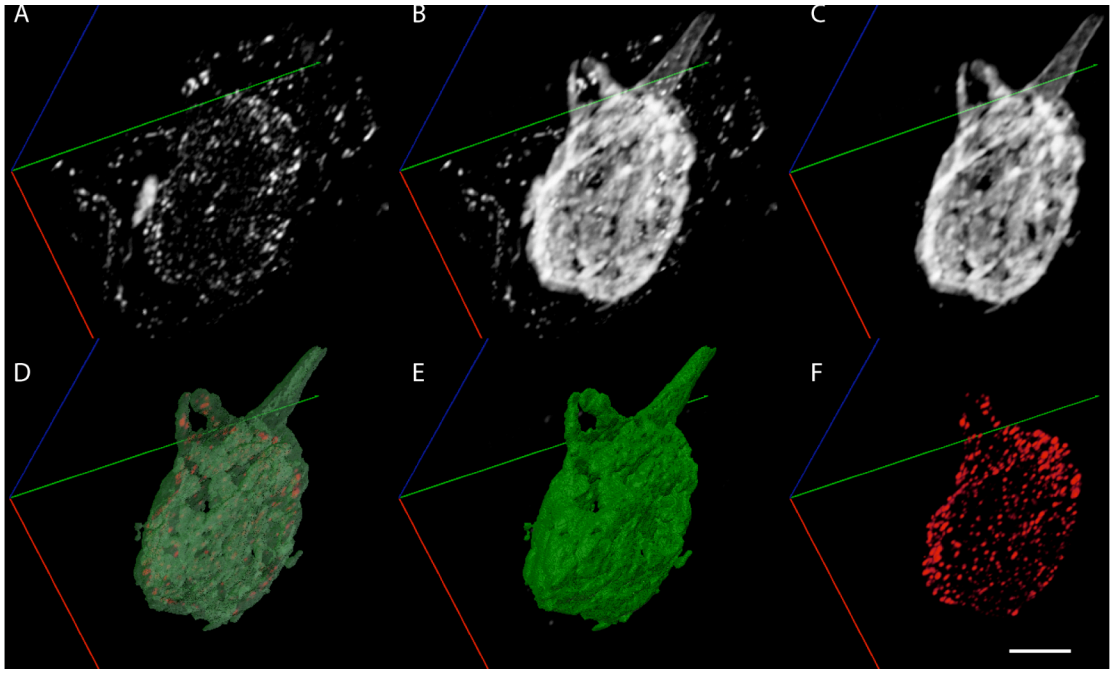

Figure 2.5: Excision of fluorescent immunolabeled Bassoon clusters from the volume of the mGFP labeled calyx.
A - Bassoon channel as seen in 3D reconstruction of confocal scan, immuno-clusters distributed within the entire scanned cube of the tissue, note the circular pattern in the middle of the cube. B - calyx channel overlaid with Bassoon channel. C - calyx has been rendered in 3 D using threshold selection so that calyx was assign value 1 and the rest of this channel content value 0. Having such selected calyx we multiplied Bassoon channel by thresholded calyx channel and in result received Bassoon signal present only within calyx volume. All clusters that did not belong to the calyx were eliminated. D - surface rendered calyx (transparent mode) with red bassoon clusters within its volume. E - surface rendered calyx (shaded mode). F - Bassoon fluorescent immuno-clusters excised from the calyx volume. Scale bar 8µm.

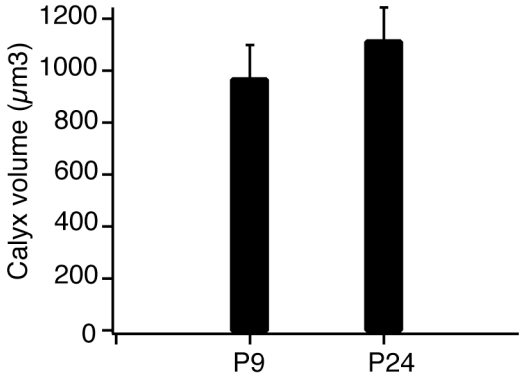

Figure 2. 6: Average volume of the calyx rendered in 3D. Comparison between two age groups shows no statistically significant difference of the calyx volume. However we have observed large variability of sizes within age group (CV for P9 = 0.5, and CV for P24 = 0.4).

2. 3 Localization of Bassoon

For the anatomical description of Bassoon localization and potential distribution changes during calyx maturation we systematically analyzed calyces at young (P8-P10) and adult age (P21-P25). We quantitatively analyzed and compared data from both age ranges.

2. 3. 1 Bassoon in young calyces (P8-P10)

Immunohistochemistry with anti-Bassoon antibody on young calyces revealed fluorescent clusters present on the inner site of the cup-like shape of calyces. Distribution of the fluorescent clusters was rather random within the entire cup-like shaped calyces (Fig. 2.7). Sporadically we observed some Bassoon fluorescent signal in thin protrusions formed extensively by young calyces (Fig. 2.7 A, B arrows). These protrusions may reflect calyceal collaterals. Hence, Bassoon also present in filopodia could indicate potential for AZ forming once a connection with target is established.

Localization of fluorescent clusters inside calyx volume was mainly toward the inner membrane but not overlapping with it (Fig. 2.8). Additionally we observed some fluorescent clusters aligned with the perimeter of a principal cell that did not belong to the calyx (Fig. 2.8 D). Here we see that fire-red fluorescent clusters of Bassoon are present in calyx but also on the opposite site from it, suggesting other synaptic contacts to the principal cell.

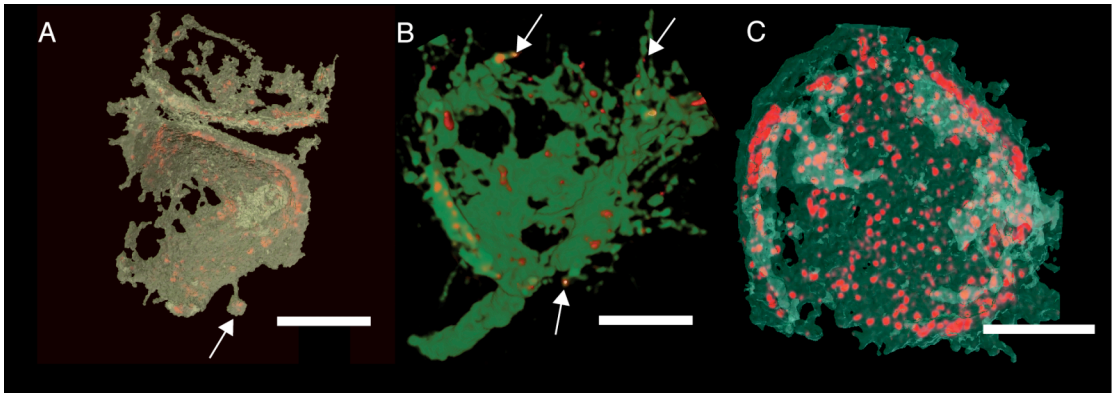

Figure 2. 7: Representative pattern of Bassoon FIHC distribution observed in young calyces.

A - one entire and one partial calyces from P9 rat surface rendered (transparent mode) to visualize Bassoon FIHC on the inner site of the calyx cup. B - calyx from P9 rat reconstructed in 3D (surface not rendered) with Bassoon FIHC surfaced rendered clusters. C - calyx from P8 rat surface rendered (transparent mode) with Bassoon FIHC clusters distributed on the inner, principal cell facing side of the calyx cup. Arrows indicate thin protrusions with FIHC Bassoon. Scale bar 10μm.

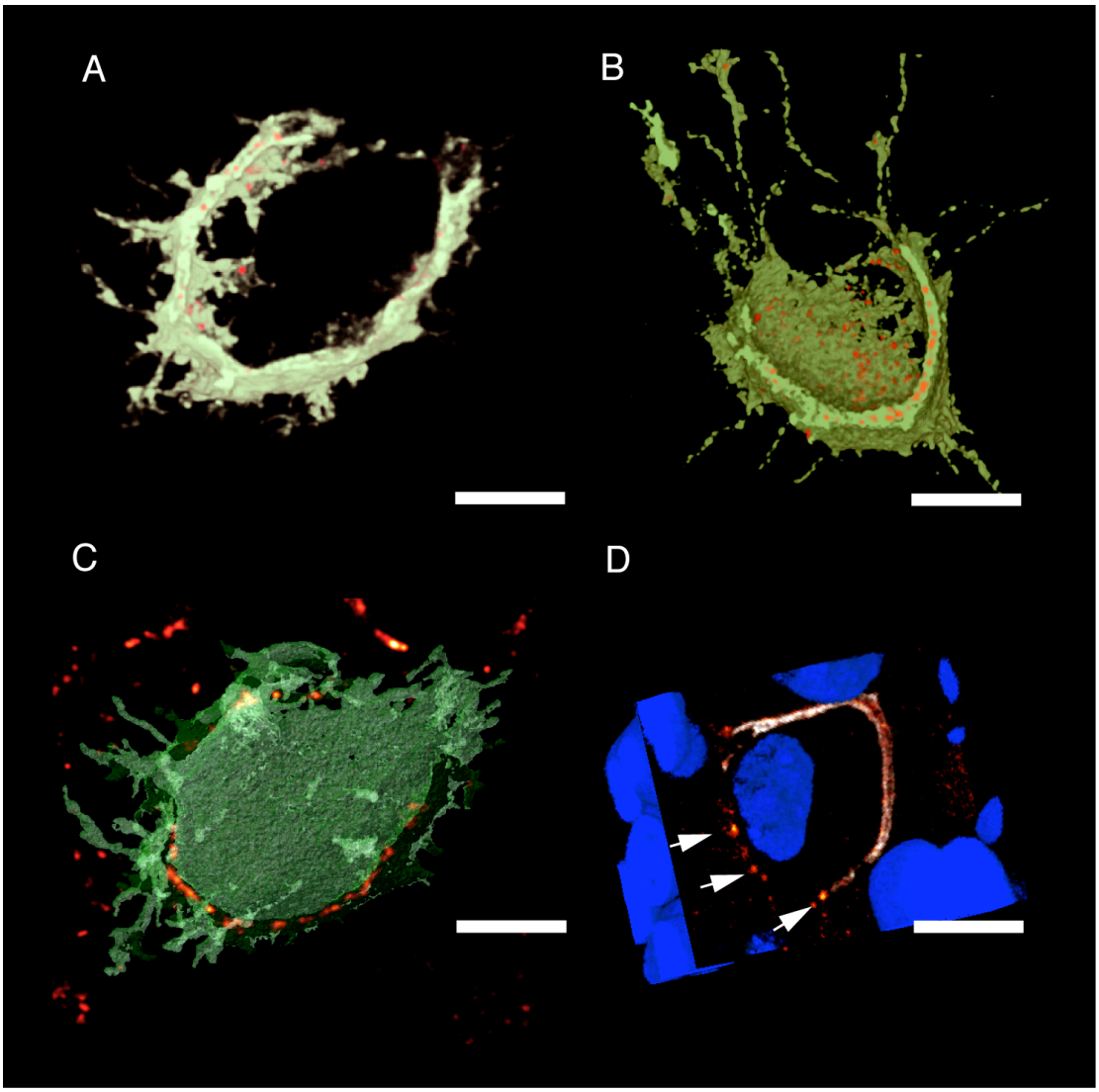

Figure 2. 8: Localization of Bassoon FIHC relative to the calyx plasma membrane labeled with mGFP.
A - cross-section through P9 calyx, the cup part of the calyx is removed to visualize Bassoon FIHC clusters-red within calyx membranes. B - cross cut P9 calyx with the side facing postsynaptic cell exposed. At the cross section of the calyceal membrane Bassoon FIHC clusters. C - transparent cross section to visualize Bassoon FIHC – fire red within single optical section in relation to fully visible 3D calyx of P9 rat. D - single optical section through both P9 calyx - white and Bassoon FIHC clusters – fire red with nuclear DAPI stain labeling nuclei of principle cells – blue. Note that some Bassoon FIHC clusters do not belong to the calyx – arrows. Scale bars 10µm.

2. 3. 2 Bassoon in adult calyces (P21-P25)

Adult calyces are fenestrated, and contain less of continues surfaces as compared to young calyces. Bassoon localization follows this anatomical modification of a calyx and it distributes within finger–like protrusions but without any obvious sub-clustering (Fig. 2.9).

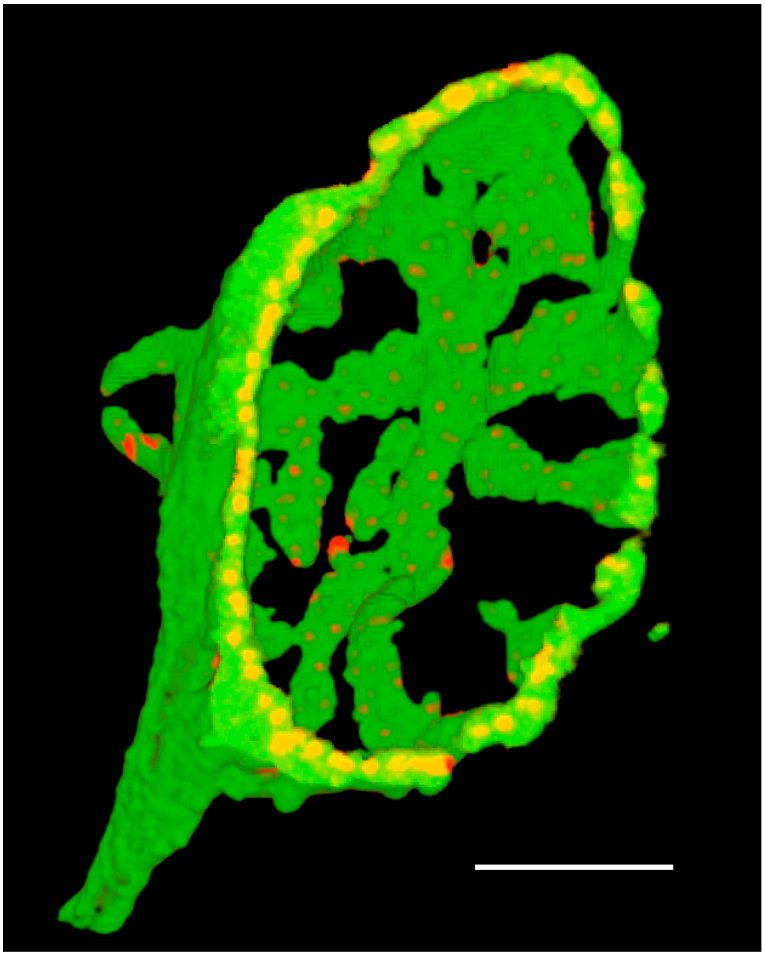

Figure 2. 9 Typical Bassoon fluorescent immunohistochemistry clusters distribution in the adult P24 calyx. Bassoon FIHC clusters-red within the inner site of the calyx, view through absent principal cell of the MNTB. Note Bassoon FIHC clusters on the rim of the cut open calyx – yellow. Calyx and Bassoon clusters shown in 3D reconstruction, surface not rendered. Scale bar 10μm.

The fluorescent signal is clearly located proximal to the membrane of the calyx facing the postsynaptic principal cell (Fig. 2.10). We observed most of Bassoon fluorescent clusters located in the vicinity of the inner membrane of the calyx, along the length of the finger like protrusions (Fig. 2.10 A). Some times we were finding clusters of Bassoon that localized exactly within fluorescently labeled membrane of the calyx. Sporadically we saw clusters that span the space between juxtaposed finger-like protrusions (Fig. 2.10 B) The latter ones most likely represented Bassoon clusters from outside the calyx located so close that our excision method could not resolve the difference.

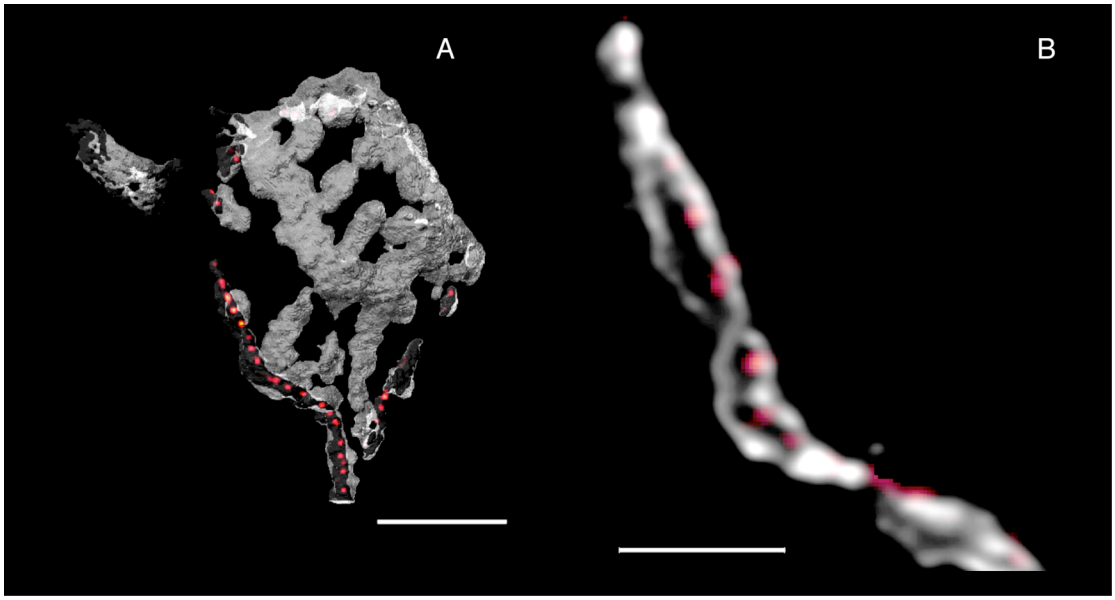

Figure 2. 10: Bassoon signal localizes to the site of the calyx that faces principal cell.
A - three dimensional, surface rendered calyx of P22 rat, cut open to visualize the inner area between plasma membranes. B - single optical section of a zoomed fragment of calyx from A. Fluorescent Immunolabeled clusters of Bassoon – red localize along the inner site of the calyx membrane, and within the membrane. Scale bars 10μm in A and 3μm in B.

The assumption that Bassoon clusters might represent active zones within calyx implies that their localization should correlate with synaptic vesicle clusters. We have checked this by using genetically encoded synaptophysin over-expression together with bassoon fluorescent immuno-labeling. We have observed that indeed synaptic vesicle clusters were mostly located between Bassoon clusters and outer membrane of the calyx. Such that Bassoon clusters would be lying directly at the site of the calyx that faces the principle cell and synaptic vesicles were above them (Fig. 2.11). In general Bassoon fluorescent signal appears closest to the plasma membrane, with clusters of synaptic vesicles filling more distant spaces.

We also observed that fluorescent Bassoon clusters that do not belong to the calyx but align along principal cell perimeter are not VGLUT1 positive (Fig. 2.12 A). These extra-calyceal inputs can be inhibitory as we also saw VGAT-positive labeling in the calyx (Fig. 2.12 B), or excitatory that are, unlike calyx, VLGUT1 negative.

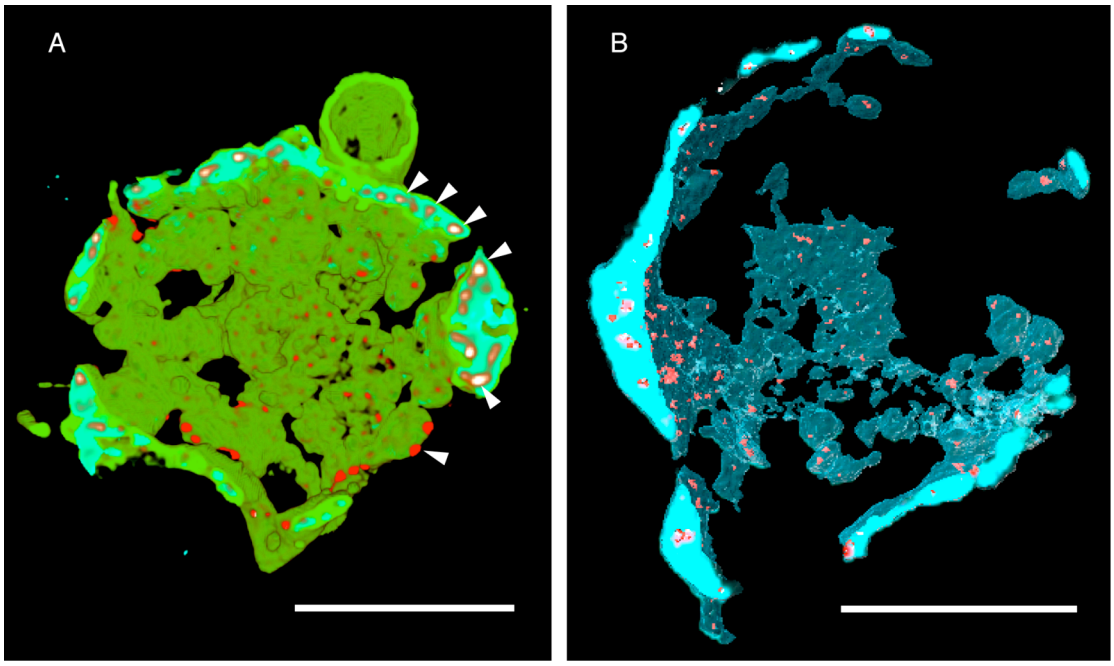

Figure 2. 11: Bassoon fluorescent immuno-signal localizes within volume of synaptic vesicles clusters in the calyx of Held.
A - calyx (P25) in 3D reconstruction with removed top part – light green. Bassoon FIHC signal – red and arrow-heads at the cross section, located within clusters of synaptic vesicles - cyan. Synaptic vesicles are labeled with antibody VGLUT1. B - surface rendered 3D reconstruction (transparent mode) of synaptic vesicle clusters – cyan labeled with genetically expressed synaptophysin in P17 calyx. Fluorescent immuno-signal of bassoon antibody – red shown in surface rendered (shaded mode) 3D reconstruction. Scale bars 10μm.

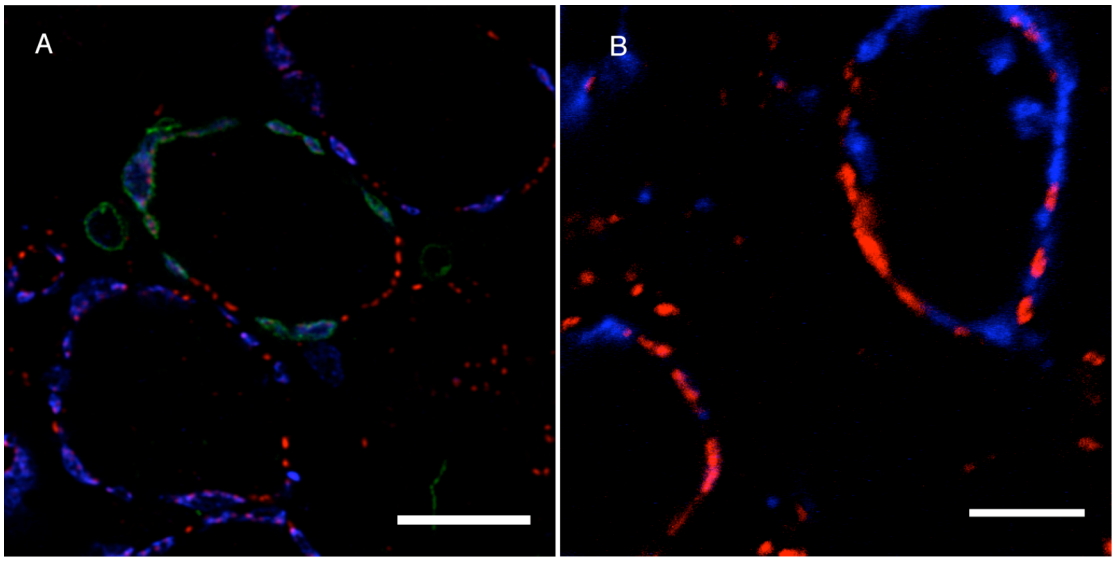

Figure 2. 12: Bassoon FIHC clusters, located outside the calyx aligned with perimeter of the principal cell, belong to VGLUT1 negative synapses and might be inhibitory.
A - calyx of P25 rat labeled with mGFP – green, immunostained for VGLUT1 protein – blue, and Bassoon – red. Note that Bassoon FIHC clusters within calyx localize closer to the membrane facing the postsynaptic cell and clusters of synaptic vesicles are above those of Bassoon. FIHC Bassoon clusters that do not belong to the calyx also do not have VGLUT1 positive clouds of SVs. B - VGLUT1 clusters – blue are interspersed with VGAT positive clusters – red, in P22 calyx. Scale bars: 10μm.

2. 3. 3 Quantification of Bassoon at two developmental stages of calyx

We assumed that a single fluorescent cluster might in fact represent an active zone or two if they are located close to each other. Therefore, we have analyzed the distribution of Bassoon clusters after rendering their surface in three dimensions. We have observed large variability in protein cluster size distribution (Fig. 2.13 A – point marks) within the age group and between the ages. At both ages P24 and P9 fluorescent signal of Bassoon localizes in small clusters 0.066 ± 0.001μm^3 (n=3394) and 0.041 ± 0.001μm^3 (n=1468) respectively. Consistent with similar size distribution between two age groups, also contribution to a total volume of calyx was similar (Fig 2.13 A – bar graph). Bassoon fluorescent clusters contribution was very small and did not differ between P24 and P9 calyces. These clusters occupied on average 0.007 ± 0.001% (n calyces = 6) and 0.006 ± 0.001% (n calyces = 6) of calyx volume at P24 and P9 respectively. Next we looked whether there is a change in total number of Bassoon fluorescent clusters per calyx over time (Fig 2.13 B). We found that number of those clusters per calyx at P24 was higher than at P9 (P = 0.02, unpaired t-test with Welch correction). At P24 we found 378 ± 42 (n=9) clusters and at P9 247 ± 18 (n=6) clusters. Since calyces can differ in size even within the same MNTB and high number of fluorescent clusters may simply reflect bigger calyx, we looked also at the density of Bassoon fluorescent signal within calyx volume (Fig. 2.13 C). In P24 calyx we found 0.3 ± 0.04 (n=6) clusters/μm^3 and in P9 calyx 0.24 ± 0.03 (n=6) clusters/μm^3. Density analysis did not show a statistically significant difference between age groups. Therefore we conclude that Bassoon content within calyx synapse does not change during development at least within the ages analyzed in this work.

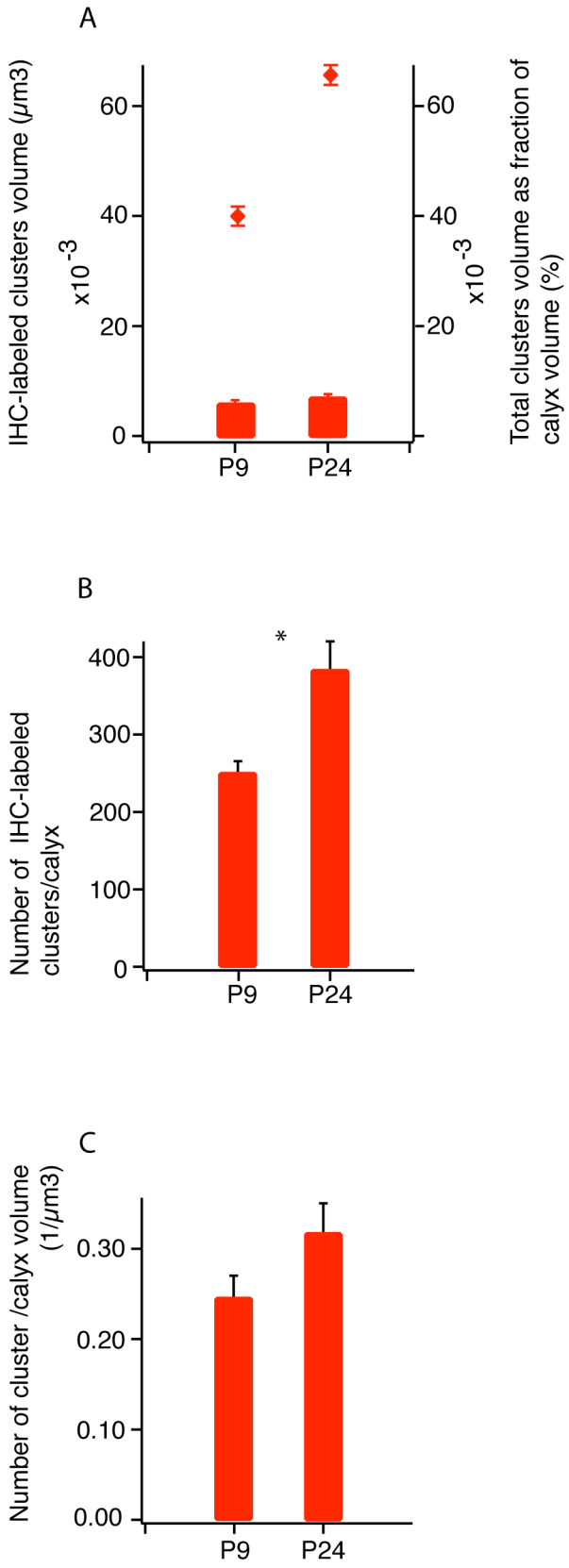

A - volume of Bassoon FIHC clusters isolated from calyces – point markers - (left y-axis). Total Bassoon FIHC clusters volume contribution to the calyx volume (right y-axis).

B - number of FIHC-labeled Bassoon clusters per calyx.

C - density of Bassoon FIHC clusters per calyx volume.

Figure 2. 13 Comparison of Bassoon FIHC, 3D surface-rendered, clusters quantification between two age groups (numbers represent mean ± SEM).

2. 3. 4 Bassoon represents active zones

Bassoon fluorescent clusters are found mostly at the calyx plasma membrane facing the postsynaptic cell. Count of fluorescent signal from immuno-labeling with anti-Bassoon antibody revealed about two fold less clusters than counts of active zones from EM studies. We also observed that immuno-fluorescent clusters tend to align between the calyx membrane and SVs clusters labeled with genetically expressed synaptophysin. Therefore, we suggest that Bassoon FIHC clusters may represent active zones, albeit at the resolution of about two AZs per single FIHC cluster.

2. 4 Localization of Piccolo

Using the same approach as for Bassoon we have analyzed immuno-fluorescent clusters of Piccolo at two developmental stages of the calyx of Held. In young (P8-P10) and adult (P21-P25) calyces we found analyzed parameters very similar to what we saw in the case of Bassoon. The two proteins are known to coexist in many but not all synapses, thus we also looked whether they co-localize in the calyx of Held. We found that Bassoon and Piccolo fluorescent immuno-clusters do indeed coexist within most fluorescent spots (Fig. 2.14). Quantification of both signals based on 3D reconstruction and surface rendering of each cluster revealed co-localization of ~ 90% between Bassoon and Piccolo.

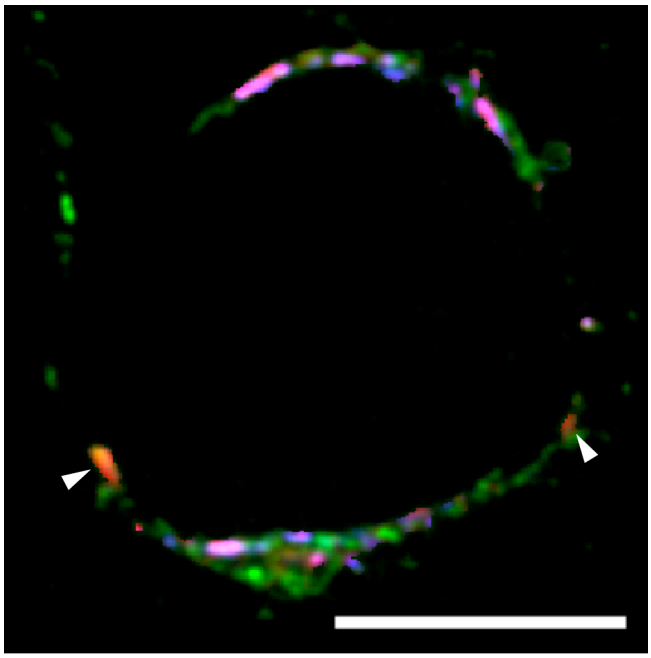

Figure 2. 14: Colocalization of Bassoon and Piccolo FIHC clusters in P9 calyx of Held. In green labeled calyx, Bassoon FIHC clusters – blue co-exist with Piccolo FIHC – red in most but not all of the fluorescent spots. Sites where Piccolo FIHC appears without Bassoon FIHC -arrowheads. Scale bar 10μm.

2. 4. 1 Piccolo in young calyces (P8-P10)

Fluorescent immuno-signal localized rather evenly within a solid area of the cup shaped calyx. Within internal volume of the calyx Piccolo fluorescent labeling was aligned toward the inner site near the plasma membrane closer to a principal cell (Fig. 2.15 A). We also saw some of the fluorescent clusters at axonal collaterals of the calyces (Fig. 2.15 B). Similarly to our observations from Bassoon, some of the fluorescent signal of Piccolo was also aligned at the perimeter of a principal cell but did not belong to the calyx (Fig. 2.16, arrow heads).

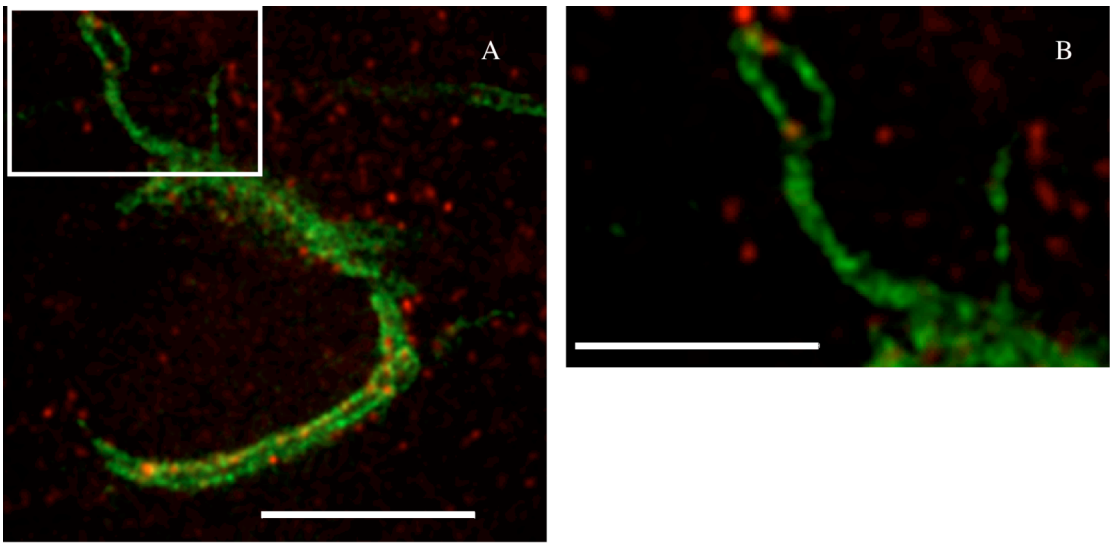

Figure 2. 15: Piccolo FIHC clusters localization in young P9 calyx.
A - in most cases Piccolo FIHC clusters - red align along membrane of the calyx - green that faces postsynaptic principal cell. B - occasionally Piccolo FIHC clusters were present at the distal ends of calyceal protrusions in young calyces. Zoomed view of calyx protrusion from the window marked in A. Scale bars: 10μm in A and 5μm – B.

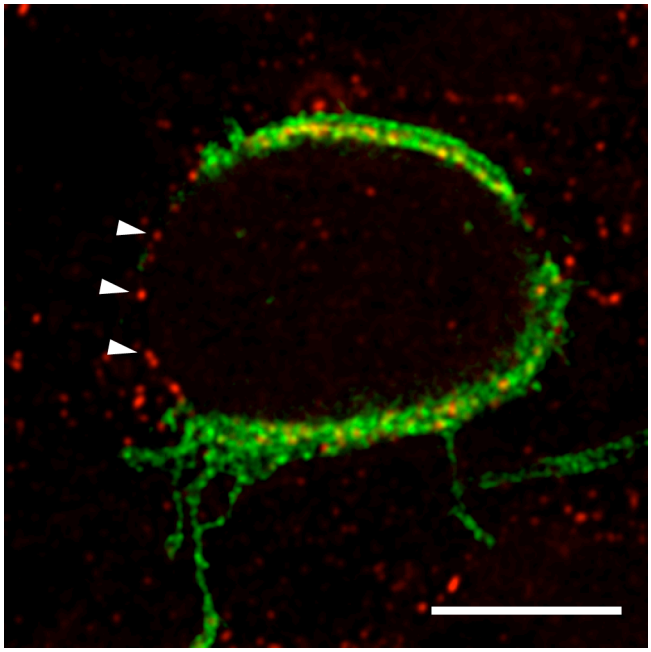

Figure 2. 16: Piccolo FIHC clusters localized within and outside the calyx. Fluorescent clusters align with the principal cell perimeter – arrowheads. Scale bar 10μm.

2. 4. 2 Piccolo in adult calyces (P21-P25)

Like in case of Bassoon clusters, Piccolo immuno-fluorescent signal was found rather evenly distributed within finger-like protrusions of adult fenestrated calyces (Fig.

2.17). No obvious sub-clustering patterns of fluorescent immuno-signal were visible. As it was in the case of young calyces, also in the adults we observed Piccolo fluorescent clusters outside the calyx area but still aligned in semi circle, suggestive of principal cell perimeter (Fig. 2.18 A - arrowheads). Piccolo fluorescent immuno-signal localized closer to the plasma membrane of the calyx that was facing a postsynaptic principal cell of the MNTB (Fig. 2.18 A and B - arrows). To establish localization of Piccolo fluorescent immuno-signal relative to SVs clusters we used genetically expressed synaptophysin together with FIHC. We found that, similarly to Bassoon, also fluorescent Piccolo signal appears to be mostly between calyx plasma membrane and SV clusters (Fig. 2.18 B).

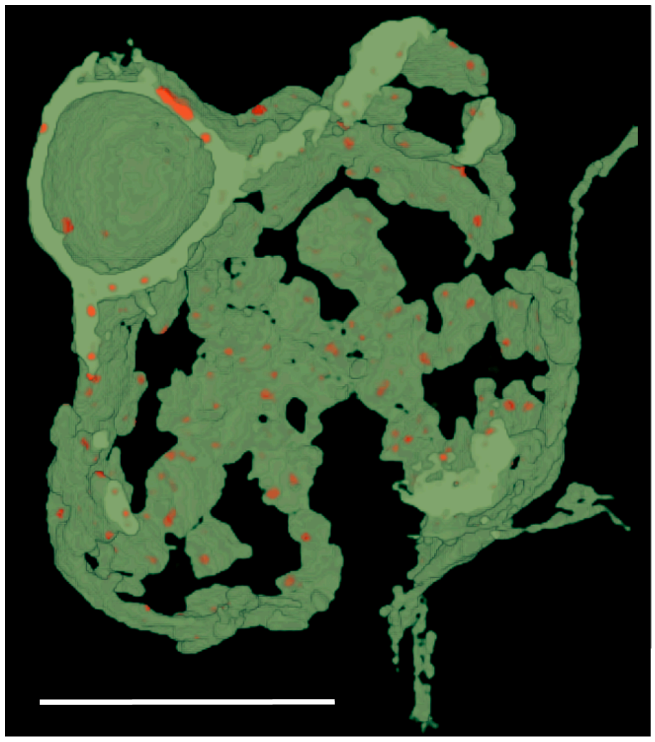

Figure 2. 17: Piccolo FIHC localize evenly within finger-like structures of an adult calyx (P21). Calyx (3D reconstruction) – green cut open to visualize its inner site spotted with Piccolo FIHC clusters – red. Scale bar 10μm.

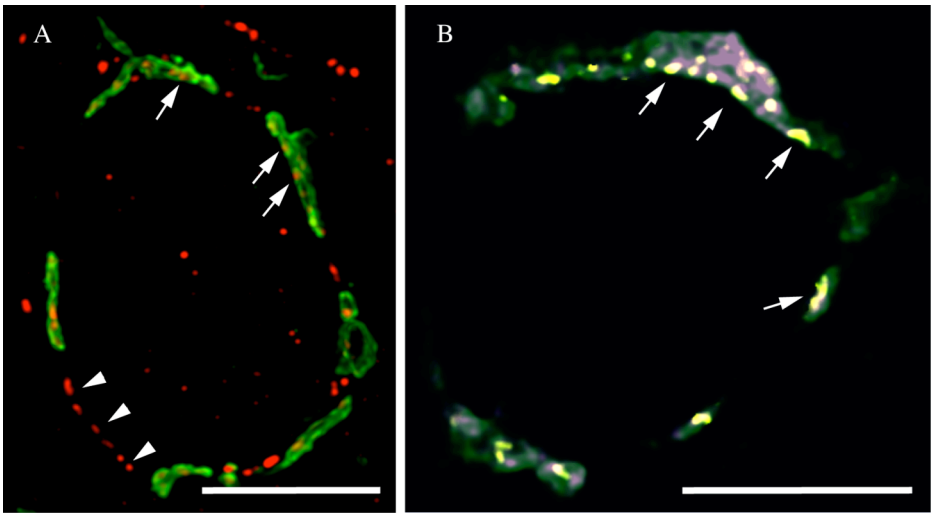

Figure 2. 18: Piccolo FIHC clusters localization within adult calyx (P21).
A - calyx labeled with mGFP – green, with Piccolo FIHC clusters within calyx membranes - arrows, and outside of them but aligned with the principal cell perimeters – arrowheads. B - Piccolo FIHC clusters – yellow localize closer to the membrane facing postsynaptic cell – arrows, with SVs clusters – purple positioned further away from this membrane. Scale bars 10µm in both images.

2. 4. 3 Quantification of Piccolo at two developmental stages of calyx

Similar to Bassoon also for Piccolo fluorescent immuno-labeling we have observed large variability in cluster size distribution (Fig. 2.19 A – left y-axis) within the age group and between the ages. Piccolo average cluster size at P24 was 0.04 ± 0.001μm^3 (n=1883) and similarly at P9 where this value was almost identical 0.05 ± 0.001μm^3 (n=1249). On average Piccolo fluorescent-immuno-clusters were occupying the same amount of calyx volume at P9 0.008 ± 0.003% (n calyces = 6) as at P24 rat 0.005 ± 0.001% (n calyces = 6) (Fig. 2.19 A – right y-axis). To find whether number of fluorescent clusters changes between the two age groups we counted the 3D rendered individual clusters and found no difference between younger and adult calyces. At P9 calyces we detected average of 206 ± 51 (n=6) per calyx and at P24 we found 310 ± 53 (n=6) (Fig. 2.19 B). Density measurements of fluorescent clusters also showed no statistical difference between young and adult calyces. Average Piccolo fluorescent clusters density at P24 calyx was 0.3 ± 0.05 (n=6) clusters/μm^3 versus 0.28 ± 0.03 (n=6) clusters/μm^3 at P9 calyx (Fig. 2.19 D). In conclusion, we found no difference in Piccolo content between young and fully developed calyces. This indicates that Piccolo just like Bassoon does not contribute to developmental changes occurring in the calyx during maturation.

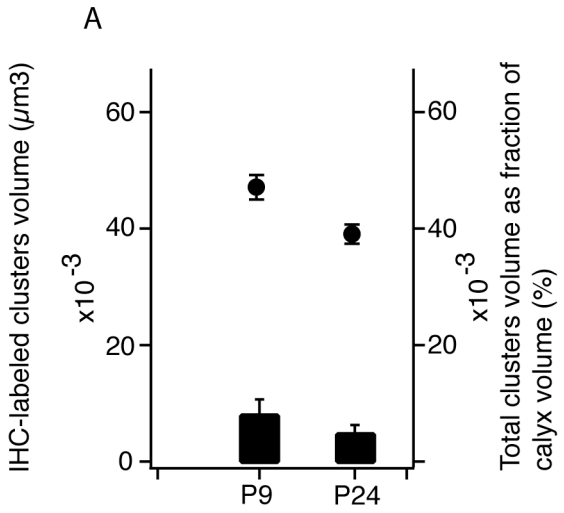

A - volume of Piccolo FIHC clusters isolated from calyces – point markers - (left y-axis).
Total Piccolo FIHC clusters volume contribution to the calyx volume (right y-axis).

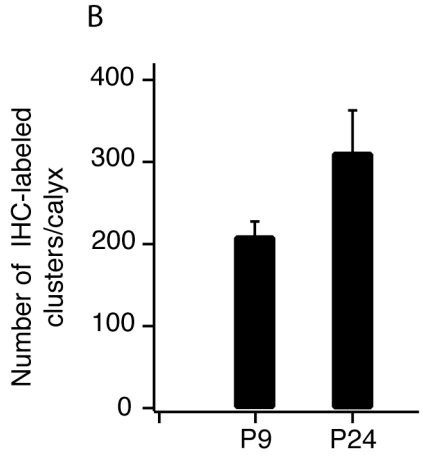

B - number of FIHC-labeled Piccolo clusters per calyx.

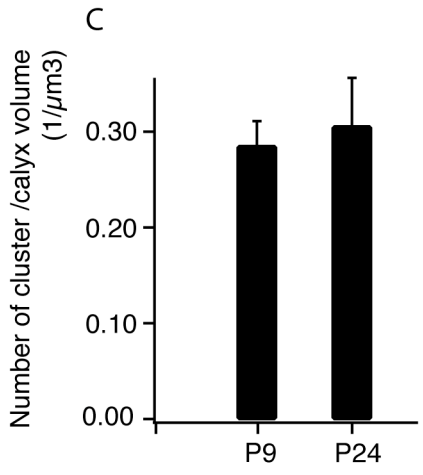

C - density of Piccolo FIHC clusters per calyx volume.

Figure 2. 19 Comparison of Piccolo FIHC, 3D surface-rendered, clusters quantification between two age groups (numbers represent mean ± SEM).

2. 4. 4 Piccolo represents active zones

Pattern of Piccolo distribution as well as specificity of localization relative to synaptic vesicle clusters was very similar to what we observed in fluorescent Bassoon clusters. Colocalization experiments have shown that both proteins co-exist in many (~ 90%) fluorescent spots. In experiments where we labeled SV (see Fig. 2.18) we observed that Piccolo localizes mostly at the membrane of the calyx facing the postsynaptic cell, below SV clusters. Morphological characterization of Piccolo strongly suggests that it indeed might represent AZs.

2. 5 Down-regulation of Bassoon and Piccolo in vivo

We characterized both proteins distribution and localization within the calyx of Held. In this way we established bases for fluorescent immunohistochemichal quantification of down-regulation of Bassoon and Piccolo. We used the short interfering RNA method to down-regulate either of the proteins. To assess down-regulation efficiency we used fluorescent immunohistochemistry on both shRNA treated and control calyces and compared the amount of protein between synapses. This approach involved simultaneous injection of two viruses, one carrying shRNA and also expressing mGFP and the second expressing only mOrange, as a control.

2. 5. 1 Two-step cloning of the shRNA into viral plasmid AAV2

We have developed two-step cloning strategy to insert RNA hairpins into adeno-associated virus serotype 2 (AAV2) plasmid. First, we used commercially available psiRNA plasmid as a shuttle plasmid in which we constructed promoter-shRNA cassette. Next, such prepared cassette was non-directionally inserted into previously prepared AAV2 plasmid (Fig. 2.20). Details about preparatory steps leading to establishing this convenient cloning are described in methods section.

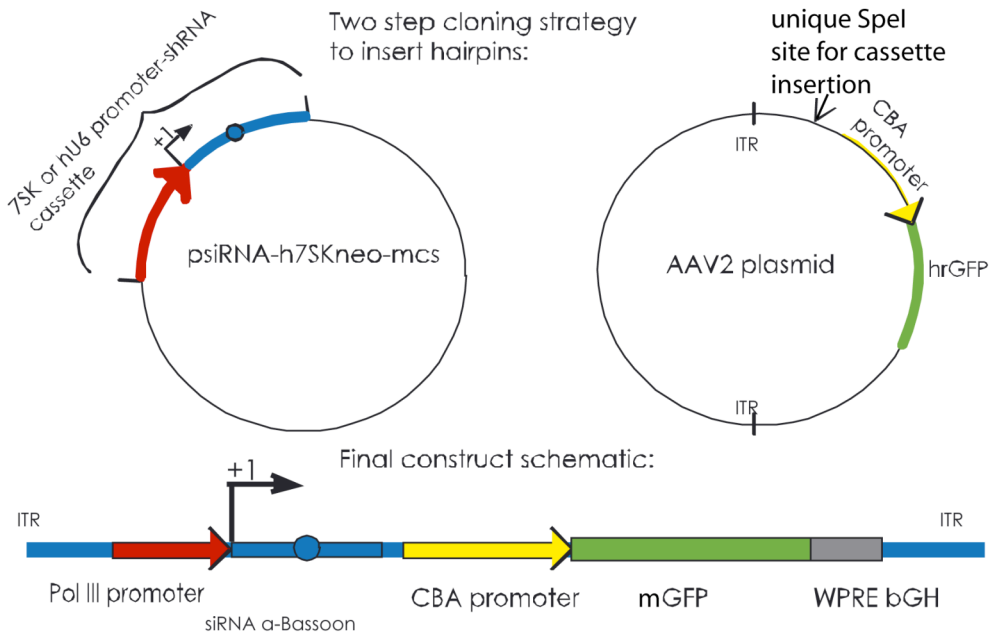

Fig. 2. 20: Schematic drawing of the two-step cloning strategy.
Left - commercially available psiRNA-h7skneo plasmid was used to construct shuttle plasmid with alternative promoter. PCR cloning was used to replace h7sk with hu6 promoter. Right - independently additional restriction enzyme recognition site was added to AAV2 plasmid to enable shRNA cassette insertion. Below - linearized construct consisting of polymerase III promoter-shRNA cassette followed by CBA promoter and mGFP represents just one of two possible directions of the shRNA cassette cloning.

2. 5. 2 Quantification of Bassoon in shRNA expressing calyces

Quantification of fluorescent immuno-signal in the calyces targeted with shRNA was based on pairs of calyces each infected with different AAV1/2 virus. One of the calyces from such a pair would express shRNA – and the fluorescent protein (mGFP), and the second calyx – mock control would express another fluorescent protein (mOrange) from second virus. Due to technical difficulties including low viral titer, of either shRNA carrying virus or mOrange, we could not find satisfying number of calyces labeled with expression proteins from shRNA and control plasmids present in the same field of view. Thus we have analyzed calyces from the same slice within the same MNTB. Due to unknown half-life of Bassoon in the synapse we incubated animal injected at P7 for 17 days (until P24) to increase chances for Bassoon removal from the AZs. We calculated average number of Bassoon fluorescent clusters per calyx from all the calyces in shRNA group and compared it to such average from mOrange group (Fig. 2.21). We have observed high variability in the number of Bassoon FIHC clusters within the control group (CV=1) but not in shRNA group. We

found no statistical difference between average number of Bassoon clusters per calyx in control mOrange group (n=8) and shRNA treated calyces (n=6). The high variability of the number of Bassoon clusters per calyx strengthens the notion that the most proper comparison of such calyces should be based on pair wise analysis. This however turned out to be very low yielding procedure.

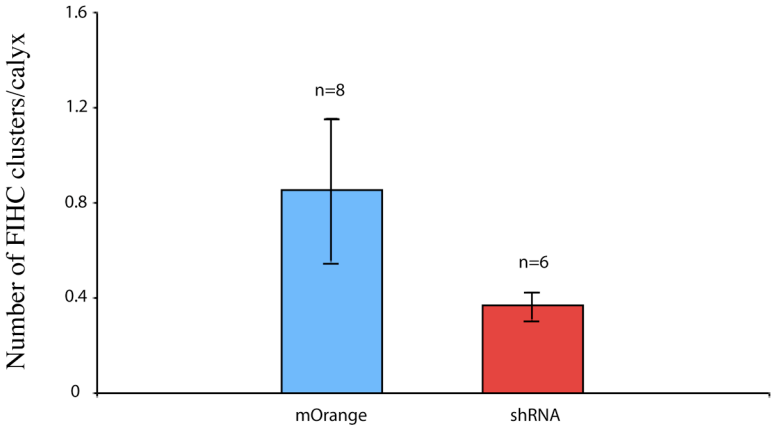

Fig. 2. 21: Quantification of Bassoon FIHC clusters in shRNA treated versus non-treated mOrange calyces.

2. 5. 3 Quantification of Piccolo in shRNA expressing calyces

Quantification of Piccolo was done using the same method as for Bassoon. Here we also used mOrange expressing calyces as virus control. We have found one pair of calyces within the same field of view and we pooled the results with additional two calyces from different fields of view but scanned at the same parameter and from the same MNTB/slice. Again total of four calyces, 2 expressing shRNA and 2 mOrange is not sufficient for any statistics, but we have observed trend toward reduced number of Piccolo clusters per calyx and calyx volume in shRNA expressing calyces (Tab. 2.1). In this analysis we used the procedure of subtracting outliers, as described in methods.

Calyx expressing	Calyx ID	Picc No./calyx Vol.	Picc No./calyx Vol.
mOrange	1	337	0.59
mOrange	2	331	0.72
shRNA	1A	267	0.28
shRNA	3	185	0.27

Table 2. 1: Comparison of the effects of shRNA against Piccolo. Number and density of Piccolo fluorescent immuno-clusters in calyces treated (shRNA) and non-treated (mOrange) with siRNA. Calyx ID: 1 and 1A indicates calyces from the same field of view; 2, and 3 are from the same MNTB/slice.

Interestingly we observed that FIHC Piccolo clusters seen in shRNA treated calyx are still present and appear in circular pattern indistinguishable from the control calyx (Fig. 2. 22 A). However at closer analysis with labeled calyx overlaying Piccolo channel it can be seen that many of the FIHC clusters from the circular pattern do not belong to the calyx (Fig. 2.22 B). Moreover FIHC clusters located within shRNA calyx appear smaller than clusters seen in the control calyx. Notably clusters that do not belong to the shRNA treated calyx also appear bigger than those from within the calyx (Fig 2. 22 arrowheads-within calyx, arrows outside calyx). This difference was not seen when we compared FIHC clusters from within the control calyx with those aligned with perimeter of the principal cell outside the calyx. Immuno-signal seen within the principal cell area indicates that some Piccolo is also present in neuronal somata.

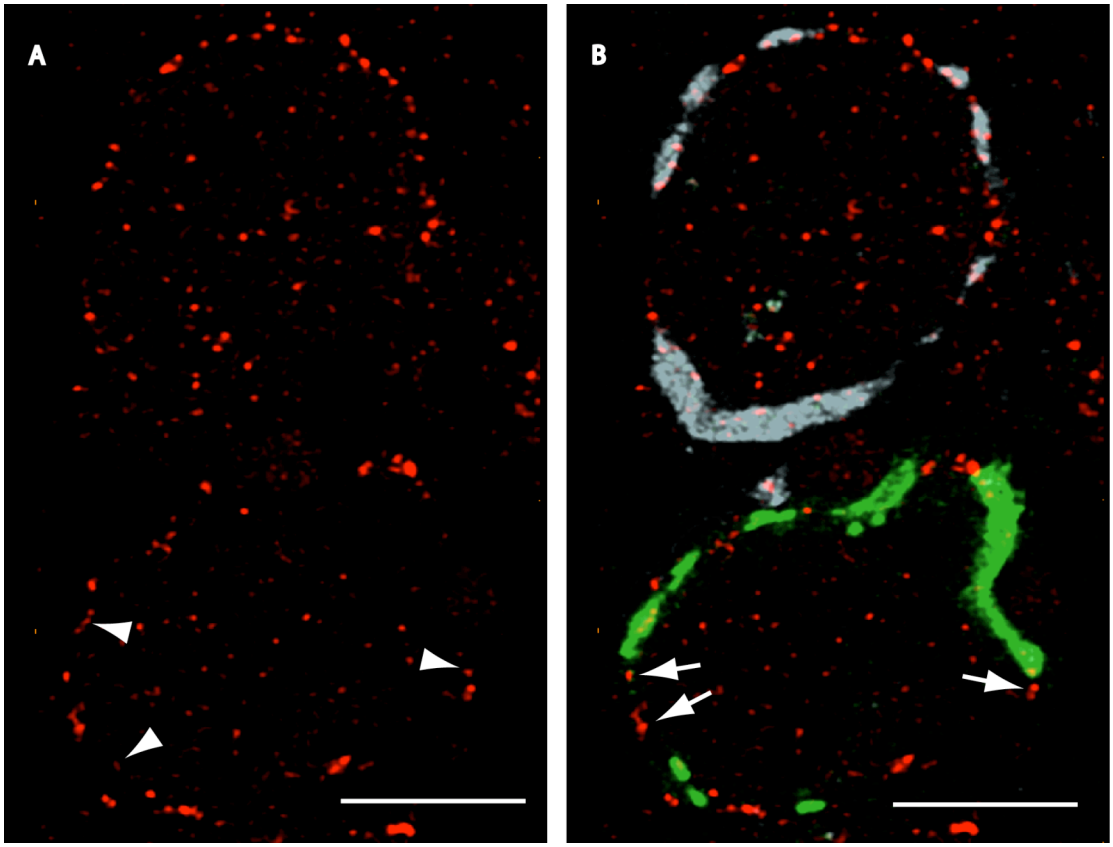

Figure 2.22: Piccolo FIHC labeling in shRNA and mOrange calyces. A - fluorescent immuno signal creates circular pattern suggestive of two calyces. Note that both patterns are very similar. B – cross section of mOrange labeled calyx – top and shRNA with mGFP labeled calyx – bottom. With calyces superimposed on Piccolo signal it is noticeable that FIHC clusters outside calyx are bigger (arrows) than those found within it (arrowheads) in the shRNA calyx, but not in mOrange control calyx. Scale bars 10μm.

3. Discussion

3. 1 Immonohistochemical localization of proteins in the calyx of Held

We have developed a novel approach of identifying and localizing proteins in the calyx of Held by combining previously described labeling of calyces via the targeted expression of fluorescent proteins *in vivo* with fluorescent immunohistochemistry *in vitro* on tissue slices. Immunohistochemistry has been widely used before in the MNTB for localization of various proteins, e.g. study of localization of mGluR2/3 at different developmental stages of rat in conjunction with EM analysis (Elezgarai et al., 2001), localization of voltage-dependent potassium channel Kv3.1b within calyx and the principal cell at different developmental stages also with additional EM analysis, (Elezgarai et al., 2003), light immunofluorescent study that identified different voltage-gated potassium channels in the calyx of Held (Ishikawa et al., 2003). In some of the immunohistochemical studies localization of the protein of interest within the calyx of Held was obtained by colocalizing it with presynaptic markers such as Rab-3A colocalized with calretinin (Felmy and Schneggenburger, 2004). One study examined the distribution of VGLUT transporters in the rat superior olivary complex (SOC) as well as within a single presynaptic terminal the calyx of Held (Billups, 2005). The author used double immunohistochemical labeling of VGLUT1 and 2 to analyze their co-localization in the calyx but without additional identification of the calyx. In another study calyces were patched and filled via patch-pipette recording with a dye Lucifer yellow and post hoc immunolabeled with antibody anti-sodium channels and anti-synaptic vesicle protein 2 (Leao et al., 2005). Approaches based on only colocalization of presynaptic markers with the protein of interest lack specific identification of the calyx. Such identification is needed because the calyx of Held is not the only presynaptic terminal present at the principal cell of the MNTB, and, these other synapses, when arranged along the perimeter of the principal cell, may pretend the pattern considered typical for calyceal origin. Other than calyceal excitatory terminals have been identified using EM in aging study of the MNTB (Casey and Feldman, 1985). Both excitatory and inhibitory additional terminals, has been also identified on the postsynaptic cell of the MNTB in the IHC study of cat superior olive complex (Adams and Mugnaini, 1990). In our study we

identified synaptic terminals labeled with anti-Bassoon but VGLUT1-negative and using ATGp showed that these terminals do not belong to the calyx. In another experiment we have found VGAT and VGLUT1 positive stain together forming circular pattern but without overlapping at any of the sites. Additionally, we have shown using various presynaptic antibodies, that circular patterns of immuno signal in the MNTB might be not unique to the calyx and represent other non-calyceal synapses. Thus, for IHC localization of the proteins within the calyx, proper labeling of it is necessary. One way of labeling namely filling the calyx with a dye via the patch-pipette recording overcomes this identification problem. However, since presynaptic recordings from the calyx of Held has been feasible up until the age of ~P14 it might be challenging to use this method for labeling adult P21 calyces. Furthermore passive, diffusion-based filling does not faithfully label thin protrusions of the calyces. Thus, injections of the virus-mediated genetically encoded fluorescent proteins to label calyces is clearly superior in the older rats. Also in the younger animals when membrane targeted GFP is expressed from the viral plasmid, level of visible details of the calyx (outer vs. inner plasma membrane with cytoplasm in between them) is superior to any patch-pipette fill for the calyx labeling.

3. 2 Localization of Bassoon and Piccolo

Combining ATGp and FIHC anti Bassoon and anti Piccolo we have described their localization relative to the calyx plasma membranes and SV clusters. Both of the proteins have been reported in the presynaptic compartments and immunocytochemical (ICC) identification of their punctate staining has been shown previously, e.g. Bassoon fluorescent signal in the hippocampal CA3 region in brain slices (tom Dieck et al., 1998), Piccolo fluorescent puncta in various regions of rat brain (Cases-Langhoff et al., 1996) and Bassoon together with Piccolo in primary hippocampal cultures (Altrock et al., 2003). These studies characterized localization of both of the proteins at the synapses and ultimately lead to acceptance of Bassoon and Piccolo being used as presynaptic markers, when present (some synapses e.g. bipolar cell ribbon synapses in the inner plexiform layer of retina, lack Bassoon (Brandstatter et al., 1999) and only contain Piccolo (Dick et al., 2001)). In our study, we were interested in describing molecular structure-function developments of the active zone proteins in the synapse. We took advantage of a large size of the calyx of

Held and were able to focus our analysis at the single synapse level utilizing 3D capabilities of the confocal microscope. We have shown that both of the proteins exist in the calyx of Held, and mostly localize at the inner site of the calyx. Furthermore, compared to SVs clusters labeled with genetically encoded synaptophysin or with antibody against VGLUT1 Bassoon and Piccolo appear below those clusters, closer to the calyceal membrane.

Our observation that Bassoon and Piccolo FIHC clusters in the calyx lay close to but not within the calyx membrane is expected because of their scaffolding role in AZ formation, big size of either of the protein (420kDa Bassoon and 530kDa Piccolo) and sandwiching effect of the antibodies. This observation is in good agreement with the EM studies of the active zone showing fuzzy electron dense material sticking out to the cytoplasm for ~ 100nm (Landis et al., 1988). To our knowledge this is the first FIHC study to describe localization of the active zone specific proteins within different compartments of three dimensionally reconstructed calyx of Held. This approach allows for quantification of FIHC clusters present exclusively within the presynaptic compartment and comparison of such data between different developmental stages of the calyx of Held.

3. 3 Bassoon and Piccolo represent active zones

We have shown using ATGp and FIHC approach that Bassoon and Piccolo are present in the calyx of Held and localize in discrete clusters distributed on the inner side of the calyx, the one that faces the postsynaptic cell. Since both of the proteins are found exclusively in the presynaptic cytoskeleton and associate with AZs (Cases-Langhoff et al., 1996; tom Dieck et al., 1998; Wang et al., 1999) they could be used to describe the localization of AZs in the calyx of Held. Our quantitative analysis yielded results numerically similar to the number of active zones known from the literature. Based on this we assume that fluorescent anti-Bassoon clusters could in fact represent active zone, baring in mind ~2 fold underestimation of active zone number due to optical spatial resolution restrictions. We have shown that the number of such FIHC clusters correspond well with previously reported number of AZs in young, P9 calyx (Saetzler et al., 2002). Specifically, Sätzler and colleagues reported 550 AZs with an average surface of 0.100μm^2. An average distance between nearest-neighbor AZs measured from their center of gravity was 0.59μm. In our study we report ~250

and ~380 FIHC clusters for Bassoon and ~210 and 310 FIHC clusters for Piccolo (P9 and P24 respectively) per calyx. The lateral optical resolution obtainable from our system is ~ 200 nm at wavelengths used for detection of the FIHC clusters. Thus, theoretically a single cluster of FIHC could represent single AZ since on average they are ~ 600 nm apart. However the axial optical resolution is about 3.5 fold lower (~700nm) than lateral, thus in practice we should assume about 2-fold underestimation of the number of AZ as represented by FIHC clusters. If we correct for this underestimation, the number of FIHC clusters agrees well with the number of AZs found in a fully reconstructed P9 calyx. Furthermore, the assumption that Bassoon and Piccolo clusters might represent active zones within calyx implies that their localization should correlate with synaptic vesicle clusters. We have demonstrated this by visualizing SVs either using genetically encoded synaptophysin-GFP expression or an antibody VGLUT1. We have shown that both Bassoon and Piccolo fluorescent signal was mostly located within the SV clusters, closer to the calyx membrane. Only a small fraction of either of the protein fluorescent cluster was not within SV clusters. Localization of fluorescent clusters within SVs strengthens our prediction about Bassoon and Piccolo representation of the AZs. However their clusters smaller fraction outside SVs is not clear, but might suggest newly arrived Bassoon and Piccolo, not yet incorporated into functional release sites.

3. 3. 1 Quantification of Bassoon and Piccolo

Any fluorescent cluster represents the sum of protein molecules together with primary and secondary antibodies plus conjugated fluorescent dye molecules present in one place. Therefore, the best way of expressing their size was to measure their volume because of their truly three-dimensional structure (as compared to ultra-thin AZs traced in EM images). For this reason we did not attempt to compare reported sizes of AZs with our finding of fluorescent immuno-clusters volumes. We found that number of AZs as represented by FIHC clusters does not change during calyx development between the age of P9 and P24. This observation might suggest that the initial increase in the number of AZs observed between ages of P5-P7 and P12-14 (Taschenberger et al., 2002) is most likely concluded by P9 and no further increase in the number of AZs occurs by P24. An alternative explanation could be that the amount of Bassoon and Piccolo proteins detected by IHC and visualized as

fluorescent clusters does not change over time, but the number of active zones increases nevertheless. This could be possible if newly formed active zones remained at distance smaller than optical resolution and thus were undetectable by our approach. Although we did detect an increase in the number of Bassoon FIHC clusters per calyx between P9 and P24, this difference disappeared when FIHC clusters density was compared suggesting different size of calyces used for Bassoon analysis at different age groups.

Comparison of Bassoon and Piccolo FIHC reveals similar number of Piccolo FIHC clusters compared to Bassoon FIHC at either age group in the calyx of Held. This observation is confirmed also by co-localization and 3D quantification of the co-localized clusters in P9 rat. Specifically we found an average ~86% (n=2) of Bassoon FIHC clusters co-localized with entire population of Piccolo FIHC clusters leaving ~14% of Bassoon FIHC clusters without Piccolo partner. Interestingly, in another two calyces, where the secondary antibodies were swapped as compared to previous two calyces, we saw different results. That is an average of 75% of Piccolo FIHC clusters co-localized with entire Bassoon FIHC cluster population, leaving 25% of Piccolo FIHC clusters without Bassoon partner. These results seem to be related to the brightness of the secondary antibody rather than biological differences in the number of Bassoon versus Piccolo clusters. This observation adds to the complications related to immunohistochemical method of quantifying co-localization of different proteins. In general, high variability in the number and size of the FIHC clusters was observed. Such variability has been reported previously in an anatomical study where Sätzler with colleagues (2002) observed high variability of the AZ sizes. They did not make any variability assessment of the number of AZs since they analyzed one 3D reconstructed EM calyx. In another study where partially reconstructed calyces were analyzed and number of AZs was approximated the authors reported some heterogeneity in AZs size but not AZs number between calyces and within any given calyx (Taschenberger et al., 2002). In our work variability that we observed might reflect truly biological differences in AZs sizes. That is if we assume that smaller AZs consisted of less Bassoon or Piccolo, they would bind fewer antibody molecules and produce less of the fluorescent signal. However, we cannot rule out the possibility that variability comes mostly from technical constraints of the method. For example, variable binding of the secondary antibody to the primary antibody, various amount of

fluorescent dye conjugated to the secondary antibody could also produce size differences of observed FIHC. These elements can introduce or enhance variability but since all of the abovementioned problems apply to all the data at random, they would cancel out in the final analysis. Nonrandom differential binding of the primary antibodies in different tissue types i.e. binding might be hindered in more myelinated tissue in such way that less antibody particles arrives to antigen, is more problematic. In almost all cases we have seen the thin surface (0.5-1μm) of the tissue stained more intensely than the remaining areas below and this was observed in either age group. However staining below this intense thin surface would very often appear equal at various depths. In a few cases we have observed a severe drop of intensities in antibody staining and those experiments were not used in the quantitative analysis. To circumvent the problem of the surface staining but without experimenter biased cropping of the raw data we decided to subtract outliers from each data set. Post-hoc we have arbitrary removed values above the calculated border defined as 1.5x(75^{th} percentile – 25^{th} percentile) from the data pool. With abovementioned technical constraints of the method in mind certain controls can be introduced to increase quantitative strength of Bassoon and Piccolo FIHC clusters analysis. To avoid uncertainty of antibodies, ideally comparison should be made at the same tissue treated with the same antibody at the same time. When comparing distribution of FIHC clusters between two calyces, ideally both of the calyces should be located within the same field of view, or at least within the same slice and MNTB, and at similar depths. In fact if these requirements are met such analysis can have great advantages for quantitative comparison of FIHC clusters because it allows for direct comparison of treated and control calyces in the same animal.

3. 4 Gene down regulation *in vivo*

We have used this unique opportunity of comparing shRNA treated calyces, which were also labeled in green, with control calyces – labeled in red, in an attempt of down regulating Bassoon and Piccolo proteins *in vivo*. We used AAV1/2 virus plasmid expressing shRNA from polymerase III promoter together with AAV1/2 plasmid expressing mOrange as a control for down regulation of Bassoon or Piccolo expression. The AAV1/2 virus is capable of multiple infection of the same cell but efficiency of such double infection is linearly related to viral titer with low titer

viruses less likely co-infecting the same cell. We used low titer viruses for expressing shRNA cassettes and control plasmids. Combined ATGp with FIHC techniques in detecting shRNA mediated protein expression down regulation theoretically offers set of advantages. First, down regulation is applicable in vivo by injecting living animal with two viral constructs one expressing shRNA and another - control plasmid. Since we used stereotaxic brain injection we targeted specifically the area of interest and avoided other brain regions. Second, since the animal recovers after the surgery we can adjust the incubation time to allow long half-life proteins to turn over. Third, recently we were capable of delivering shRNA as early as at P2 before the time of calyceal formation (P3-P4). Fourth, using quantitative 3D FIHC approach we could detect a decrease in the protein level by counting the number of fluorescent clusters and measuring volume of those clusters. Fifth, comparing FIHC clusters in treated and non-treated calyces we analyze protein content in its most relevant site – the synapse. Finally, such approach allows for best assessment of down regulation of the AZ protein at the synaptic site and directly justifies functional approach via electrophysiological methods.

In practice we have encounter certain hard to predict yet significant obstacles. First, since we did not know the time needed for clearance of native Bassoon or Piccolo proteins from the AZs in the calyx of Held we first constructed viral plasmids carrying shRNA against mRNA of each of the protein separately. It was important to establish half-life of these proteins because in the calyx of Held electrophysiological postsynaptic recordings are possible up to an age of P18 in rats, since thick myelination hampers accessibility of the cell. Thus P18 is the upper limit of the incubation time after viral infection. We developed coordinates and surgical procedure for targeting ventral cochlear nucleus (VCN) with viral injection as early as at P2 and this sets the lower limit for the incubation time after infection. Thus half-life of the protein of interest should not exceed two weeks if physiological study is considered. Only after defining the incubation time we planed to target both proteins simultaneously. Second, efficiency we observed when injecting low titer viruses was below optimal. Third, injections of P2 animals are more variable than that of P7 and older and additionally ~24hrs needed by AAV to reach full expression capability plus time for increase in shRNA concentration most likely set back the actual action of shRNA to occur within but not ahead of calyces formation. Fourth, calyces labeled

with mGFP with shRNA were differently labeled than that of control - mOrange volume fill calyces. This brought certain risk of missing FIHC clusters located close to the membrane in the volume filled calyces, because in those calyces membranes are not well defined. It could cause bias toward detecting less FIHC clusters in volume fill calyces, vs. membrane labeled ones. Finally, the preliminary results with effects described below were obtained from P24 (Bassoon) and P25 (Piccolo) rat after 22 - 23 days of incubation, raising the possibility of a very long turnover of the proteins already present in the AZs. The above mention factors and additional technical variables, like primary and secondary antibody good performance all need to coincide to make successful image.

The above described problems together with technical variables turned out to be a low yielding strategy. Therefore, even though that many trials were made only small sample of data was collected consisting of shRNA treated and control calyces. This said we established data for Piccolo where we demonstrated (with low n) that indeed shRNA might be down regulating expression of Piccolo and with our FIHC method we are able to detect it. We have never seen down regulation of neither of the proteins when scrambled control shRNA was applied as compared to wild type calyces.

3. 5 Improvements of the *in vivo* down regulation system

Our work has shown potential capabilities of combined shRNA ATGp and FIHC system in down regulation experiment but it also revealed some shortcomings of the approach. Fortunately most of the practical problems can be solved. The very first complications showed themselves at the constructing of the plasmids. We have observed that cloning of the shRNA-casette in AAV2 plasmid can sometimes alter the ITR located close to the insertion site of the cassette and impair packaging of the viral plasmid to its capsid. From our experience most of these alterations can be detected by analytical digest of the AAV2 with endonuclease SmaI after the cloning. However, such sensitivity of AAV2 to any cloning needs to be taken in account for the future cloning of two shRNA-cassettes against Bassoon and Piccolo each. It is obvious now that large insert consisting of two promoters driving each shRNA would have to be assembled outside AAV2 plasmid, and cloned into it in one step. After that, besides sequencing of new constructs, screening could be introduced to streamline assessment

of down regulation efficiency of shRNAs used. In this work our collaborators provided the shRNA sequences tested in the primary hippocampal cultures that we used in the experiments for down regulating Bassoon and Piccolo. However shRNA tested in vitro does not necessarily work in vivo system. Thus after inserting these sequences into AAV2 plasmid and producing the virus we started directly with in vivo tests. We assumed that since our collaborators did in vitro tests we do not need to perform another testing in the neuronal cultures with Western blot as a quantification method. Nevertheless, from today's point of view, such an in vitro test seems to be necessary regardless of whether shRNA sequences were tested somewhere else or not. This is because such testing, including a Western blot technique, would: 1) test shRNA-cassette expressing from our AAV1/2 virus, in contrast to naked or non virus expressed siRNAs, 2) would shorten and ease the way to obtain confirmation of efficiency of the tested shRNA, 3) could reveal an approximate time needed by the protein to be down regulated, which could be used to estimate incubation time in the in vivo system, 4) would be a proof of case for any promoter – shRNA expression cassette, even if later it would not work in vivo. In this way we could relatively quickly screen through multiple viral constructs carrying shRNA-cassette inserts. Only after passing the screen, we would use qualifying virus for in vivo system. In use of FIHC cluster count in shRNA treated and control calyces, similarity of calyx detection is important because it is a number or a volume of FIHC clusters that is compared between two treatments. However doing experiments we observed difference in the calyx labeling that depended on the expressed fluorescent protein. In this work we used shRNA-cassette expressed from AAV2 plasmid that also encoded membrane targeted GFP, and mOrange fluorescent protein expressed from the control virus that was not carrying any shRNA. The mGFP labels with an outstanding precision delineating membranes of calyces thus shows FIHC clusters of Bassoon or Piccolo close to membrane localization. The mOrange fills volume of the calyx and often under represents narrow areas like stalks on which calyceal swellings develop, any FIHC cluster that would localize in the stalk would not be counted. Furthermore since mOrange does not show membrane localization of the calyx it often leads to FIHC clusters appearing just above or merely touching mOrange labeled calyx. These in turn may cause under representation of the number or volume of FIHC clusters belonging to given calyx. On the other hand such bias toward under representation of

FIHC clusters in the control calyces only strengthens our results but it also miss represents real potential of shRNA in down regulation of Piccolo. Therefore in the future we plan to swap these two fluorescent proteins between constructs. In such way that mGFP would be expressed from the control plasmid and mOrange would be expressed from plasmid carrying shRNA-cassette. This would produce two-fold effect. First we could use mGFP-expressing virus at higher titers, so that it would also infect cells expressing control plasmid. By doing so we could only need to look for a hint of mOrange within mGFP expressing calyx to qualify it as shRNA targeted calyx. Second we would be able to always use mGFP for identifying calyces and quantifying their FIHC cluster content in a very consistent way. This approach should allow for more precise estimation of down regulation potential of shRNA used.

The last but not least improvement that we will need to introduce for the future experiments stems out of ongoing developments in understanding of siRNA system workings. When we have started our experiments the shRNA approach was very little known. Short RNA sequence that would not match any known gene, so called scrambled sequence, was an accepted control for siRNA down regulation at the times. With time, it became obvious that shRNA can act at two different pathways within a cell, one utilizing sequence specific matching leading to cleavage of the complementary mRNA of the host cell. The other pathway triggered by partly mismatched siRNA leading to non-specific cleavage of non-targeted mRNA. These observations lead to introduction of changes in accepted control for shRNA specificity. Namely that shRNA has to lose its specific down regulation capabilities when only one nucleotide is mismatch with the targeted mRNA. Therefore we will have to redesign and create new control shRNA for our future experiments with down regulation of Bassoon and Piccolo.

3. 6 Summary and outlook

We are interested in understanding molecular mechanisms underlying neurotransmitter release. The calyx of Held, the model synapse we focused on, offers a unique opportunity to study developmental structure-function modifications leading to increased efficacy of transmission. For our study we chose two active zone associated cytoskeletal proteins Bassoon and Piccolo to follow potential changes in the molecular structure of release sites in the calyx of Held at P7-9 and P21-25 old

rats. We chose these AZ-associated proteins for two reasons. Because results from previous studies using rat calyx EM analysis suggest possible addition of AZs during calyx development. As well as because of an observation of a fraction of silent synapses in the Bassoon knock out (KO) mouse hippocampal culture. Protein content analysis in the Bassoon KO mouse revealed increased amount of Piccolo suggesting possible share of function between the two proteins.

We have developed a novel approach of single calyx 3D fluorescent immunohistochemical analysis combined with acute targeted gene perturbation method. We demonstrated that Bassoon and Piccolo are present in the calyx of Held, and their FIHC clusters number and distribution within the calyx area resembles that of AZs. We conclude therefore that in the calyx of Held both Bassoon and Piccolo represent localization of AZs. We then compared changes of FIHC clusters between two age groups P7-9 and P21-25, and found no statistically significant difference in number and size of the clusters. Using Bassoon antibody we have also identified non-calyceal synapses located at the perimeter of principal cells, that were also VGLUT1 negative, suggesting that they are inhibitory synapses, or VGLUT1 negative excitatory ones.

To look for functional implications of Bassoon and Piccolo presence in the AZ we first attempted to down-regulate Bassoon and Piccolo content in the calyx in vivo using the RNA interference method. We have constructed several viral plasmids carrying shRNA expressed from polymerase III promoter against Bassoon or Piccolo. We then took advantage of combined ATGp and FIHC approach and attempted to quantify perturbation of Bassoon and Piccolo in the calyx. However, due to several reasons such as shRNA itself being a relatively novel method with rules governing its efficiency in down regulating target mRNA not well understood, and low titers of the viruses carrying shRNA cassettes and strict rules of FIHC, we have encountered problems in achieving reproducible results. We have managed, however, to obtain preliminary data demonstrating that our ATGp and FIHC approach can be functional.
Our research established solid base for any future FIHC based localization of presynaptic proteins in the calyx of Held. We have also reconfirmed presence of non-calyceal synapses on the principal cells of the MNTB. It would be interesting to better immunoshitochemically characterize those different types of synapses, as well as ultimately trace their axons back to the cell bodies. This would be interesting to

describe, because the calyx of Held already seems to be more than just a relay synapse. Another open question stemming from our work is whether Bassoon and Piccolo can take over their function, and whether down regulation of both of the proteins would cause similar effects to those observed in Bassoon KO hippocampal cultures.

One more interesting question is more provocative than previous ones. We have sporadically observed Bassoon FIHC clusters on the outer site of the calyx, away from the postsynaptic cell. Similarly in a subset of only few experiments that we made we have seen VGAT positive staining located on the outer site of the calyx. There is an increasing notion that the calyx might possess additional release sites located on the outer site, that are used for sending signals to the glia astrocytes (Kettenmann personal communication). It would be very interesting to follow on our preliminary observations in a systematic way to find out whether those release sites show AZ specific immunohistochemical blueprint.

4. Material and Methods

4. 1 Genetic techniques

4. 1. 1 Standard methods of molecular biology

Standard molecular biology methods like cutting DNA with restriction endonucleases, ligation, agarose gel electrophoresis, transformation and culture of bacteria *Escherichia coli*, dephosphorylation of DNA terminals were done according to standard protocols from laboratory handbook by J. Sambrook, E.F. Fritsch and T. Maniatis "Molecular cloning: a laboratory manual." vol. 1-3 (2 Ed., 1989)

4. 1. 2 Isolation of plasmid DNA from *E.coli*

For isolation of low amounts of DNA (up to 10μg) the "QIAprep Miniprep Kit" was used while for larger amounts (up to 500μg) the "QIAprep Maxiprep Kit" was used, (both from QIAgen company). Isolation procedure was according to company manual. The principle of the DNA isolation in this system is based on three steps: alkaline lysis of bacteria, adsorption of DNA to the silica column at the high salt concentration and elution from the column at the low salt concentration.
The purified DNA is of very high purity and can be directly used for further processing like sequencing, transformation etc.

4. 1. 3 Sequencing

Sequencing of pAAV2 plasmids without region of ITRs and fragments of psiRNA-neo-shRNA plasmids was done in house. The DNA for sequencing was mixed with the "Big Dye Terminator Mix V3.1" (ABI) and run in the Capillary Sequencer "3100 Genetic Analyzer" (ABI). Typically sequenced fragments would reach the length of 300 bp. Sequencing of final constructs of AAV2-"promoter-shRNA" plasmids was done commercially by MWG with our own primer design. All the sequencing primers for sequencing were design by us. The primers used for sequencing of different constructs are listed in table 4.1.

Sequencing target	Primers sequence	Primer ID
plasmid AAV2 primers		
5' ITR	5'-ACGCGGCTACAATTAATACA-3'	AD05
5' CBA	5'-TGCCCAGTACATGACCTTA-3'	AD06
5' Xba, BamH1/GFP	5'-CTTGGTTTAATGACGGCTT-3'	AD07
3' end of GFP	5'-TACAAAGGCATTAAAGCAGC-3'	AD08
3' end of WPRE	5'-TCTAGTCGAGCCCCAGC -3'	AD09
3' end of KpnI	5'-TATGTAACGCGGAACTCCA-3'	AD10
3' ITR	5'-ACCATAGTCCCGCCCCT-3'	AD11
3'end of KpnI	5'-AAATTGGGGGTGGGGA-3'	AD14
3'end of KpnI	5'- CAAGTGGGCAGTTTACCGT- 3'	AD15
3'end of EcoRI, EcoRV and HindIII	5'-ACGGTATCGATGCGGG-3'	AD16
5'end bGH and ITR	5'-CCTCTTCCGCGTCTTCG-3'	AD17
5'end bGH and ITR	5'-GGCCCTCAATCCAGCG-3'	AD18
3'end XbaI and BamHI	5'-CCTTGGTCACGCGGAT-3'	AD19
plasmid psiRNA-neo-hU6 or h7sK		
to confirm promoter	5'-GATCCGGCAAACAAACC-3'	AD22
to confirm promoter	5'-CCAAAAAGTCTTCCTAGCTC-3'	AD23
final construct pAAV2 plasmid with promoter-shRNA caseette inserted		
promoter-shRNAcassette	5'-TCCAACCAAACCGACTCTGA-3'	AD66
promoter-shRNAcassette	5'-AGATGGGGAGAGTGAAGCAGAACG-3'	AD67

Table 4.1: List of primers. Table is organized chronologically to reflect progressing order of making virus constructs for shRNA *in vivo* delivery (top to bottom). Plasmids psiRNA were used as shuttles to assemble a promoter-shRNA cassette – the original contained the h7SK promoter, and newly constructed had h7SK replaced with hU6 promoter. The final pAAV2 viral plasmid with inserted cassette of promoter-shRNA, ready for virus production.

4. 1. 4 Polymerase Chain Reaction-based cloning

The PCR – cloning method was used for extraction of DNA fragment of interest from one plasmid with simultaneous alterations of 5' and 3' ends of such extracted DNA and cloning it into another plasmid. In principle forward and reverse primers were designed to be complementary for about 18 – 25 bp with the DNA fragment of interest and their additional 12 – 15 bp were carrying sequences recognizable by desired restriction enzymes, those fragments were not complementary. The product of such PCR would be the DNA of interest flanked by the restriction enzyme sites that were needed for further cloning steps. All the primers for PCR-cloning were designed by us. PCR – based cloning was used:

A) in constructing psiRNA shuttle plasmid to insert hU6 promoter after removing of commercially inserted h7sk promoter,

B) in constructing AAV2 – mGFP plasmid, from originally available AAV2-hrGFP plasmid.

Specifically:

A) Inserting hU6 promoter into plasmid psiRNA-7sK-neo-mcs

1. Excise fragment ClaI (2649) – Bsu36I (2913).
2. PCR humanU6 polymerase III promoter from psiRNA-hu6-neo-mcs (Ambion cat#7209) with primers:

- 5PhU6=AD13=5'primer with ClaI & XbaI

5-GACCATCGATTCTAGACCCCAGTGGAAAGACGC-3
ClaI XbaI

- 3'PhU6=TS-AD04=3'primer with BbsI and Bsu36I

5-GCTACCTCAGGTGAAGACCCGGATCCCGCGTCCTTTC-3
BSu36I BbsI

3. Ligate PCRed hU6 promoter with digested psiRNA-~~7sK~~-neo-mcs (as in "1")
4. Confirm liagation with analytical digest

XbaI should yield two bands: 2670, 712

XbaI is unique in original psiRNA-7sK-neo-mcs – linerarizes this plasmid.

B) Cloning of membrane targeted GFP to AAV2-hrGFP plasmid

The mGFP was PCRed from pBKS plasmid with the forward primer containing BamHI (a) and reverse primer containing HindIII (b) recognition sites:

(a) – 5' CAT AGC GGA TCC ATG GGT TGC TGT TTC TCC – 3'

(b) – 5' CAT AGC AAG CTT TTA CTT GTA CAG CTC GTC CAT G – 3'

Final product of PCR the mGFP flanked with BamHI and HindIII sites was digested with BamHI and HindIII restriction enzymes and purified.

After excising hrGFP from AAV2 plasmid with the abovementioned two restriction enzymes, the digested PCR mGFP was ligated with linearized AAV2 plasmid. Total of 16 clones were finally selected for analytical digest with following restriction enzymes: AvaII - to ensure mGFP insertion to AAV2 plasmid and SmaI – to check the integrity of ITRs. SmaI recognition site is located in the middle of ITR sequences thus if ITR sequence was destroyed SmaI site would also be lost. Twelve out of 16 clones passed the analytical digest as positive and out of those 10 clones were

screened for their brightness via transfection into primary hippocampal culture. Total of four clones were the brightest and out of them one was selected for test in the virus production. The viral titer with this clone was as good as the other highest titer constructs and reached ~$7x10^6$ infectious particles per ml. This construct was further used in siRNA plasmid production.

Creating a unique site for insertion of the shRNA cassettes.

The AAV2 plasmid was altered before the transfer of shRNA cassette could take place. We first designed short oligoneucleotide containing SpeI recognition site in the middle and flanked by KpnI sites on 5' and 3' ends. One of the KnpI sites was made to be lost after cloning into AAV2 plasmid. The cloning was based on a single unique KpnI site present in the AAV2 plasmid. After inserting unique site for SpeI restriction enzyme we obtained the master plasmid for any further shRNA-casettes cloning.

4. 1. 5 RNAi

Both Bassoon and Piccolo have two (each) different target sequences both near the N-terminal. Two shRNAs are produced against each target sequence one is driven from hU6 and the other h7sk polymerase III promoter. The list of shRNA anti Bassoon and shRNA anti Piccolo sequences and their complementary target sites are listed below:

BASSOON

hU6-2425/2627

In bassoon gene aligns to bp: 555 – 573

hU6- 3233/3435

In bassoon gene aligns to bp: 543 – 571

h7sK-2627/2829

In bassoon gene aligns to bp: 555 – 573

h7sK-3435/3637

In bassoon gene aligns to bp: 543 – 571

PICCOLO

hU6-4041/4243

In piccolo gene aligns to bp: 336 – 354

hU6-4849/5455c
In piccolo gene aligns to bp: 642 – 660

h7sK-4445/4243
In piccolo gene aligns to bp: 336 – 354

h7sk-5253/5455c
In piccolo gene aligns to bp: 642 – 660

Design of short hairpin sequences

Terminals of the short hairpin sequences required specific design to fit into the shuttle plasmids of our choice. First - 5' ends of hairpin sequences had to be specially designed because the polymerase of hU6 promoter has a preference to initiate transcription with purine (Guanine or Adenine), human 7sK promoter is very permissive, and second the 3' ends of the hairpin had to incorporate poly-thymidine (polyT) tail used as termination site for the polymerase III. Additionally the general design of an entire short hairpin insert was constrained by the type of the cloning sites available in the psiRNA plasmids namely BbsI recognition sites. The BbsI restriction enzyme cleaves DNA six nucleotides away from its recognition sequence. This kind of cloning offers possibility to insert the short hairpin sequence at close proximity to the polymerase III promoter. We have designed the shRNA sequences with the 5' overhang designed either for h7sk or hU6 promoters (Fig. 4.1)

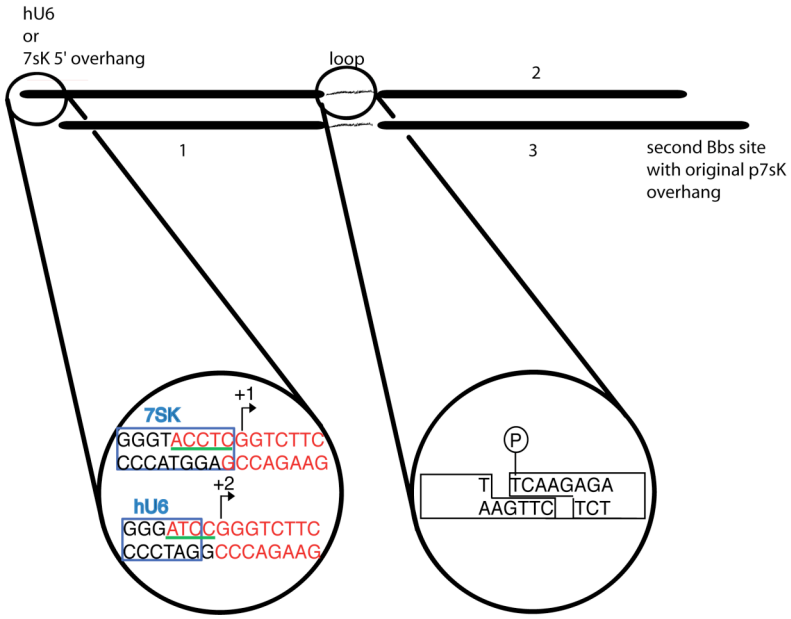

Figure 4. 1: A schematic of short hairpin RNA design. Each hairpin was assembled from 4 short oligonucleotides (labeled here as: hU6/h7sk overhang, 1, 2 and 3). Five prime overhang was designed to ligate with h7sk or hU6 promoter. Left zoomed window shows: 3' end sequence of h7sk or hU6 prmoter– blue box and blue letters; recognition site (GTCTTC) and cleavage site of BbsI - red letters; reconstructed parts of the h7sk or hU6 sites included into shRNA short oligo design – red letters with green underline.
Right zoomed window shows how each elementary oligonucleotide was separated from each other at the loop site (the loop sequence TTCAAGAGA). The loop sequence had one 5'end phosphorylated to facilitate ligation.

4. 2 Immunohistochemistry

Antibodies used in this work are summarized below.

. antibody	developed in	mono/polyclonal	catalogue No.	Company
mAb7f	mouse	mono	Gundelfinger, ED	
gp-44a	guinea pig	poly	Gundelfinger, ED	
PSD95 (SAP90)	rabbit	poly	cat: 124002	SySy
Synaptophysin	mouse	mono	cat: 101011	SySy
VGAT	mouse	mono	cat: 131011	SySy
CASK	rabbit	poly	cat: 150002	SySy
VGLUT1	rabbit	poly	cat: 135303	SySy

Table 4. 2: List of primary antibodies with catalogue number and company name.

Secondary antibodies were purchased from Molecular Probes and were conjugated with Alexa Fluor:

goat anti-mouse, A546 cat: 21123; A647 cat: 21235

goat anti-rabbit, A568 cat: 11011, A647 cat: A21244

goat anti-guinea pig, A647 cat: A21450

4. 2. 1 Tissue preparation

Rats were overdosed with intraperitoneal injection of Narcoren (70mg/kg of body weight). Intracardial perfusion of normal rat ringer (contains: 135.0 mM NaCl, 5.4 mM Kcl, 1.8 mM $CaCl_2$, 1.0 mM Mg Cl_2, 5.0 mM Hepes, pH7.2) was followed by perfusion of 4% paraformaledhyde solution in 0.1M phosphate buffer (contains: 0.1M Na_2HPO_4 and 0.1M NaH_2PO_4). The brain was extracted from the skull and post-fixed for 90 to 120 min in 4% PFA solution at 4ºC. After post-fixation brains were moved to 0.1M PB solution and stored at 4ºC for 2-12hrs until further processing.

4. 2. 2 Staining of presynaptic proteins in free floating sections

Coronal sections of the auditory brainstem were cut on a vibratome (HR2, Sigmann Elektronik) at 50-100μm of thickness. All further processing was done at 4ºC.

Sections were always incubated at 1 – 2 sections per volume of 1ml/well. For processing sections were incubated in 0.4% - 1% (depending on the age of the rat) of Triton X100 and 5% normal goat serum (Jackson ImmunoResearch Laboratories, Inc., cat. # 005-000-121) in PB for 60–120 min. Primary antibodies were diluted in 1% NGS and 0.2% TX100 in PB and tissue was incubated for 12 to 20 hrs at 4ºC. After the primary antibody incubation stringent rinsing with 2% NGS in PB was applied. The secondary antibody was also prepared in 1% NGS and 0.2% TX100 and sections were incubated at 4ºC for 12 hrs. After final rinsing sections were mounted in SlowFade Gold antifade reagent (Molecular Probes, cat. # S36936).

4. 3 Acute targeted genetic perturbation (ATGp)

ATGp method was developed previously in our lab (Wimmer et al., 2004). Briefly, this method is based on stereotaxic delivery of viral gene shuttles to VCN. In principle this approach allows for selective targeting of the calyx of Held terminals. This method facilitates acute manipulation of protein composition in the synapse at *in vivo* system.

4. 3. 1 Virus systems suitable for gene transfer

We used two different viral systems, sindbis and adeno-associated virus.

These viruses offer different advantages for the use in acute gene transfer but also have their own disadvantages. We will describe each of the systems separately and point out unique features utilized for gene transfer. We also describe detail production protocols for each of the virus.

4. 3. 1. 1 Sindbis virus

Sindbis virus is well suited for protein expression for its fast onset and high expression level. Additionally because of cytotoxicity observed at ~30hrs after the onset of expression it is useful for only short time of incubation. Therefore we used Sindbis for expression of fluorescent proteins in young animals (P7-P9) with injection at P6-P8, and incubation for ~ 18 - 24 hrs, to avoid toxic side effects of the virus. This time of incubation yielded satisfactory results of labeling for the calyx identification.

4. 3. 1. 2 Adeno-Associated virus

Hybrid virus containing AAV2 ITRs and AAV1 capsid proteins was used for its natural tropism toward neurons (supported by AAV2) and enhanced expression level. However onset and level of expression are lower than that known for alpha viruses, thus we used the AAV1/2 for adult animals (P21 – P25). We injected young P7 –P9 pups and incubated them for a period of minimum 10 days.

4. 3. 2 Generation of viral particles

Protocol for production of AAV1/2 viral particles was based on commercially available Stratagene protocol (cat. # 240071) and optimized in our lab by technical assistant. Protocol for Sindbis production previously described (Wimmer et al., 2004) followed standard protocol from Invitrogen (cat. # K750-01)

4.3.2.1 Production of Sindbis virus

Sindbis is an alpha virus belonging to the togaviridae family. It is a positive, single-stranded RNA virus that does not integrate into the host genome. In order to make it accessible for safe gene delivery, the wild type viral genome was split and inserted into two plasmids. The gene of interest is cloned into pSinRep5 that contains the genes for the nonstructural proteins 1-4 (nsp1-4). The nsps ensure the intracellular replication of the virus genome as well as of the subgenomic RNA that serves as functional mRNA in the host cell. The helper plasmid p26S encodes for the structural proteins, which produce the protein capsid, and the envelope proteins. Packaging of the helper plasmid into capsids is prevented due to a lack of the packaging signal. Both plasmids were introduced into the baby hamster kidney (BHK) production cell line by electroporation. After 20 – 24 hours of incubation BHK cells produced viral particles containing only the RNA with the transgene and nsps. An overview of Sindbis virions production is shown in Fig. 4.2.

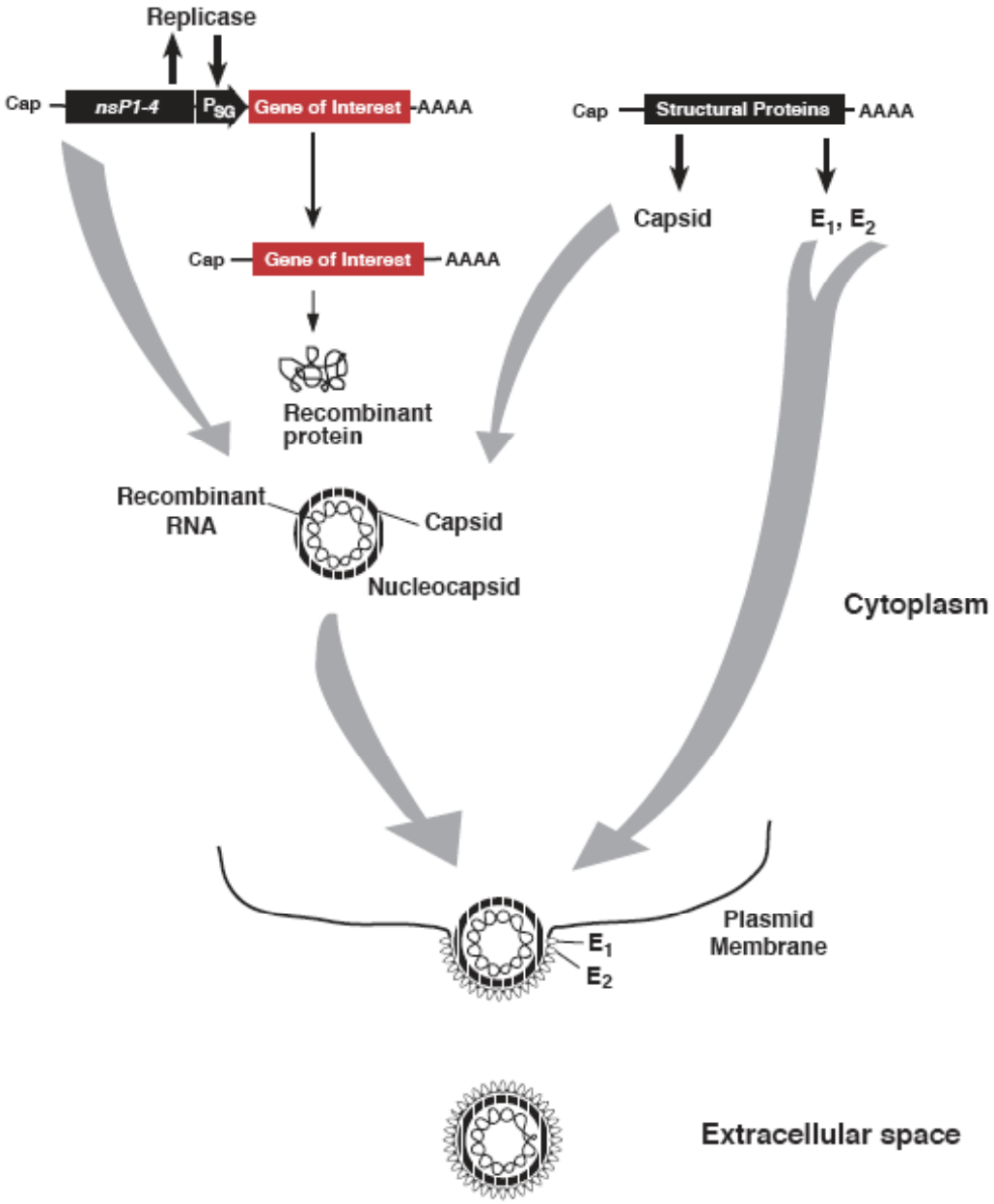

Figure 4.2: Preparation of recombinant virions. Baby hamster kidney cells (BHK) are made competent for RNA uptake by electroporation. Cells produce infectious but replication deficient virions encoding the gene of interest (red) and the nonstructural proteins 1-4 (nsp1-4). The RNAs are flanked with a 3´-poly adenylyl tail (AAAA) and with the 5´-methyl guanylyl (Cap). E1 and E2 are the envelope proteins encoded by the helper plasmid. Modified from Invitrogen Sindbis expression manual.

In vitro transcription of the viral RNA

The recombinant plasmids pSinRep5 and the helper plasmid p26S were linearized by a restriction digest at their linearization sites XhoI. The DNA was purified by extraction with phenol / chloroform and precipitated with ethanol / ammonium acetate. The in vitro transcription was prepared as follows (Gurevich, Pokrovskaya et al. 1991):

1-3µg DNA (in 7µl RNAse-free water)
2.5µl 10x transcription buffer
2.5µl 100mM DTT
7.5µl NTPs (ATP, CTP, UTP)
1.25µl GTP
1.25µl 5'-methylguanosin-Cap (Cap-analogue)
1µl RNAse inhibitor
2µl SP6-polymerase

Following one hour incubation at 37°C, a volume of 1.5 µl was denatured for 10 min at 85°C and analyzed on a gel containing 1% agarose. RNA was stored at - 70°C and used within 2 hours.

Electroporation of baby hamster kidney cells

These manipulations, including the harvesting and injection were performed in biosafty level II environments. Two 10 cm plates with BHK cells were used, cells were 80-90 % confluent. Cells were washed with 1x PBS and αMEM and then detached with 2.5 ml / plate trypsin. Trypsination was stopped after ~2 min with αMEM. Following gentle centrifugation, the pellet was re-suspended in αMEM and washed with cation free PBS. Cells were again collected and re-suspended in 500 µl PBS without cations. This volume was mixed in an electroporation cuvette (Gene Pulser cuvettes, Biorad) with 15µl of
recombinant RNA and 10µl helper RNA.

Cells were electroporated two times with the following parameters:

0.45kV
1.25µF external capacity
2.2-2.5ms time constant
1125V/cm2

After a short incubation on ice, cells were plated on one 10 cm plate with 10 ml

complete αMEM.

Harvest and concentration of viral particles

Transfected BHK cells were incubated for 20 – 24 hours at 37ºC, 5% CO_2 incubator. The medium was collected in 50ml Falcon tubes and centrifuged to remove cell debris. The supernatant was filtered through 100K Amicon Filter (Millipore, UFC9 10024), which restricts passage to molecules <100.000 MW and centrifuged at 4500 rpm. Typically 150 µl remain after 30 min of centrifugation, which contain the concentrated virions. BSA was added to a final concentration of 50 µg/ml to preserve the activity of viral particles after freezing and thawing. Therefore, virus was diluted with filtered BSA/PBS (1:5.5), aliquoted and immediately shock-frozen in methanol dry ice and stored at –70°C.

4. 3. 2. 2 Production of AAV virus

Cell culture

For one batch of virus 1-10 (1 for vector check, 5 for "small-scale" and 10 for "large-scale" virus production) 15 cm dishes with 1.0-1.2 x 10^7 AAV 293 cells per plate in 25 ml DMEM were used. The cells should be less than passage 30. The plates should be approx. 70-80% confluent by the time of transfection.

Transfection

1. Three hours before transfection get 2 x HeBS buffer, 2.5 M $CaCl_2$ and distilled H_2O out to warm up to room temp.
2. Prewarm the DMEM to 37ºC in a water bath.
3. In Nunc 50 ml tubes prepare the transfection mixture:
   Per 15 cm dish use:
   12.5μg AAV plasmid
   19μg Helper plasmid pDP1 (#174)
   19μg Helper plasmid pDP2 (#175)
   150μl 2.5 M $CaCl_2$
   Add ddH_2O to final volume of 1.25 ml
4. Make the transfection solution up in 50 ml Nunc tube, adding ingredients in the following order – water, $CaCl_2$, plasmids. Mix well this DNA/$CaCl_2$ mix.
5. Take an aliquot of transfection mix and **quickly** add 1.25 (12,5) ml of 2 x HeBS buffer with a pipetter. Keep vortexing for a further 10-15sec and leave

the solution to stand on the bench (total of 1-2 min max) for optimal formation of the precipitate. A very fine white precipitate should form, clearly visible to the naked eye. This will be very obvious when comparing this mix to a polystyrene tube containing water only.

6. Add 22.5 (225) ml of the DMEM growth medium to DNA/ $CaCl_2$ /HeBS-mix. Take the plates out of the incubator and remove medium by aspiration. Add transfection solution (25 ml to each plate) dropwise, slowly on the cell monolayer. The medium must be prewarmed at 37°C. Add the medium very gently to the cells. After transfection solution is added shake but do not stir the plates.
7. Return the tissue culture plate to the 37°C incubator.
8. 16 hours after transfection remove the medium and replace with 25 ml per plate of fresh DMEM. Transfection efficiency must reach 50-80% to be considered succesfull. This is determined by counting cells which simultaneously fluorescence green (GFP-vector) and red (mRFP-helper).

Harvesting cells 60-72 hours after transfection:

1. Prepare the ice-ethanol bath and 37°C water bath.
2. Remove media from cells and discard. Wash the cells in 1xPBS, i.e. carefully add 25ml warm 1xPBS to the plate, swirl and remove (discard). Add 25ml of 1xPBS to each plate and detach cells by using a cell scraper and collect in 50 ml tissue culture tubes.
3. Pellet cells at 200g (Rotina 1050 rpm) for ~15 min, RT.
4. Discard supernatant and resuspend cell pellets in 150mM NaCl, 50mM Tris pH 8.5. Volume to use is 1 ml per 15 cm plate. Transfer the cell suspension to a fresh 50ml tube.
5. Subject the cell suspension to three or four rounds of freeze/thaw by alternating the tubes between the ice-ethanol bath and 37°C water bath, vortexing briefly after each thaw. Each freeze and each thaw will require approximately 10 min. incubation time.
6. Add Benzonase endonuclease (Sigma #E1014) to a final concentration of 25-50U/ml. Mix contents of tube thoroughly.
7. Incubate in a 37°C waterbath for 1hr, before removing cell debris by centrifugation at 3000g (Rotina 4500 rpm) x 15min, 4°C.

8. Filter the supernatant trough a 13 or 32 mm 0.45μm Acrodisc syringe filter into a fresh tube and freeze at –20ºC until column purification (= crude lysate).

Heparin column purification

1. Defrost samples at room temp.
2. Pre-equilibrate the column (1- 5-ml Heparin Agarose type I columns, Sigma #H 6508) with PBS-MK pH 7.2 (4-5 x volume of HepAg).
3. Load the 1-10 ml of crude lysate prepared above onto the column and incubate for 1-2 h at room temperature with constant agitation (alternatively, use a Harvard infusion pump set with a flow rate of 1ml/min).
4. Wash column with PBS-MK pH 7.2 (4-5 x volume of HepAg) by gravity flow (using the infusion pump - a flow rate of 1ml/min).
5. Elute virus off column with PBS-MK 0.5M NaCl pH 7.2 (3 x volume of HepAg).
6. Concentrate virus eluate using 15ml AMICON ULTRA- (100000MWCO; Millipore), centrifuge at 3000g for 15 min. Wash the virus preparation by adding 3-4 times 15 ml PBS to the concentrator. Flow through – discard. Centrifuge down to as small a volume as possible (approximately 200ul).
7. Sterilise by filtration through a 13mm 0.2μm syringe filter. Do not use a larger diameter filter.
8. Run 10μl purified vector on a Coomassie protein gel to see how pure it is (only viral proteins should be present).

Titration of recombinant AAV

Determination of infectious particles by Fluorescence Cell Assay (FCA)

Transfection of the cells requires 5 days. On day 1 the cells are split. On day 2 the cells are infected. One day 5 the cells are visually monitored using a fluorescence microscope. At ~ 24 hr prior to infection, seed 24-well dish with $5x10^4$ HT 1080 cells/w in DMEM, at about 70% confluence. Prepare a 10-fold serial dilution of your virus stock. Infect cells by adding AAV directly to the medium of the cells or mix virus stock with fresh DMEM immediately before adding it to the cells. At 48 to 72 hr post infection, count the number of positive (fluorescence) cells using a fluorescence microscope.

4. 3. 3 Stereotaxic injections

All procedures involving animals were performed according to the German law for animal protection. Sprague-Dawley rats were used for the entire experiment. The technique of stereotactic VCN injections was developed by V. Wimmer and T. Kuner (Wimmer et al. 2004).

Injection capillaries were pulled on a horizontal P87 puller (Sutter Company, USA) from 5 µl micro pipettes (intraMAR, BlauBrand). Very long, tube-like tips were obtained after setting the time variable to zero. Tips were trimmed with scissors to a length of ~1cm immediately before use. The tips had an inner diameter of 10-20µm. The pipettes have a calibrated scale (1µl) to estimate the injection volume. Rats were injected with ~1µl virus solution under binocular control.

The stereotax (Cartesian Instruments, USA) was subjected to a calibration procedure according to the manufacturers guidelines before each experiment. The anesthetized animal was fixed in the head stage with ear bars and a tooth ring. The scalp was opened and the bregma, a common point at the intersection of sutures between frontal and parietal bones was observed on the rostral cranium. The bregma served as the zero point and all other positions were referred to bregma. Therefore the head had to be adjusted until bregma was localized in zero position of the stereotax in all three dimensions. By means of a cross hairs equipped ocular, bregma was first zeroed in the X Y Z axis.

4. 3. 3. 1 Surgery

Rats were anesthetized with isoflurane inhalation anesthesia with oxygen used as gas carrier delivered directly to rat snout via stereotaxic gas mask. Initial concentration of isoflurane was at 3-5% for about 4-5mins, and sustained concentration of 1 – 1.8% for the duration of the surgery. Local anesthetic Licain (Lidocaine, 1%) was injected (50 – 100μl) subcutaneously under the scalp at ~10 min ahead of skin incision to ensure total pain blockade. Skin was cut open with scalpel along the midline in anterio-posterior direction. After zeroing the stereotax coordinates on Bregma point on the skull, and establishing Lambda point position, little hole was drilled (~1.5mm diameter) in the skull at the injection site area as determined by Cartesian coordinates. Body temperature was monitored throughout the whole surgery with a rectal probe

and hold constant at 37.5°C.

4. 3. 3. 2 Cartesian coordinates

The coordinates used for injections were as follows.

For P7 -9 rats:		and for P21 and older rats:	
Y	X	Y	X
-9.8	1.3	-10.5	0.9
-9.5	1.3	-10.2	0.85
-9.2	1.25	-9.9	0.85
-9.9	1.15	-10.4	0.75
-9.6	1.1	-10.1	0.7
-9.3	1.1	-9.8	0.7
-9.0	1.05	-9.5	0.7

For all the injections vertical Z coordinate was always set to + 0.45. Angled injection arm was advanced along the VCN axis into $Axial_1$= 9.2 and $Axial_2$ = 9.4 coordinates ensuring maximal filling of the nucleus.

4. 3. 3. 3 Injection

The stereotaxic injections into VCN and tissue processing were done as reported previously (Wimmer et al., 2004). Briefly, the VCN of rats was injected with 1μl of virus solution. After *in vivo* protein expression for the time periods indicated below, rats were transcardially perfused, brains were sectioned and examined with confocal microscopy. For analysis of young (P7-P9) rats sindbis virus was used and rats were injected at P6 - P8 and sacrificed 24 h later. For analysis of older rats (P21- P24) the P7 – P9 rats were injected and sacrificed ~14 days later.

4. 4 Confocal microscopy

Sections of fluorescently immuno-labeled brainstem slices were imaged on confocal microscope at the in-house imaging facility. Confocal microscope technical parameters, as well as details of image acquisition will be described in the following sections.

4. 4. 1 Confocal microscope hardware and software

- LEICA TCS SP2 confocal microscope equipped with:
- two microscope stages (upright, inverted)
- Ar UVLaser (352, 364 nm)
- Ar Laser (457, 476, 488,514 nm)
- HeNe Laser (543 nm)
- HeNe Laser (633 nm)
- Acousto Optical Beam Splitter (AOBS) as main beam splitter for free selection of and rapid switching between reflected / transmitted wavelengths
- Spectral scanner with adjustable windows for fluorochromes showing blue to dark red fluorescence and for different Green Fluorescent Protein Variants (CFP, GFP, YFP) and dsRed
- 4 PMTs (epifluorescence and reflection mode)
- One PMT (transmission mode)
- Maerzhaeuser XY stage (manual and software-controlled mode)
- Software for sequential / simultaneous / time lapse / spectral recording / and for photobleaching experiments

Scans were made on the above Leica TCS SP2 confocal microscope with 63x objective and 1.3 NA, with glycerol based immersion medium of 1.45 refractive index for collecting stacks of optical sections or 20x objective for overview images. All the hardware used was controlled from Leica confocal software version 2.61 Build 1537.

4. 4. 2 Acquisition parameters

Scans were made at 512 or 1024 format at 8 bit resolution with PMTs and lasers settings to ensure the whole range of grayscale values. At lower magnification for scans that were not deconvolved four times line averaging was used. After collecting images at 1.8 to 3 - fold oversampling, data was deconvolved with Huygens2 software (Scientific Volume Imaging).

4. 5 Processing of image data and statistics

All our data is based on fluorescent indirect immunohistochemistry performed on slices. Revealing localization of antibody-bound antigens by fluorescently labeled secondary antibody was done with the confocal microscopy. Like any method, also this one is not free from methodological challenges and requires careful consideration to overcome potential technical problems. We will describe theoretical consideration of limitations and shortcomings of immunohistochemistry combined with confocal visualization in respect of quantitative approach. We will also suggest possible solutions to some of these problems.

4. 5. 1 Theoretical considerations of problems in IHC/confocal study

Using immunohistochemistry for labeling antigens of interest requires well characterized antibodies, whose specificity has been established rigorously. In the case of antibodies used in this study, anti-Piccolo and anti-Bassoon, such characterization has been thoroughly performed earlier (Dick et al., 2001; tom Dieck et al., 1998 respectively). Even then, however, immuno-labeled proteins are notoriously difficult to quantify. This is due to several factors that increase the complexity of immuno-labeling approaches. Factors related to antibody characteristic, like number of primary antibodies binding to antigen, number of secondary antibody molecules binding to primary and finally number of fluorescent molecules conjugated to secondary antibody are all variable and impossible to quantify in tissue stainings. The above factors render an estimation of a number of Bassoon or Piccolo particles within any given fluorescent cluster very hard if not entirely out of reach.

Visualization of a signal created by fluorescent dye molecules conjugated to the secondary antibody using confocal microscope creates its own set of issues worth careful considerations. Confocal imaging offers great three-dimensional capabilities by creating series of thin optical sections along depth (z-axis) facilitated by confocality of the pinholes. It uses specific laser-generated light of defined wavelengths to excite each fluorophore separately. Light from the excited fluorescent molecule passes through appropriate wavelength filter (or Acousto-optic Tunable Filters AOTF) and falls on the photomultiplier (PMT). Fluorescent signal collected

from two different sources, located in a tissue sample, passed in two separate channels, can differ in intensity due to:

- number of fluorescent molecules generating that signal,
- quantum yield which determines brightness of a dye
- presence of highly diffractive structures on the light path that can cause increased dispersion and ultimate loss of signal

PMTs allow the user to optimize the range of scanned intensities and prevent clipping, which is collecting an entire signal at either too high or too low intensities (e.g. at 0 or 255 grayscale values when scanned at 8 bit) instead of using the full range. In this study we have decided to preserve the full range of scale and always scan at optimal intensity settings for each sample rather than using the same setting of intensity for a given antibody between age groups (but compare Billups, 2005). Keeping the same PMTs setting between age groups could miss signal in tissue samples from old animals. In these animals densely packed myelinated axons of the medial nucleus of the trapezoid body (MNTB) hinder visibility of calyces.

4. 5. 2 Deconvolution with Huygens2 software

Collected images were processed at Huygens2 software for deconvolution. This processing reduces noise, removes blur and improves visible resolution.
Deconvolution was run using High quality Classic Maximum Likelihood Estimation (CMLE) algorithm with estimated point spread function (PSF).

4. 5. 3 Quantitative analysis in three dimensions

All 3D reconstructions, surface rendering and volume measurements were done in Amira 4.1.1 software (Mercury Computer Systems, Inc). Excision of the immuno-labeled signal from the pre-labeled calyces was done via thresholding of the calyx channel and multiplying it by the Bassoon or Piccolo channel. The outcome of the procedure was a channel with immuno-labeled clusters of original intensity retained only within the calyx volume.
Due to the non-specific surface labeling, the data had a consistent bias towards extremely large immuno-clusters at the surface located parts of the calyx (e.g. a 100x the size of any clusters from below the surface). These extremely large clusters were

removed and to avoid any experimenter bias we used mathematically defined outliers. On the cluster size data we calculated the outliers with the border size defined as 1.5 x (75^{th} percentile - 25^{th} percentile). The clusters above the border size were subtracted from the raw data set (they account for ~20%). All further analysis was done on the data without outliers. A nonparametric statistical test (unpaired t-test with Welch correction) was used to compare semi-quantitative data obtained from measurements of fluorescently labeled immno-clusters. Data are expressed as mean ± standard error of the mean.

For quantification of calyces treated with shRNA as compared to WT control, set of rules was developed to minimize variability introduced by fluorescent imaging method itself. These included keeping constant laser power, PMT gain, and offset, using the same FIHC preparation, ensuring similar scanning time, avoiding comparing calyces if at least one of them was located at the surface. These rules could be fulfilled thoroughly only if we compared treated and control calyces located within the same field of view.

Once such pair of calyces was found, the processing methods including, clusters excision from the calyx volume and 3D cluster reconstruction were applied. We have used thresholding method to identify FIHC clusters. In such case if a protein was down regulated FIHC clusters would appear smaller (less bright clusters) or there would be less of them in total. To take in account both of these cases we always have set threshold first at the shRNA treated calyx, assuming that these clusters might be less bright, due to reduced number of antibody bound antigens. We would then reuse the same threshold value in control calyces. In result if the protein expression was reduced in shRNA treated calyx then in the control we would detect more or bigger (or either) of FIHC clusters. For this reason we have quantified both the number of FIHC clusters as well as their total volume.

List of abbreviations

AAV	adeno-associated virus
AMPAR	L-alpha-amino-3-hydroxy-5-methyl-4-isoxazolepropionate receptor
AP	action potential
AZ	active zone
bp	base pairs
CA3	*cornu Ammonis*
CN	cochlear nucleus
CNS	central nervous system
div	day *in vitro*
dsRNA	double strand RNA
E15	embryonic day 15
EM	electron microscopy
EPSC	excitatory postsynaptic current
FIHC	fluorescent immunohistochemistry
GABA	gamma-amino butyric acid
GABAR	gamma-amino butyric acid receptor
GBC	globular bushy cell
GFP	green fluorescent protein
GlyR	glycine receptor
H-NMR	H-nuclear magnetic resonance
IHC	immunohistochemistry
IPL	inner plexiform layer
ITR	internal terminal repeats
KAR	kainate receptor
kbp	kilo base pairs
kDa	kilo Dalton
KO	knock out
LSO	lateral superior olive
ME-MRI	Manganese-enhanced magnetic resonance imaging
miRNA	micro RNA
MNTB	medial nucleus of the trapezoid body

NMDAR	N-methyl-D-aspartate receptor
nt	nucleotide
P9	postnatal day 9
PB	phosphate buffer
PBS	phosphate buffer saline
PCR	polymerase chain reaction
PSD	postsynaptic density
PTV	piccolo-bassoon transport vesicles
RNAi	RNA interference
RRP	readily releasable pool
SEM	standard error of the mean
shRNA	short hairpin RNA
SOC	superior olivary complex
SV	synaptic vesicle
VCN	ventral cochlear nucleus
VNTB	ventral nucleus of the trapezoid body
WT	wild type

References

Adams JC, Mugnaini E (1990) Immunocytochemical evidence for inhibitory and disinhibitory circuits in the superior olive. Hear Res 49:281-298.

Ahmari SE, Buchanan J, Smith SJ (2000) Assembly of presynaptic active zones from cytoplasmic transport packets. Nat Neurosci 3:445-451.

Altrock WD, tom Dieck S, Sokolov M, Meyer AC, Sigler A, Brakebusch C, Fassler R, Richter K, Boeckers TM, Potschka H, Brandt C, Loscher W, Grimberg D, Dresbach T, Hempelmann A, Hassan H, Balschun D, Frey JU, Brandstatter JH, Garner CC, Rosenmund C, Gundelfinger ED (2003) Functional inactivation of a fraction of excitatory synapses in mice deficient for the active zone protein bassoon. Neuron 37:787-800.

Angenstein F, Hilfert L, Zuschratter W, Altrock WD, Niessen HG, Gundelfinger ED (2007) Morphological and Metabolic Changes in the Cortex of Mice Lacking the Functional Presynaptic Active Zone Protein Bassoon: A Combined 1H-NMR Spectroscopy and Histochemical Study. Cereb Cortex.

Angenstein F, Niessen HG, Goldschmidt J, Lison H, Altrock WD, Gundelfinger ED, Scheich H (2006) Manganese-Enhanced MRI Reveals Structural and Functional Changes in the Cortex of Bassoon Mutant Mice. Cereb Cortex.

Awatramani GB, Turecek R, Trussell LO (2004) Inhibitory control at a synaptic relay. J Neurosci 24:2643-2647.

Banks MI, Smith PH (1992) Intracellular recordings from neurobiotin-labeled cells in brain slices of the rat medial nucleus of the trapezoid body. J Neurosci 12:2819-2837.

Baslow MH (2003) N-acetylaspartate in the vertebrate brain: metabolism and function. Neurochem Res 28:941-953.

Bennett MV (1997) Gap junctions as electrical synapses. J Neurocytol 26:349-366.

Betz A, Okamoto M, Benseler F, Brose N (1997) Direct interaction of the rat unc-13 homologue Munc13-1 with the N terminus of syntaxin. J Biol Chem 272:2520-2526.

Betz A, Thakur P, Junge HJ, Ashery U, Rhee JS, Scheuss V, Rosenmund C, Rettig J, Brose N (2001) Functional interaction of the active zone proteins Munc13-1 and RIM1 in synaptic vesicle priming. Neuron 30:183-196.

Billups B (2005) Colocalization of vesicular glutamate transporters in the rat superior olivary complex. Neurosci Lett 382:66-70.

Blatchley BJ, Cooper WA, Coleman JR (1987) Development of auditory brainstem response to tone pip stimuli in the rat. Brain Res 429:75-84.

Bollmann JH, Sakmann B (2005) Control of synaptic strength and timing by the release-site Ca2+ signal. Nat Neurosci 8:426-434.

Bollmann JH, Sakmann B, Borst JG (2000) Calcium sensitivity of glutamate release in a calyx-type terminal. Science 289:953-957.

Borst JG, Sakmann B (1998) Facilitation of presynaptic calcium currents in the rat brainstem. J Physiol 513 (Pt 1):149-155.

Brandstatter JH, Fletcher EL, Garner CC, Gundelfinger ED, Wassle H (1999) Differential expression of the presynaptic cytomatrix protein bassoon among ribbon synapses in the mammalian retina. Eur J Neurosci 11:3683-3693.

Cases-Langhoff C, Voss B, Garner AM, Appeltauer U, Takei K, Kindler S, Veh RW, De Camilli P, Gundelfinger ED, Garner CC (1996) Piccolo, a novel 420 kDa protein associated with the presynaptic cytomatrix. Eur J Cell Biol 69:214-223.

Casey MA, Feldman ML (1985) Aging in the rat medial nucleus of the trapezoid body. II. Electron microscopy. J Comp Neurol 232:401-413.

Cuttle MF, Tsujimoto T, Forsythe ID, Takahashi T (1998) Facilitation of the presynaptic calcium current at an auditory synapse in rat brainstem. J Physiol 512 (Pt 3):723-729.

Deken SL, Vincent R, Hadwiger G, Liu Q, Wang ZW, Nonet ML (2005) Redundant localization mechanisms of RIM and ELKS in Caenorhabditis elegans. J Neurosci 25:5975-5983.

Dermietzel R, Spray DC (1993) Gap junctions in the brain: where, what type, how many and why? Trends Neurosci 16:186-192.

Dick O, Hack I, Altrock WD, Garner CC, Gundelfinger ED, Brandstatter JH (2001) Localization of the presynaptic cytomatrix protein Piccolo at ribbon and conventional synapses in the rat retina: comparison with Bassoon. J Comp Neurol 439:224-234.

Dresbach T, Hempelmann A, Spilker C, tom Dieck S, Altrock WD, Zuschratter W, Garner CC, Gundelfinger ED (2003) Functional regions of the presynaptic cytomatrix protein bassoon: significance for synaptic targeting and cytomatrix anchoring. Mol Cell Neurosci 23:279-291.

Elbashir SM, Harborth J, Lendeckel W, Yalcin A, Weber K, Tuschl T (2001) Duplexes of 21-nucleotide RNAs mediate RNA interference in cultured mammalian cells. Nature 411:494-498.

Elezgarai I, Diez J, Puente N, Azkue JJ, Benitez R, Bilbao A, Knopfel T, Donate-Oliver F, Grandes P (2003) Subcellular localization of the voltage-dependent potassium channel Kv3.1b in postnatal and adult rat medial nucleus of the trapezoid body. Neuroscience 118:889-898.

Elezgarai I, Bilbao A, Mateos JM, Azkue JJ, Benitez R, Osorio A, Diez J, Puente N, Donate-Oliver F, Grandes P (2001) Group II metabotropic glutamate receptors are differentially expressed in the medial nucleus of the trapezoid body in the developing and adult rat. Neuroscience 104:487-498.

Elmqvist D, Quastel DM (1965) A quantitative study of end-plate potentials in isolated human muscle. J Physiol 178:505-529.

Erles K, Sebokova P, Schlehofer JR (1999) Update on the prevalence of serum antibodies (IgG and IgM) to adeno-associated virus (AAV). J Med Virol 59:406-411.

Fedchyshyn MJ, Wang LY (2005) Developmental transformation of the release modality at the calyx of held synapse. J Neurosci 25:4131-4140.

Felmy F, Schneggenburger R (2004) Developmental expression of the Ca2+-binding proteins calretinin and parvalbumin at the calyx of held of rats and mice. Eur J Neurosci 20:1473-1482.

Fenster SD, Kessels MM, Qualmann B, Chung WJ, Nash J, Gundelfinger ED, Garner CC (2003) Interactions between Piccolo and the actin/dynamin-binding protein Abp1 link vesicle endocytosis to presynaptic active zones. J Biol Chem 278:20268-20277.

Fenster SD, Chung WJ, Zhai R, Cases-Langhoff C, Voss B, Garner AM, Kaempf U, Kindler S, Gundelfinger ED, Garner CC (2000) Piccolo, a presynaptic zinc finger protein structurally related to bassoon. Neuron 25:203-214.

Fire A, Xu S, Montgomery MK, Kostas SA, Driver SE, Mello CC (1998) Potent and specific genetic interference by double-stranded RNA in Caenorhabditis elegans. Nature 391:806-811.

Fire AZ (2007) Gene silencing by double-stranded RNA. Cell Death Differ 14:1998-2012.

Forsythe ID, Tsujimoto T, Barnes-Davies M, Cuttle MF, Takahashi T (1998) Inactivation of presynaptic calcium current contributes to synaptic depression at a fast central synapse. Neuron 20:797-807.

Friauf E, Ostwald J (1988) Divergent projections of physiologically characterized rat ventral cochlear nucleus neurons as shown by intra-axonal injection of horseradish peroxidase. Experimental Brain Research 73:263-284.

Friauf E, Hammerschmidt B, Kirsch J (1997) Development of adult-type inhibitory glycine receptors in the central auditory system of rats. J Comp Neurol 385:117-134.

Gao G, Vandenberghe LH, Alvira MR, Lu Y, Calcedo R, Zhou X, Wilson JM (2004) Clades of Adeno-associated viruses are widely disseminated in human tissues. J Virol 78:6381-6388.

Garcia J, Gerber SH, Sugita S, Sudhof TC, Rizo J (2004) A conformational switch in the Piccolo C2A domain regulated by alternative splicing. Nat Struct Mol Biol 11:45-53.

Geal-Dor M, Freeman S, Li G, Sohmer H (1993) Development of hearing in neonatal rats: air and bone conducted ABR thresholds. Hear Res 69:236-242.

Gerber SH, Garcia J, Rizo J, Sudhof TC (2001) An unusual C(2)-domain in the active-zone protein piccolo: implications for Ca(2+) regulation of neurotransmitter release. Embo J 20:1605-1619.

Glendenning KK, Hutson KA, Nudo RJ, Masterton RB (1985) Acoustic chiasm II: Anatomical basis of binaurality in lateral superior olive of cat. J Comp Neurol 232:261-285.

Grandes P, Streit P (1989) Glutamate-like immunoreactivity in calyces of Held. J Neurocytol 18:685-693.

Gray EG (1959) Axo-somatic and axo-dendritic synapses of the cerebral cortex: an electron microscope study. J Anat 93:420-433.

Guinan JJ, Jr., Li RY (1990) Signal processing in brainstem auditory neurons which receive giant endings (calyces of Held) in the medial nucleus of the trapezoid body of the cat. Hear Res 49:321-334.

Hamilton AJ, Baulcombe DC (1999) A species of small antisense RNA in posttranscriptional gene silencing in plants. Science 286:950-952.

Heuser JE, Reese TS (1973) Evidence for recycling of synaptic vesicle membrane during transmitter release at the frog neuromuscular junction. J Cell Biol 57:315-344.

Ishikawa T, Nakamura Y, Saitoh N, Li WB, Iwasaki S, Takahashi T (2003) Distinct roles of Kv1 and Kv3 potassium channels at the calyx of Held presynaptic terminal. J Neurosci 23:10445-10453.

Jonas P MH (1999) Ionotropic Glutamate Receptors in the CNS: Springer-Verlag.

Kandler K, Friauf E (1993) Pre- and postnatal development of efferent connections of the cochlear nucleus in the rat. J Comp Neurol 328:161-184.

Kim S, Ko J, Shin H, Lee JR, Lim C, Han JH, Altrock WD, Garner CC, Gundelfinger ED, Premont RT, Kaang BK, Kim E (2003) The GIT family of proteins forms multimers and associates with the presynaptic cytomatrix protein Piccolo. J Biol Chem 278:6291-6300.

Kuwabara N, DiCaprio RA, Zook JM (1991) Afferents to the medial nucleus of the trapezoid body and their collateral projections. J Comp Neurol 314:684-706.

Landis DM, Hall AK, Weinstein LA, Reese TS (1988) The organization of cytoplasm at the presynaptic active zone of a central nervous system synapse. Neuron 1:201-209.

Leao RM, Kushmerick C, Pinaud R, Renden R, Li GL, Taschenberger H, Spirou G, Levinson SR, von Gersdorff H (2005) Presynaptic Na+ channels: locus, development, and recovery from inactivation at a high-fidelity synapse. J Neurosci 25:3724-3738.

McAlpine D (2005) Creating a sense of auditory space. J Physiol 566:21-28.

Meinrenken CJ, Borst JG, Sakmann B (2002) Calcium secretion coupling at calyx of held governed by nonuniform channel-vesicle topography. J Neurosci 22:1648-1667.

Meinrenken CJ, Borst JG, Sakmann B (2003) Local routes revisited: the space and time dependence of the Ca2+ signal for phasic transmitter release at the rat calyx of Held. J Physiol 547:665-689.

Morest DK (1968) The growth of synaptic endings in the mammalian brain: a study of the calyces of the trapezoid body. Z Anat Entwicklungsgesch 127:201-220.

Ohtsuka T, Takao-Rikitsu E, Inoue E, Inoue M, Takeuchi M, Matsubara K, Deguchi-Tawarada M, Satoh K, Morimoto K, Nakanishi H, Takai Y (2002) Cast: a novel protein of the cytomatrix at the active zone of synapses that forms a ternary complex with RIM1 and munc13-1. J Cell Biol 158:577-590.

Paddison PJ, Caudy AA, Bernstein E, Hannon GJ, Conklin DS (2002) Short hairpin RNAs (shRNAs) induce sequence-specific silencing in mammalian cells. Genes Dev 16:948-958.

Pei Y, Tuschl T (2006) On the art of identifying effective and specific siRNAs. Nat Methods 3:670-676.

Purves D AG, Fitzpatrick D, Katz L, Lamantia AS, McNamara JO, Williams SM (2004) Neuroscience, 3 Edition. Sunderland, Massachusetts, USA: Sinauer Associates, Inc.

Pyle JL, Kavalali ET, Piedras-Renteria ES, Tsien RW (2000) Rapid reuse of readily releasable pool vesicles at hippocampal synapses. Neuron 28:221-231.

Rajewsky K, Gu H, Kuhn R, Betz UA, Muller W, Roes J, Schwenk F (1996) Conditional gene targeting. J Clin Invest 98:600-603.

Richter K, Langnaese K, Kreutz MR, Olias G, Zhai R, Scheich H, Garner CC, Gundelfinger ED (1999) Presynaptic cytomatrix protein bassoon is localized at both excitatory and inhibitory synapses of rat brain. J Comp Neurol 408:437-448.

Rizzoli SO, Betz WJ (2005) Synaptic vesicle pools. Nat Rev Neurosci 6:57-69.

Rodriguez-Contreras A, de Lange RP, Lucassen PJ, Borst JG (2006) Branching of calyceal afferents during postnatal development in the rat auditory brainstem. J Comp Neurol 496:214-228.

Rowland KC, Irby NK, Spirou GA (2000) Specialized synapse-associated structures within the calyx of Held. J Neurosci 20:9135-9144.

Saetzler K, Soehl LF, Bollmann JH, Borst JGG, Frotscher M, Sakmann B, Luebke JHR (2002) Three-dimensional reconstruction of a calyx of Held and its postsynaptic principal neuron in the Medial Nucleus of the Trapezoid Body. The Journal of Neuroscience 22:10567-10579.

Scherer LJ, Rossi JJ (2003) Approaches for the sequence-specific knockdown of mRNA. Nat Biotechnol 21:1457-1465.

Schneggenburger R, Neher E (2000) Intracellular calcium dependence of transmitter release rates at a fast central synapse. Nature 406:889-893.

Schoch S, Gundelfinger ED (2006) Molecular organization of the presynaptic active zone. Cell Tissue Res.

Shibasaki T, Sunaga Y, Fujimoto K, Kashima Y, Seino S (2004) Interaction of ATP sensor, cAMP sensor, Ca2+ sensor, and voltage-dependent Ca2+ channel in insulin granule exocytosis. J Biol Chem 279:7956-7961.

Smith PH, Joris PX, Carney LH, Yin TC (1991) Projections of physiologically characterized globular bushy cell axons from the cochlear nucleus of the cat. J Comp Neurol 304:387-407.

Somogyi P, Cowey A (1981) Combined Golgi and electron microscopic study on the synapses formed by double bouquet cells in the visual cortex of the cat and monkey. J Comp Neurol 195:547-566.

Spirou GA, Brownell WE, Zidanic M (1990) Recordings from cat trapezoid body and HRP labeling of globular bushy cell axons. J Neurophysiol 63:1169-1190.

Takao-Rikitsu E, Mochida S, Inoue E, Deguchi-Tawarada M, Inoue M, Ohtsuka T, Takai Y (2004) Physical and functional interaction of the active zone proteins, CAST, RIM1, and Bassoon, in neurotransmitter release. J Cell Biol 164:301-311.

Taschenberger H, von Gersdorff H (2000) Fine-tuning an auditory synapse for speed and fidelity: developmental changes in presynaptic waveform, EPSC kinetics, and synaptic plasticity. J Neurosci 20:9162-9173.

Taschenberger H, Leao RM, Rowland KC, Spirou GA, von Gersdorff H (2002) Optimizing synaptic architecture and efficiency for high-frequency transmission. Neuron 36:1127-1143.

Thomas KR, Capecchi MR (1987) Site-directed mutagenesis by gene targeting in mouse embryo-derived stem cells. Cell 51:503-512.

Tolbert LP, Morest DK, Yurgelun-Todd DA (1982) The neuronal architecture of the anteroventral cochlear nucleus of the cat in the region of the cochlear nerve root: horseradish peroxidase labelling of identified cell types. Neuroscience 7:3031-3052.

tom Dieck S, Altrock WD, Kessels MM, Qualmann B, Regus H, Brauner D, Fejtova A, Bracko O, Gundelfinger ED, Brandstatter JH (2005) Molecular dissection of the photoreceptor ribbon synapse: physical interaction of Bassoon and

RIBEYE is essential for the assembly of the ribbon complex. J Cell Biol 168:825-836.

tom Dieck S, Sanmarti-Vila L, Langnaese K, Richter K, Kindler S, Soyke A, Wex H, Smalla KH, Kampf U, Franzer JT, Stumm M, Garner CC, Gundelfinger ED (1998) Bassoon, a novel zinc-finger CAG/glutamine-repeat protein selectively localized at the active zone of presynaptic nerve terminals. J Cell Biol 142:499-509.

Vaucheret H, Beclin C, Fagard M (2001) Post-transcriptional gene silencing in plants. J Cell Sci 114:3083-3091.

Wadel K, Neher E, Sakaba T (2007) The Coupling between Synaptic Vesicles and Ca(2+) Channels Determines Fast Neurotransmitter Release. Neuron 53:563-575.

Wang X, Kibschull M, Laue MM, Lichte B, Petrasch-Parwez E, Kilimann MW (1999) Aczonin, a 550-kD putative scaffolding protein of presynaptic active zones, shares homology regions with Rim and Bassoon and binds profilin. J Cell Biol 147:151-162.

Wang Y, Sudhof TC (2003) Genomic definition of RIM proteins: evolutionary amplification of a family of synaptic regulatory proteins(small star, filled). Genomics 81:126-137.

Wang Y, Sugita S, Sudhof TC (2000) The RIM/NIM family of neuronal C2 domain proteins. Interactions with Rab3 and a new class of Src homology 3 domain proteins. J Biol Chem 275:20033-20044.

Wang Y, Liu X, Biederer T, Sudhof TC (2002) A family of RIM-binding proteins regulated by alternative splicing: Implications for the genesis of synaptic active zones. Proc Natl Acad Sci U S A 99:14464-14469.

Wang Y, Okamoto M, Schmitz F, Hofmann K, Sudhof TC (1997) Rim is a putative Rab3 effector in regulating synaptic-vesicle fusion. Nature 388:593-598.

Warr WB (1972) Fiber degeneration following lesions in the multipolar and globular cell areas in the ventral cochlear nucleus of the cat. Brain Res 40:247-270.

Wimmer VC, Nevian T, Kuner T (2004) Targeted in vivo expression of proteins in the calyx of Held. Pflugers Arch 449:319-333.

Wimmer VC, Horstmann H, Groh A, Kuner T (2006) Donut-like topology of synaptic vesicles with a central cluster of mitochondria wrapped into membrane

protrusions: a novel structure-function module of the adult calyx of Held. J Neurosci 26:109-116.

Yang YM, Wang LY (2006) Amplitude and kinetics of action potential-evoked Ca2+ current and its efficacy in triggering transmitter release at the developing calyx of held synapse. J Neurosci 26:5698-5708.

Zhai R, Olias G, Chung WJ, Lester RA, tom Dieck S, Langnaese K, Kreutz MR, Kindler S, Gundelfinger ED, Garner CC (2000) Temporal appearance of the presynaptic cytomatrix protein bassoon during synaptogenesis. Mol Cell Neurosci 15:417-428.

Zhai RG, Vardinon-Friedman H, Cases-Langhoff C, Becker B, Gundelfinger ED, Ziv NE, Garner CC (2001) Assembling the presynaptic active zone: a characterization of an active one precursor vesicle. Neuron 29:131-143.

Zhang L, Volknandt W, Gundelfinger ED, Zimmermann H (2000) A comparison of synaptic protein localization in hippocampal mossy fiber terminals and neurosecretory endings of the neurohypophysis using the cryo-immunogold technique. J Neurocytol 29:19-30.

Acknowledgments

At the end I would like to thank everybody from the lab for his or her help, understanding, and coping with me.

I would like to thank particularly Prof. Dr. Thomas Kuner for his support with the project, for his time generously shared with me during our discussions, and for all I learnt from him.

I would like to thank Prof. Dr. Bert Sakmann for taking me on board of his department and providing financial support of my work, and his ongoing interest in the progression of my project.

I would also like to thank Dr. Guenther Giese for his help with the confocal microscope.

Many thanks to Frau Marlies Kaiser for her help with miscellaneous issues related to life in Cell Physiology dept.

And last but not least I would like to express many thanks to my family for ongoing support.